

INGV-DPC Project S4 – Shakemap project

Research Unit S4/01

Responsible:

Alberto Michelini, INGV-CNT Roma

2.1 Achievement of Project Deliverables

Following the list deliverables listed in the approved project, the research unit (RU) has achieved the following applicative deliverables.

- Prototype implementation of the USGS-ShakeMap package at INGV.
- Prototype of the web site “Integrated Italian Seismic network” accessible at <http://earthquake.rm.ingv.it> where earthquake locations, ground motion maps (PGA, PGV, instrumental intensity), and moment tensors for $M > 3.5$ earthquake are published.
- implementation of fully non-linear earthquake, global search methods for earthquake location.

In addition, the main research achievements obtained by the RU during the project are:

- Three-dimensional velocity model for the Italian peninsula and neighboring areas and associated regionalization of Green’s functions to the end of full waveform modeling.
- new method for the fast determination of earthquake magnitude for $M > 7.5$ earthquakes at teleseismic distances.

In detail, the RU has been involved in Tasks 1, 2, 3 and partly in 5 of the approved project. Here it follows a description of the work done and the results obtained in each task during the two year project. Other deliverables are listed in the reports of the individual tasks.

Task 1 - Data organization, integration and exchange

The project has developed a data archiving-distribution system of the INGV network administered by the National Earthquake Center (CNT). This system allows the users to access the data in various ways depending on the analysis needs. By its nature, the developed system is still under development.

The archived data to be distributed consist of both full waveforms and of various types of parametric data (e.g., station location coordinates, instrumental response, filtering procedures, arrival time of phases, earthquake locations).

Real time data. It has been developed a continuous data stream procedure that allows, in principle, for the distribution of all the data acquired by the national network. Core to the data stream distribution is the implementation of the *SeedLink Server* that gathers in real-time all the data acquired by the CNT. The data are converted in *miniseed* format to be archived in the same format independently from their original format. For the data acquired by the Nanometrics stations (all broadband, BB), the existent plugin has been rewritten and improved to insure no loss of data. For the data acquired by the GAIA-INGV seismic data logger, the SeedLink Server has been implemented locally on each data logger. The latter is capable to produce *miniseed* data directly at the station.

Station Data-base. During the course of the project, the station metadata database (DB) has been completed. This DB has been designed to keep track of the day-to-day functioning of the

station. This is of great benefit to the technical personnel that can promptly recover the history of the stations and their performance.

Event Data-base. The event DB has been populated with the revised earthquake locations obtained by the seismologists on duty in the seismic center. In less than 30' (often in less than 15') the DB is adjourned as a new event has been recorded and located by the seismologists on H24 duty in the INGV seismic center. The data of the DB are used to generate maps published on the INGV recent earthquake web page.

The 15-days seismic bulletins, obtained from the phase data of the Italian Seismic Network read manually by the CNT analysts, have also become available and are published on the INGV web site. More specifically, the users can access the "Bollettino Sismico" (January 1985 – April 2005), the ING Catalog (1450 BC – 1985 AD), the CSTI 1.1 (1981-1996), the CPTI 04 (217 a.c. – 2002) and the CSI 1.1 (1997-2002).

Continuous Data Archiving. The data recorded in real time are transferred to the waveform archive after checking for possible data gaps. A more thorough checking of the waveforms is postponed to a later stage of the data processing. For what concerns the data completeness, we have developed a procedure that allows for retrieving the data after interruptions of the data carrier. This procedure works both for the SeedLink local server and the Nanometrics stations.

The very broad band data distribution occurs through the automatic request procedures NetDC (SEED format) e AutoDRM (GSE format). In addition, the entire continuous data can be accessed from within INGV using the "ad hoc" developed software "rdseedtcp" or, more generally, using the ArcLink protocol. Through ArcLink, it is possible to distribute the data from a distributed archive of waveform servers.

Event Data Archiving. It has been developed a procedure that, after each earthquake determination, prepares the waveform event data in SAC format together with the station response functions as poles-and-zeros and sensitivity. These data are distributed on the web as gzipped tar ball for each event.

Task 2 – Definition of crustal models

The ultimate goal of this task is that of determining the Green's functions (GFs) over the entire Italian territory and neighboring areas in order to be able to model the observed ground motion. To this purpose it is necessary to determine the velocity structure of both P- and S-waves for the Crust and the Upper Mantle. During the project this goal has been pursued in various ways – broadband waveform inversion for velocity model parameters, cross-correlation of seismic noise at pairs of stations, travel-time tomography, receiver functions.

As anticipated, the GFs are the main ingredients for forward waveform modeling of arbitrary focal mechanisms (point and finite fault sources) and/or for retrieving the moment tensor (or the finite fault) through inversion of the data of the Italian broadband stations. To this end, it has been completed a study (*Li et al., BSSA in press*) in which the Italian territory has been subdivided in laterally homogeneous regions (i.e., 1D velocity models). This regionalization has been accomplished through inversion of broadband data of the recently installed Italian broadband network and of MedNet together with several thousands of P- and S-wave arrival times. In order to obtain the regionalized 1D models, we have used the genetic algorithm (GA) to search the velocity model parameters from a set of 39 earthquakes with known focal mechanism (Fig. 1). This study, however has evidenced the limitations of the 1D regionalization above for geological complex areas such as the Italian peninsula.

In a second work (still underway) similarly driven toward determination of the velocity structure, we have employed a recently proposed technique which exploits the seismic noise recorded at pairs of stations for long periods of time (*Shapiro and Campillo, 2004; Shapiro et al., 2005*). In practice, the technique is based on stacking the cross-correlation of ambient noise between

pairs of stations. As result, the true Green's function between the station pairs are obtained. From all these GFs It is then possible to determine the inter-station group velocities for periods comprised between 5 and 30 s (Fig. 2). At these periods the seismic wavefield is confined within the Crust and the Upper mantle. Our first results show well defined group velocities in general agreement with the previously proposed models and with the previously identified Moho depths (see below).

In a third study, we have followed an approach based essentially on the calculation of receiver functions to define the 3D model for the Moho in the Apennines region. The approach followed consists of two separate steps:

Step 1: The computation of the Moho depth underneath each seismic station with Receiver Function (RF) technique. This technique uses the P-S conversion at the velocity interface to produce 1D S-wave velocity models and the depth of the conversion (the Moho, in our case).

Step 2: The integration of Moho depth information from RF and Controlled Seismic Sources (CSS) data and 3D P-wave velocity model of the area. The final result is a 3D image of the Moho depth underneath the Italian peninsula.

In detail, in this work it has been addressed the crust-mantle boundary under the Apennines, using teleseismic receiver function (RF). We analysed teleseismic records of the National Seismic Network, together with data from temporary networks (mainly RETREAT and CATSCAN campaigns). The data set used comprises about 7700 high s/n ratio waveforms from 138 broadband seismic stations. The RF data-set was investigated using different methods. We started with a single station analysis of the RF dataset computed for each seismic station, to provide a S-velocity profile under each station. As an example, in Fig. 3 we illustrate the results for seismic stations deployed along the CROP-04 seismic line, during the CATSCAN experiment (*Steckler et al, 2007, submitted to Geology*).

The well known stacking method of Zhu and Kanamori (*Zhu and Kanamori, 2000*) has been also applied to extract first-order information about the bulk crustal seismic properties. We obtained results for a dense linear array deployed during the RETREAT campaign (*Piana Agostinetti et al, 2007, in preparation*).

Finally, we have integrated results from the RF with those independently obtained by controlled seismic sources (CSS) experiments all over Italy. The Moho depths derived from both CSS and RF are used, weighted accordingly with the estimation errors, as observational points to fit the Moho topography. The P-wave velocity model, continuous through the area, is used both to define the boundary between the Adriatic and the Tyrrhenian plates and to introduce constraints on the mean P-wave velocity in the crust (Fig. 4).

Task 3 – Rapid estimates of the seismic source, implementation and verification of the ShakeMap package, development of the www.iisn.org

This task involves many activities driven toward the accurate representation of the earthquake source and its effects on the resulting wavefield. Although core to the task is the implementation for Italy of the USGS-ShakeMap package (*Wald et al. 1999*), a number of other different procedures of importance to better describe the earthquake process have been implemented. These include fully nonlinear algorithms for earthquake location, early warning estimates of source location and magnitude, moment tensor and finite source determinations, and the development of web portal where to publish the results. As a corollary, a method for the calculation of the space-temporal estimates of seismic hazard has been also put under testing. In the following we provide a brief description of the activities and the results accomplished.

ShakeMap

During the first year of the project it had been installed version 3.1 of the USGS-ShakeMap package (. The package itself generates maps of ground shaking in terms of various peak ground motion (PGM) parameters (PGA, PGV, SA at 0.3, 1.0 and 3.0 s and instrumentally derived intensities). In practice and while grossly simplifying the problem, ShakeMap can be assimilated to

a seismologically based interpolation algorithm that exploits observed ground motion data and seismological knowledge to determine maps of ground motion at local and regional scales. Thus and in addition to the data, fundamental ingredients toward obtaining accurate maps are i.) the attenuation relations of ground motion with distance at different periods and for different magnitudes and ii.) realistic descriptions of the amplifications that the local site geology - the site effects – induce on the incoming seismic wavefield. In the current version of the package the generation of the peak ground motion maps relies on regional attenuation laws and on local site amplifications based on the S-wave velocities in the uppermost 30 m (V_{S30}). Thus fidelity to the “true” ground motion depends heavily on the data available and on the attenuation and site corrections imposed.

It is also worthwhile to stress that the scale the shakemap procedure is implemented is of the order of tens to hundreds of kilometers and the overall aim is to provide a fast, first-order assessment of the ground shaking. Clearly, this length scale prevents from resolving local site amplifications unless observed data are available. Thus shakemaps are a useful tool in the first minutes to hours after the earthquake has occurred and its relevance progressively decreases as information about the real damage becomes available.

In the implementation carried out at INGV and to the purpose of near real-time generation of maps (few minutes from earthquake occurrence), the data are mainly provided by the broadband network complemented by strong motion data when available (currently about 60 broadband stations include also strong motion sensors). With regard to the “seismological information” required for proper interpolation, the attenuation laws previously determined by Malagnini and co-authors have been used (*Morasca, et al., 2006; Malagnini, et al., 2002; Malagnini, et al., 2000*; see Fig. 5). For the site correction part, the V_{S30} have been initially taken from the rough classification of the Italian territory in terms of three litho-types – rock, stiff, and soft (1000, 600 and 350 m/s, respectively) and toward the end of the project a more detailed description of V_{S30} based on the geology (1:100,000 maps) and on five different site classification (A=1000, B=600, C=300, D=150 and E=250 m/s) has become available from the activities of Task 5 of the project (Fig. 6)

More technically, the generation shakemaps relies currently on two independent data flux streams. The first which has been used from the very beginning of the project, avails of the Earthworm processing package and of the modules *gmew* and *localmag* – the latter opportunely modified – whereas the second data stream gets the data directly from the event waveform data in SAC format described in the task 1 of this report. For each earthquake shakemaps are determined i.) immediately using the automatic earthworm location (max 4-5 minutes from event occurrence); ii) automatically after manual location revision by the seismologists on duty in the seismic center (max 30 minutes and on average 10 minutes after the event) and iii) manually after re-downloading the SAC data using “ad hoc” procedures independent from the earthworm automatic processing. This redundancy while determine the shakemaps has insured cross-checking between the results and increased reliability for the obtained maps. To this end, we have also installed the module *plotreg* of ShakeMap that plots the actual data versus the regression curves adopted. This latter module is particularly important in that it allows for prompt checking of the PGM data scatter and it helps to identify possible instrumental malfunctioning at a glance. To keep track of the various maps generated, a unique event identification coding has been envisaged and implemented so that it is always possible to maintain a history for each map. Maps are all published on an INGV internal server (wood.int.ingv.it) and the official ones are “pushed” to the publicly accessible server earthquake.rm.ingv.it using a procedure developed during the project (see <http://earthquake.rm.ingv.it/shakemap/shake/index.html> for standard shakemap layout and <http://earthquake.rm.ingv.it/earthquakes.php> for the event layout access).

An example of the shakemap determined for a M3.8 earthquake in northern Italy (near Brescia) is provided in Fig. 7 where it is made use, in addition to the CNT station data, of the strong motion data recorded by the strong motion network of the Milano INGV section. The PGA map shows well the importance of near source data and of possible amplifications induced by the local site geology.

In this particular case the map has been processed off-line to include the additional data provided by the Milano section.

In order to verify the performance of the shakemap package for a large earthquake, we have used strong motion data available at the Internet-Site for European Strong-Motion Data (ISESD, *Ambraseys et al., 2004*) and determined shakemaps for the Friuli, 1976 main shock, the Colfiorito September 26 (M5.7 and M5.9) events and the Irpinia-Vulture M6.9 (11/23/1980). Here, for conciseness, we show the shakemaps obtained for the Irpinia earthquake in Fig. 8 in terms of PGA, PGV, SA at 0.3 and 1.0 s and as instrumentally derived intensity compared to the reported macroseismic field (Fig. 9). In describing the results it is important to note that i.) the event featured multiple rupture along different parts of the fault (i.e., roughly at 0, 20 and 40 s from origin time) which individually were never larger of an equivalent M6.6 earthquake, and ii) the attenuation relations currently implemented do not account for the finite source. These factors on one side contribute to make the largest accelerations never larger than those expected for each single event (i.e., the largest acceleration of 0.32 g was recorded at Sturmo, STR) resulting in instrumental intensities that are somewhat lower than those expected for a M6.9 rupturing at once. On the other, we note that, regardless of the assumption made on the point source attenuation laws employed, the finiteness of the fault is nevertheless well represented because the PGM recorded at the stations permit a reasonable reconstruction of the observed ground motion accounting themselves for the finiteness of the fault. In future developments, it is thought that adoption of other intensities scales (e.g., Arias intensity captures the potential destructiveness of an earthquake as the integral of the square of the acceleration-time history) that take into account also the source duration could be employed to generate more engineering oriented maps of ground motion. In any event, comparison with the macroseismic intensities (Fig. 9) provided by the Database of Macroseismic Information (<http://emidius.mi.ingv.it/DBMI04/>) although plotted using different intensity scales (MCS versus MII) do not differ significantly indicating an overall agreement between the observed intensities and those potentially available within few minutes from the earthquake. This is eventually the final goal of the shakemap approach toward fast earthquake shaking assessment.

Early Warning.

Real-time determination of earthquake location and size is a big challenge for immediate shutdown of, for example, high risk manufactories (chemical plants), high velocity trains, and, in general, anything that, as result of the strong ground motion shaking, can become particularly harmful to people and the environment. During the course of the project it has been implemented the software ElarmS proposed by *Allen and Kanamori (2003)* to determine within few seconds earthquake location and magnitude. The procedure as implemented at INGV (*Olivieri et al., submitted for publication*) relies on some of real-time modules of the earthworm package and, for testing purposes, it is triggered 10 minutes after the earthquake has occurred. ElarmS is capable to provide first locations (and magnitudes) after the 4th station has detected the first P-wave arrival time. In Figure 10, we show the detection capabilities of the Italian network applied to the set of M>5 earthquakes that have occurred in Italy since 1900. The gray scale indicates the distance (km) to the 4th station detecting the P-waves. In its current station configuration and assuming $V_p \approx 6.0$ and no data transmission delays, the figure shows it possible to provide early warning estimates ranging from less than 4 s along most of peninsular Italy to several seconds in northern Italy (NE-Italy and in parts of Lombardy and Piedmont). The plot shows, for example, that early warning for the Irpinia region could be done in a matter of a few seconds whereas for the Friuli area more than 16 s would be necessary to provide a first location. This result stresses the importance of real-time data exchange among different networks and institutions.

Non-linear Earthquake location

It has been implemented the software NonLinLoc (*Lomax, et al., 2000; Lomax, et al., 2001; Lomax, 2005; <http://www.alomax.net/nlloc>*; NLL hereafter) and the Java visualization applet

SeismicityViewer. NLL is run automatically using the phases of the earthquakes detected by the INGV automatic systems implemented on the servers tokyo and kyoto operating in the seismic center. In addition, a new *earthworm* module, *nll_mgr*, has been developed that uses NLL as standard location program replacing *hypoinverse* which is distributed with *earthworm*. NLL adopts the “Equal Differential Time” misfit function which is particularly robust in presence of data outliers (*Lomax et al., submitted for publication*). An example of NLL earthquake determination is provided in Fig. 11 which shows the event off the coast of Sardinia.

Energy-Duration Magnitude

It has been developed a new magnitude scale denominated M_{ED} (energy-duration magnitude; *Lomax et al., in press*). This magnitude scale avails of estimates of short-period (1 Hz) duration and of seismic energy estimates determined between the arrival of P- and S-waves at teleseismic distances larger than 30° . It has been found that M_{ED} is particularly accurate for earthquakes $M > 7.5$ and, through the determination of the energy-to-moment ratio it is capable to indicate the tsunamigenic potential of a given earthquake. Noticeably, M_{ED} has shown to provide a magnitude of 9.2 for the great Sumatra earthquake (12/26/2004) less than 20 minutes earthquake occurrence. This magnitude estimate was estimated several months later using the Earth’s free oscillations whereas it is well known that only after several hours after the earthquake the magnitude was upgraded to M9 giving the true dimension of the catastrophe. Similarly, after the 2006 July 17, Java earthquake, the initial magnitude was $M=7.2$ (17 min after OT), the CMT magnitude, available about 1 hr after OT, was $M_{CMT}=7.7$; the energy-duration results for this event give $M_{ED}=7.8$, with a very long source duration of about 160 s, and a very low of the energy-to-moment ratio, indicating a possible tsunami earthquake. This estimate would have been possible within 17 minutes. In Figure 12, we show the comparison between the values of M_{ED} and those of M_{CMT} .

Moment Tensor

During these two years we have developed an automatic moment tensor procedure capable of releasing, once the H24 INGV seismic center has located $M_I \geq 3.5$ earthquakes, moment tensor solutions within about 5 minutes (*Scognamiglio et al., submitted for publication*).

Real-Time Automatic Algorithm Design (AUTO-TDMT) and Reviewed MT solution (REV-TDMT)

Moment tensor solution are computed for Italian earthquakes using data from the high quality INGV and MedNet regional broadband network, using the complete waveform inversion methodology, originally proposed by *Dreger and Helmberger (1993)* and later implemented by *Dreger (2003)*. The algorithm inverts complete, three-component broadband displacement waveforms to estimate the point-source solution, while does not solve for the isotropic component that is constrained to zero. The goodness of the solution is determined comparing synthetics with the observed data, and is measured through the variance reduction parameter (VR).

The AUTO-TDMT computation technique is triggered by a UNIX *crontab* command, which checks every 2 minutes for a new $M_I \geq 3.5$ earthquake. The procedure starts by downloading the velocity waveforms from all the stations having recorded the event, within 300 km of epicentral distance. If the magnitude is higher that $M_I=5.0$, the distance range is extended to 500km.

Data are corrected for the instrument response, integrated to obtain displacement, and band-pass filtered in the frequency band 0.02-0.05 Hz for events with $M_I \geq 3.8$, and in the 0.02-0.1 Hz range, for events with magnitude smaller than 3.8. The AUTO-TDMT procedure selects the optimal station set to apply the moment tensor inversion. This procedure takes into account the signal to noise ratios of the data, and the stations distribution relative to the event location and magnitude.

To investigate the dependence of the solution on depth, the procedure repeats the inversion for several point-source depths. Among all the moment tensor solutions obtained for all the explored depths, the procedure chooses those with the largest overall variance reduction.

The AUTO-TDMT procedure determines earthquake focal mechanism, moment magnitude, percentage of double couple, preferred depth, and the solution quality value. The quality parameter (A to D with A best) depends on the number of the stations used, the azimuthal coverage, and the variance reduction.

All the moment tensor solutions with at least quality C are automatically published on the web-page <http://earthquake.rm.ingv.it>.

A seismologist subsequently reviews all the moment tensor solutions. Reviewing solutions implies the proper knowledge of how the inversion code, and the automatic procedure work. To make the revision procedure easier and accessible, we have developed a web-interface. This interface is actually under test.

An Example of Moment Tensor Determination

We show an example of how the AUTO-TDMT procedure worked for a small Apennine earthquake, the 2007 March 29, $M_I = 3.9$ Monti Sibillini Earthquake.

The event has been recorded by 61 broadband stations within the distance range of 28-297 km. The results of the AUTO-TDMT are shown in Figure 13. Panel a.) is the moment tensor solution, while panel b.) shows focal mechanisms and the associated variance reductions for each inverted centroid depth. The quality of this solution is C.

Overall, this is a quite good automatic solution. It gives us a reasonable moment magnitude, a fair fit at 3 of the 7 inverted stations, a centroid depth consistent with the earthquake location given by the seismic center (lat 42.83°N, lon 13.21°E, depth 5.7 km). To improve the quality of the solution and the DC component we have replaced 3 stations with other stations of the correspondent sector and we have adjusted the *zcor* parameter, in particular for MAON. All these steps result in a better seismograms fit. In this example, the final depth is that one already selected by the AUTO-TDMT because it gives the better result.

The REV-TDMT has Quality A and $M_w = 3.9$ (fig. 2). The inferred moment tensor solution is consistent with the kinematic of the region.

Quick Regional Centroid Moment Tensor

During the second year of the project, we have inserted in the project web portal the moment tensor solutions obtained by Pondrelli and co-authors using the Regional Centroid Moment Tensor technique. This method is based on the inversion of surface waves of intermediate period - 35 s – recorded at regional distance. We compute Regional Centroid Moment Tensors (RCMT) routinely since 1997 for intermediate- magnitude earthquakes (about $4.5 < M < 5.5$) occurring in the Euro-Mediterranean region, and we maintain a catalog of solutions (Pondrelli et al., 2002, 2004, 2006; <http://www.ingv.it/seismoglo/RCMT/>). Our catalog occasionally also lists events with magnitudes as low as 4.0, obtainable when the station distribution is particularly favorable.

The surface wave Quick Regional Centroid Moment Tensor calculation is fast, allowing rapid determination of source mechanisms, a feature of great importance for scientific and relief operations following an earthquake (Ekström et al., GRL, 1998) . We compute QRCMTs since 2000 (Morelli et al., Orfeus Newsletter, 2000; http://mednet.rm.ingv.it/quick_rcmt.php) and the increase of availability of on-line seismographic data helped to get a faster computation and to lower the magnitude threshold. We started with the QRCMT determination of event with a magnitude close to 5.0 using the data from 3 to 5 stations, while now we obtain the source parameters also for earthquakes with $M \leq 4.5$ using data from 5 to 10 stations. For the fast determination, we presently rely mainly on seismograms recorded by MedNet (Mediterranean Network) stations.

Kinematic inversion on finite fault

During the two years of the project, we have implemented and tested the kinematic inversion procedure on finite fault proposed by *Dreger and Kaverina (2000)*. The procedure uses mainly broadband and strong motion waveforms, but it can invert also for GPS and InSar data.

This procedure is able to rapidly determine earthquake source parameters (slip distribution, rise time, rupture velocity) through a non-negative least squares solver. The inverse problem is simplified considering only source models with constant rise time and constant rupture velocity on the fault plane. To resolve the fault plane ambiguity, the procedure inverts the data testing the two possible fault planes given by the moment tensor inversion.

The hypocenter location and moment magnitude are given by moment tensor inversion (see previous section).

The fault dimension are assumed 20% larger than those inferred by the empirical relationships of *Wells and Coppersmith (1994)* for the corresponding magnitude, allowing the rupture to be unilateral and bilateral. The rise time is set through the *Somerville et al. (1999)* empirical relationship.

Once the fault dimension and rise time are fixed, the inversion is performed for both planes over a range of constant rupture velocities: the best rupture velocity for each plane is that which gives maximum variance reduction (*Dreger and Kaverina, 2000*). Moreover, the variance reduction values allow for the determination of the causative fault plane. Obviously this distinction is unnecessary when the causative active fault is well constrained by other data.

The frequency band used for the inversion depends on the hypocenter-station distances: it is usually assumed 0.1-1 Hz frequency band for set of data at distances around 50-100 km while lower frequency bands are used for larger distances (100-400 km). The minimum magnitude to apply this procedure is approximately $M_w \sim 5.5$. The Green's functions have been computed using a frequency-wavenumber approach developed by *Saikia (1994)*. We have collected a precompiled catalog of Green's function for different velocity models.

We are finishing to implement a short procedure, triggered by the AUTO-TDMT procedure (see above) that, when an earthquake with $M_l > 5.5$ occurs, sets up directories and files to be used for the finite fault inversion.

The procedure has been tested for three real events: 2000, Western Tottori earthquake; $M_w = 5.6$; 2002 Greece earthquake; $M_w = 5.7$; 1980 Irpinia earthquake, $M_w = 6.9$. 2000, Western Tottori, $M_w = 5.6$

2000, October 6, Western Tottori earthquake, $M_w = 6.7$

The 2000 Western Tottori earthquake has been recorded by a large number of strong motion data. The frequency band used for the inversion is 0.15-0.7 Hz, because all the stations are closer than 80 km. The velocity structure is that one given by the Disaster Prevention Research Institute, Kyoto.

We tested rupture velocities between 1.5 and 3 km/s for both planes.

The best solution is for the plane1 (left panel of Figure 14a), that is identified, from the literature, as the causative fault plane. The best slip distribution and rupture velocity ($V_r = 1.6$ km/s) of plane1 are very similar to the source model parameters inferred by *Piatanesi et al. (2007)*.

2002, May 21, Greece, $M_l = 5.1$

This regional event has been recorded by several digital broadband stations of the new seismic network operated in Greece by the National Observatory of Athens (NOA). All these stations have hypocentral distances larger than 100km. The source model has been inverted for 0.05-0.3 Hz frequency band. The velocity structure used to compute the Green's function is given by NOA.

The best inverted source models for both of the planes show a circular slip distribution smeared out around the hypocenter (see Figure 14b). Besides, the best variance reduction of the two planes is very similar. All these factors indicate that for this event is not possible to distinguish between the two planes.

1980, Irpinia earthquake, Mw=6.9

The 1980 Irpinia Earthquake is one of the most important historical Italian earthquakes. It is a complex event that involves at least three distinct ruptures starting in a time span lasting approximately 40 sec. The main event (0s) was followed by a rupture episode after about 20s and one after 40s. We tried to infer the source model of the 0sec event. The quality of the accelerometric stations prevent us to obtain a stable and well constrained inversion. The main problem is the lack of absolute timing on the accelerograms. We associated to the data the same triggering time given by *Cocco and Pacor (1993)*.

We used for the inversion only Bagnoli (BGIA), Sturno (STRA) and Calitri (CLTA) stations, being aware of the strong site amplification effects at high frequency on some stations (*Rovelli et al. 1988*).

Figure 14c shows the comparison between data and synthetics for the well known causative fault plane (str,dip,rake)=(315°,60, -90) (*Bernard and Zollo, 1989*): yellow panels indicate the inverted records, while the other panels indicate stations with zero weight during the inversion (i.e. not inverted stations).

Web portal

The web portal has been developed to include the main results of the analysis described above. In its current form, published on <http://earthquake.rm.ingv.it>, it is possible to access most of the results of the analysis obtained in the project.

To this end, there have been written several *bash* scripts which are triggered by the unix crontab command which checks for new locations provided by the seismic center. For each event, the following products are determined in near real-time:

- epicentral map with the stations used for the location;
- map of the catalogued epicenters and centroid moment tensors;
- web publication of the Time Domain Moment Tensor (TDMT) and of the Quick Regional Centroid Moment Tensor (QRCMT) if available;
- web publication of the PGA and PGV ShakeMap;
- availability of the *shape file* of the shakemap for ground motion representation using GIS;
- availability of the tar archive file of the SAC event waveforms;
- parse the information provided by the seismic center and from the CNT data-base (DB) to 'retrieve' the information about the earthquake and publish it.

All this information is inserted within a unique event directory and a DB is populated. This DB is also accessed by GoogleMap for additional plotting or for information retrieval.

In the web portal are also inserted the reviewed TDMT and QRCMT solutions and the procedure has been designed to contemplate possible updates of the products presented above up to one week after the event (e.g., revised locations, shakemaps).

In Fig. 15, some screen-shots of the developed web portal are shown.

Space-temporal seismic hazard

The algorithm developed during the project provides the users with quantitative estimates of the probability of occurrence of new earthquakes on specific areas of the target territory. The algorithm avails of the earthquake data detected by the Italian National seismic network. The software adopted for the estimation of the space-temporal seismic hazard is based on epidemic models of the ETAS type (*Epidemic Type Aftershock Sequence*) (*Console et al., 2001; 2003; 2005; 2006; 2007*). In epidemic models each event can be either inducing to another earthquake or induced by a previous one. The expected seismicity rate in any particular point of the target area for a given threshold value can be determined through the contribution of all the previous events using a kernel

function that involves: magnitude, distance and time of occurrence of every previous events. The magnitude distribution assumed follows the Gutenberg-Richter law. The parameters used by the software have undergone a first phase of training using the INGV data set so that to obtain a maximum likelihood estimates of the parameters. The time span for training is from July 1987 to December 2005 for $M > 2.0$ earthquakes. It has been used the statistical software ZMAP (Wiemer and Wyss, 1994) used at ETH Zurich to verify the data completeness.

Since January 2006 it has been tested the procedure described above on the server wood dedicated to the project. The goal is to determine the occurrence probability of new medium to large size events detected in real time by the INGV seismic monitoring center. The results are displayed as time-dependent maps showing every 5 minutes both the expected rate density of $M > 4.0$ earthquakes overall Italy, given as events/day/km², and the probability of ground motions larger than 0.01 g in areas of the size of 100 x 100 km in the next 24 hours, around the zone of maximum expected rate density. In order to verify the results of the predictions, it has been used the statistical method ROC (Relative Operative Characteristics) known also as Molchan diagram. This method is also used to assess the meteorological forecasts. In essence it addresses the capability of the model to predict or to generate false alarms. The results obtained in this study show that the ETAS model is capable to obtain predictions some hundreds of times more accurate than a purely random model.

Task 5 – Site effects estimation at the stations and use of GIS for the classification of the Italian territory

A geologic map with soil class differentiation has been elaborated starting from the 1:100,000 Italian geological map (Servizio Geologico Nazionale). Geologic units have been unified in five different classes A, B, C, D and E according to the EuroCode8 previsions, EC8, after Draft 6 of January 2003 on the base of the ground acceleration response. For the classification we have followed lithological and age criteria as in Table 1.

Ground type	Description of stratigraphic profile	Vs ,30 (m/s)
A	<i>Rock or other rock-like geological formation, including at most 5 m of weaker material at the surface</i>	> 800
B	<i>Deposits of very dense sand, gravel, or very stiff clay, at least several tens of m in thickness, characterised by a gradual increase of mechanical properties with depth</i>	360 – 800
C	<i>Deep deposits of dense or mediumdense sand, gravel or stiff clay with thickness from several tens to many hundreds of m</i>	180 – 360
D	<i>Deposits of loose-to-medium cohesionless soil (with or without some soft cohesive layers), or of predominantly soft-to-firm cohesive soil</i>	<180
E	<i>A soil profile consisting of a surface alluvium layer with vs values of type C or D and thickness varying between about 5 m and 20 m, underlain by stiffer material with vs > 800 m/s</i>	-----

Figure 6b shows the resulting Geological-Class Map (GCM). An ASCII file has been elaborated with ArcInfo software; the obtained matrix is represented by velocity values with space interval of 0.016667 degrees for the ShakeMap program. We attributed to the A, B, C, D, E classes velocity values corresponding respectively with 1000, 600, 300, 150 e 250 m/s.

References

- Allen, R. and H. Kanamori (2003). The Potential for Earthquake Early Warning in Southern California, *Science* 2 May 2003: 786 □ DOI: 10.1126/science.1080912
- Ambraseys N.N., Smit, P., Douglas, J., Margaris, B., Sigbjörnsson, R., Ólafsson, S., Suhadolc, P. and G. Costa (2004). Internet site for European strong-motion data, *Boll. Geof. Teor. Appl.*, 45, 3, 113-129.
- Bernard P., and A. Zollo, 1989, The Irpinia (Italy) 1980 earthquake: detailed analysis of a complex normal faulting, *J. Geophys. Res.* 94, 1631-1647.
- Console, R. and M. Murru (2001), A simple and testable model for earthquake clustering, *J. Geophys. Res.*, 106, 8699-8711.
- Console, R., A.M. Lombardi, M. Murru and D. Rhoades (2003), Bath's law and the self-similarity of earthquakes, *J. Geophys. Res.*, 108 (B2), 2128, doi: 10.1029/2001JB001651.
- Console, R., M. Murru, and A.M. Lombardi (2003), Refining earthquake clustering models, *J. Geophys. Res.*, 108, 2468, doi: 10.1029/2002JB002130.
- Console, R., M. Murru, and F. Catalli (2005), Physical and stochastic models of earthquake clustering, *Tectonophysics*, 417, 141-153.
- Console, R., D.A. Rhoades, M. Murru, F.F. Evison, E.E. Papadimitriou and V.G. Karakostas (2006), Comparative performance of time-invariant, long-range and short-range forecasting models on the earthquake catalogue of Greece, *J. Geophys. Res.*, 111, B09304, doi:10.1029/2005JB004113.
- Console, R., M. Murru, F. Catalli, and G. Falcone (2007), Real time forecasts through an earthquake clustering model constrained by the rate-and-state constitutive law: Comparison with a purely stochastic ETAS model, *Seismological Research Letters*, 78, 49-56.
- Cocco, M. and F. Pacor, 1993, The rupture process of the 1980 Irpinia, Italy, earthquake from the inversion of strong motion waveforms, *Tectonophysics*, 218, 157-177.
- Dreger, D. S. (2003). TDMT_INV: time domain seismic moment tensor inversion, *International Handbook of Earthquake and Engineering Seismology*, W.H.K. Lee, H. Kanamori, P.C. Jennings, and C. Kisslinger (Editors), Vol B, 1627 pp.
- Dreger D.S., and Helmberger D.V. (1993). Determination of source parameters at regional distances with 3-component sparse network data, *J. Geophys. Res.*, 98, 8107-8125.
- Dreger D., and Kaverina A., 2000, Seismic remote sensing for the earthquake source process and near-source strong shaking: A case study of the October 16, 1999 Hector mine earthquake, *J. Geophys. Res.*, 27 (13), 1941-1944.
- Lomax A., 2005: A Reanalysis of the hypocentral location and related observations for the great 1906 California Earthquake - *Bull. Seism. Soc. Am.*, 95, 861-877.
- Lomax A., Virieux J., Volant P. e Berge C., 2000: Probabilistic earthquake location in 3D and layered models: Introduction of a Metropolis-Gibbs method and comparison with linear locations - in Thurber C.H. e Rabinowitz N. (eds.): *Advances in seismic event location* - Kluwer, Amsterdam, 101-134.

- Lomax A., Zollo A., Capuano P. e Virieux J., 2001: Precise, absolute earthquake location under Somma-Vesuvius volcano using a new 3D velocity model - *Geophys. J. Int.*, 146, 313-331.
- Morasca , P. , L. Malagnini, A. Akinci, D. Spallarossa, and R.B. Herrmann (2006). Ground-Motion Scaling in the Western Alps, *Journal of Seismology*, Vol. 10, pp. 315-333.
- Malagnini, L., Akinci, A., Herrmann, R. B., Pino, N. A. , and L. Scognamiglio (2002). Characteristics of the ground motion in northeastern Italy. *Bull. Seism. Soc. Am.*, 92, 6, 2186-2204.
- Malagnini, L., Herrmann, R.B., and M. Di Bona., Ground motion scaling in the Apennines (Italy) (2000). *Bull. Seism. Soc. Am.*, 90, 1062-1081.
- Piatanesi A., A. Cirella, P. Spudich and M. Cocco, 2007, A global search for earthquake kinematic rupture history: Application to the 2000 western Tottori, Japan earthquake, *J. Geophys. Res.*, in press.
- Pondrelli, S., A. Morelli, G. Ekström, S. Mazza, E. Boschi, and A. M. Dziewonski, 2002, European-Mediterranean regional centroid-moment tensors: 1997-2000, *Phys. Earth Planet. Int.*, 130, 71-101, 2002
- Pondrelli S., A. Morelli, and G. Ekström, European-Mediterranean Regional Centroid Moment Tensor catalog: solutions for years 2001 and 2002, *Phys. Earth Planet. Int.*, 145, 1-4, 127-147, 2004.
- Pondrelli, S., S. Salimbeni, G. Ekström, A. Morelli, P. Gasperini and G. Vannucci, The Italian CMT dataset from 1977 to the present, *Phys. Earth Planet. Int.*, doi:10.1016/j.pepi.2006.07.008, 159/3-4, pp. 286-303, 2006.
- Rovelli A., O. Bonamassa, M. Cocco, M. Di Bona and S. Mazza, 1988, Scaling laws and spectral parameters of the ground motion in active extensional areas in Italy, *Bull. Seism. Soc. Am.*, 78: 530-560.
- Shapiro N. M., M. Campillo (2004), Emergence of broadband Rayleigh waves from correlations of the ambient seismic noise, *Geophys. Res. Lett.*, 31, L07614, doi:10.1029/2004GL019491.
- Shapiro N. M, Campillo, M., Stehly, L. and M. H. Ritzwoller (2005), High resolution surface wave tomography from ambient seismic noise, *Science*, 307, 1615-1617.
- Somerville, P.G., K. Irikura, R. Graves, S. Sawada, D. Wald, N. Abrahamson, Y. Iwasaki, T. Kagawa, N. Smith, and A. Kowada, Characterizing crustal earthquake slip models for the prediction of strong ground motion, *Seism. Res. Lett.*, 70, 59-80, 1999.
- Wald, D. J., Quitoriano, V., Heaton, T. H., Kanamori, H., Scrivner, C. W., and Worden, C. B., (1999). TriNet "ShakeMaps": Rapid Generation of Peak Ground Motion and Intensity Maps for Earthquakes in Southern California *Earthquake Spectra* 15, 537.
- Wald, D. J., Worden, C. B., Quitoriano, V., and K. L. Pankow (2006). ShakeMap® Manual, technical manual, users guide, and software guide, available at <http://pubs.usgs.gov/tm/2005/12A01/pdf/508TM12-A1.pdf>, 156 pp.
- Wells D.L. and K.J. Coppersmith, 1994, New empirical relationships among magnitude, rupture length, rupture width, rupture area, and surface displacement, *Bull. Seism. Soc. Am.*, 84 (4): 974-1002.
- Wiemer, S., and M. Wyss (1994), seismic quiescence before the Landers (M=7.5) and Big Bear (M=6.5) 1992 earthquakes, *Bull. Seismol. Soc. Am.*, 84, 900-916.
- Zhu, L., H. Kanamori, Moho depth variation in southern California from teleseismic receiver functions, *J. Geophys. Res.*, 105(B2), 2969-2980, 10.1029/1999JB900322, 2000.

2.2 Specific problems which have prevented success

Overall, the work accomplished by the CNT research unit is to be considered successful as nearly all the deliverables promised when the project was approved have been achieved. However and while focusing on the shakemap implementation and the waveform analysis (moment tensor, finite fault inversion), the whole part aimed toward the fast data exchange between networks and institutions – instrumental for obtaining more accurate maps of peak ground motion - cannot be considered fully successful. In fact, we have found very difficult the real-time data exchange. This is particularly true both locally for the networks and the institutions in the north-eastern Italy that, for reasons mainly tied to local policies of the Friuli-Venezia Giulia Civil Protection, had not been allowed to share their data and at the national level with the “Servizio Sismico Nazionale” which similarly and mainly for technical reasons has not been capable to provide the important strong motion data acquired by the “Rete Accelerometrica Nazionale”. These factors have hampered the impact on the national level that the project was supposed to achieve at its completion.

2.3 Relevant publications which have arisen directly from this project

incomplete

JCR publications

Li, H., Michelini, A., Zhu, L., Bernardi, F., and M. Spada (2007). Crustal velocity structure in Italy from Analysis of Regional Seismic waveforms, in press in *Bull. Seism. Soc. Am.* .

Lomax, A., Michelini, A., and A. Piatanesi (2007). An energy duration procedure for rapid determination of earthquake magnitude and tsunamigenic potential, in press in *Geophys. J. Int.* .

Lomax, A., Michelini, A. and A. Curtis. Earthquake location, Nonlinear, submitted to the Springer *Encyclopedia of Complexity and Systems Science*.

Olivieri M., R. M. Allen, G. Wurman. The potential for Earthquake Early Warning in Italy using ElarmS, submitted to BSSA.

Scognamiglio L., E. Tinti, and A. Michelini. Real-Time Regional Moment Tensor Estimation Using the Italian Broadband Network, submitted BSSA, July 2007.

Piana Agostinetti et al, 2007, in preparation.

Steckler et al, 2007, submitted to Geology.

Not JCR publications

Abstracts

Olivieri, M., Michelini, A., Lomax, A. (2007). New robust automatic earthquake locations for the Italian Region, EGU2007-A-05106 Abstract 2007 EGU General Assembly, Vienna 15-20 April, 2007.

Lomax, A., Michelini, A., and A. Piatanesi (2007). Rapid, energy-duration estimates of seismic moment and implications for rupture scaling and dynamics, EGU2007-A-06885 Abstract 2007 EGU General Assembly, Vienna 15-20 April, 2007.

Michelini, A., Malagnini, L., Worden, B. C., D. J. Wald and the S4 Team (2007). Near real-time shakemaps in Italy, EGU2007-A-07774 Abstract 2007 EGU General Assembly, Vienna 15-20 April, 2007.

Scognamiglio, L.; Tinti, E.; Lauciani, V.; Quintiliani, M.; Michelini, A.; Malagnini, L.; Dreger, D. (2007). Near real-time regional moment tensor estimation using Italian broadband stations, EGU2007-A-09654 Abstract 2007 EGU General Assembly, Vienna 15-20 April, 2007.

Michelini, A., and the S4 Team (2007). Earthworm and ShakeMap developments at INGV, invited presentation at the NERIES-ORFEUS Observatory Meeting, Sinaia (Romania) 6-10 May, 2007.

Figures

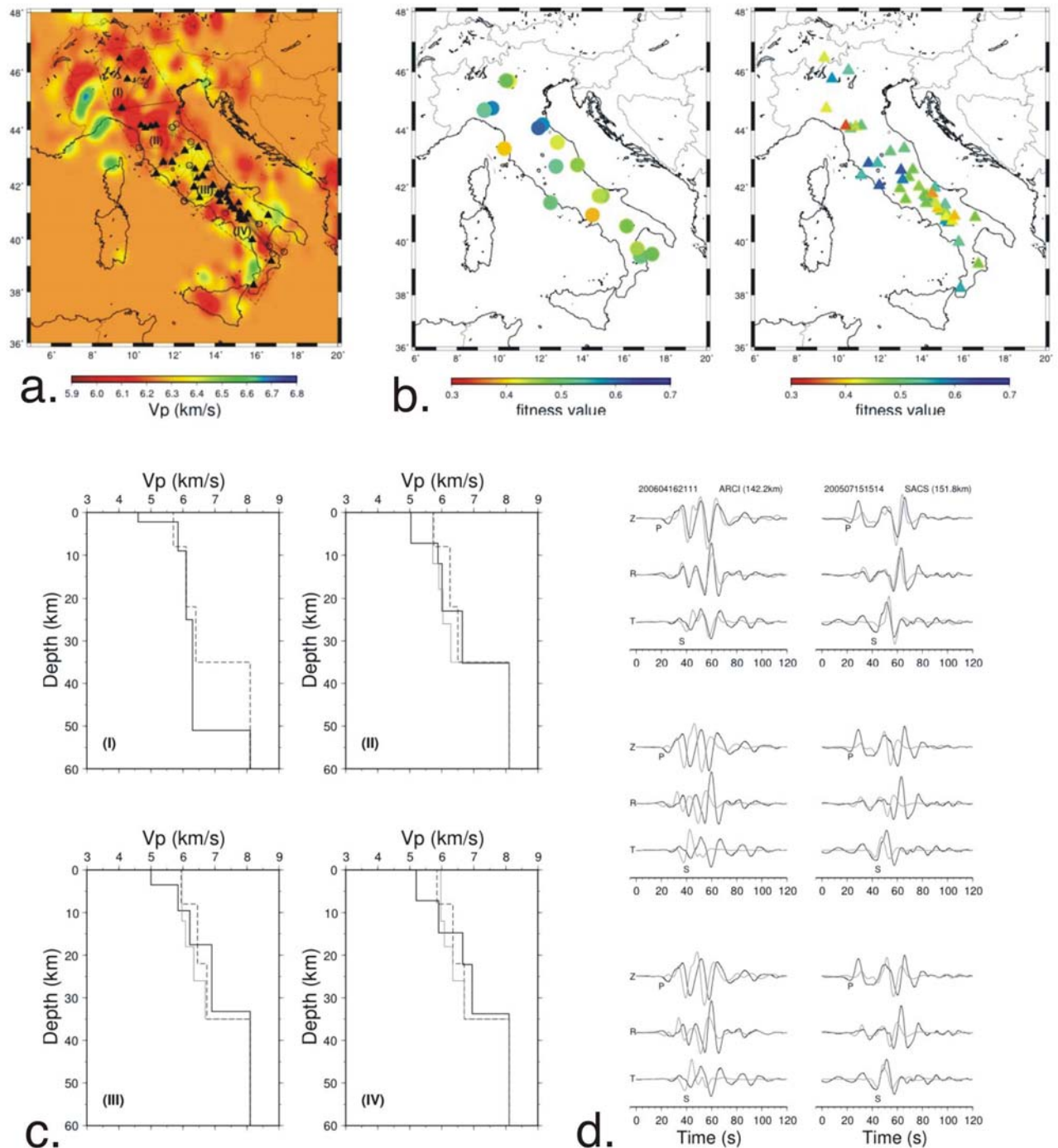


Figure 1. Results of the regionalization in laterally homogeneous velocity structures of the Italian peninsula. a.) Polygonal areas and paths used to determine the velocity models; b.) Fitness values calculated from the velocity models (P) determined in this study for all events (left) and stations (right) used in the Genetic Algorithm (GA) inversions. c.) 1-D velocity models obtained from the GA for the four regions (solid line) plotted together with previously proposed models. d.) Comparison of synthetic waveforms with observation for Region (II), the northern Apennines. Top: Comparison of synthetic waveforms from the best-fit velocity model obtained in this study (gray) with observed waveforms (black). Middle: Comparison of synthetic waveforms from the velocity model averaged from recent P-wave tomography results (gray) with observed waveforms (black). Bottom: Comparison of synthetic waveforms from the minimum 1D velocity model from Chiarabba and Frepoli (1997) (gray) with observed waveforms (black).

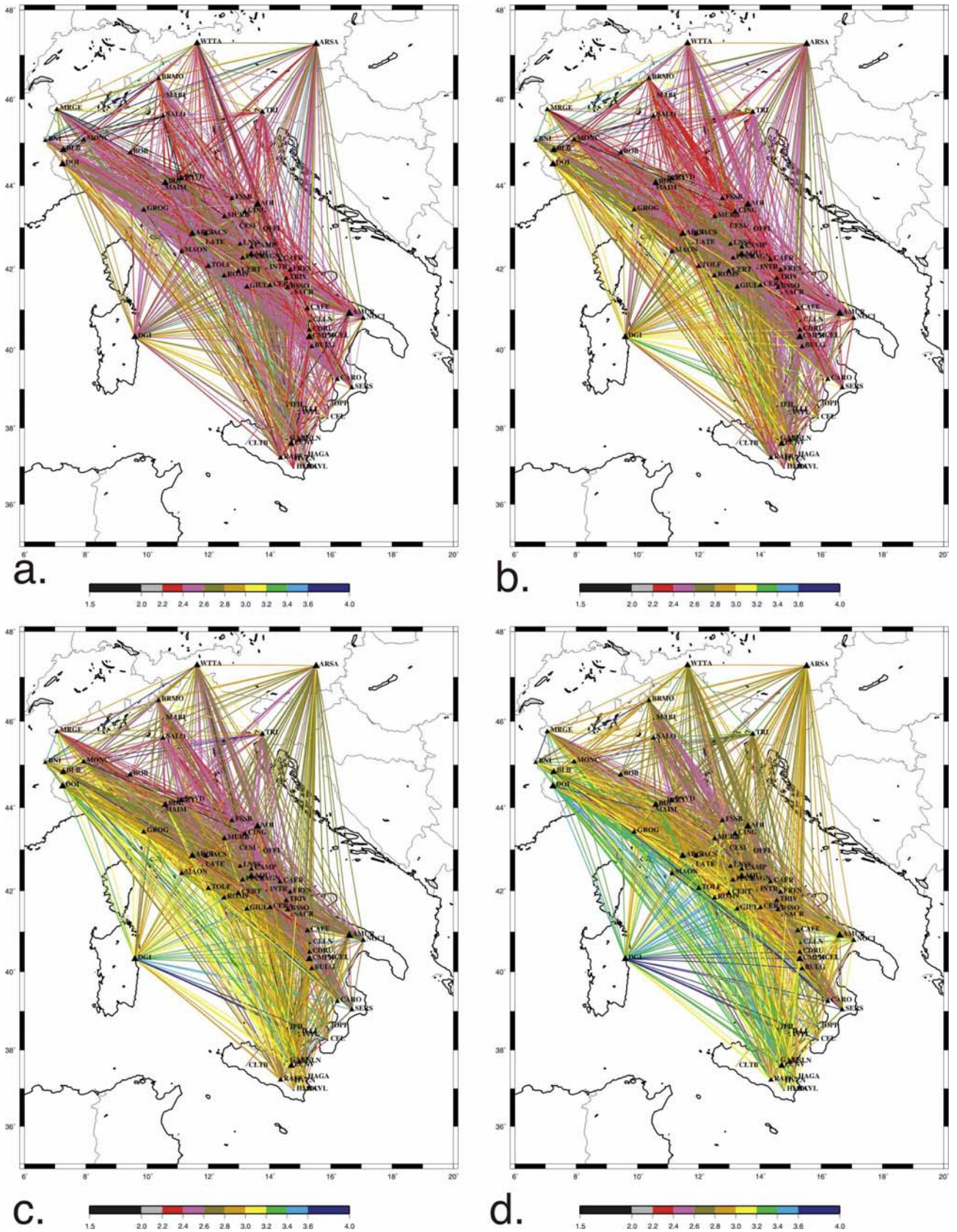
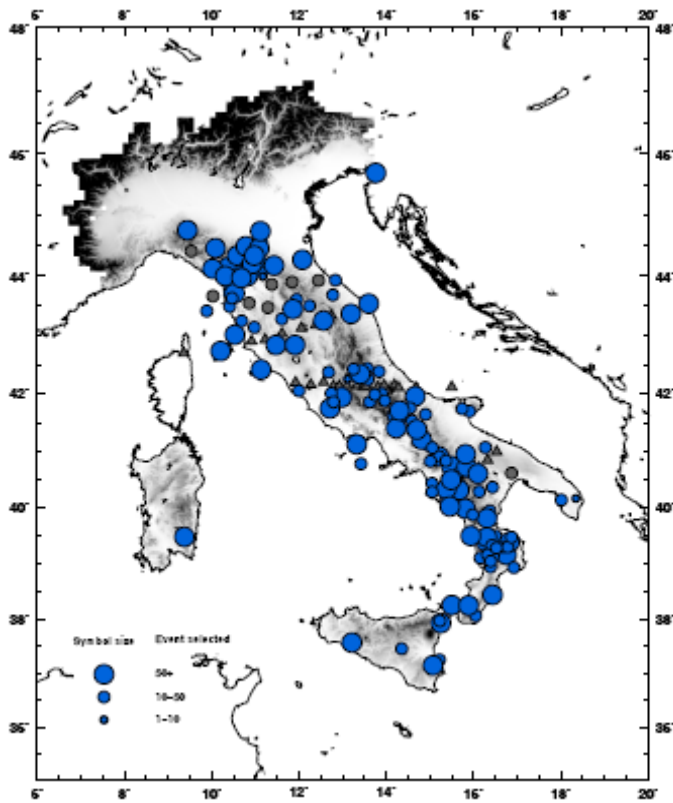
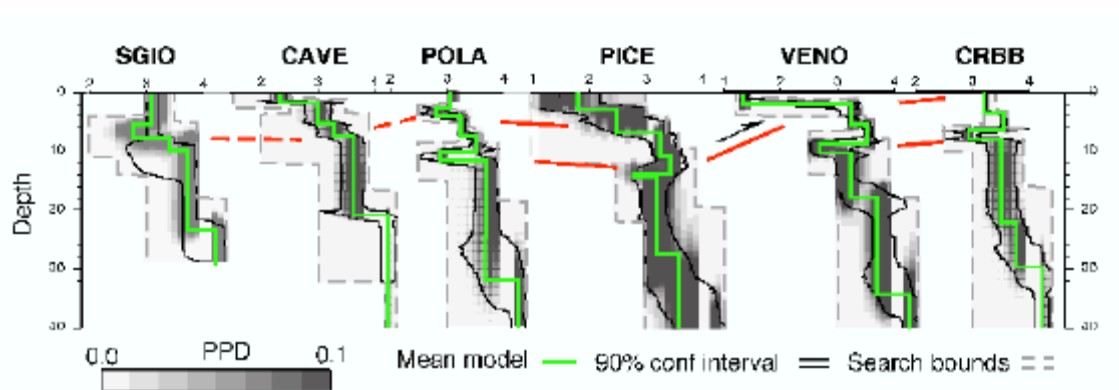


Figure 2. Average Rayleigh wave group velocities at different periods between the station pairs used in the ambient noise cross-correlation analysis. a) 10.2 s; b) 14.6 s; c.) 20.5 s and d.) 24.9 s. Note the clear distinction between paths within the Tyrrhenian basin and those along the Apennines. As expected, faster velocities occur for longer period waves.

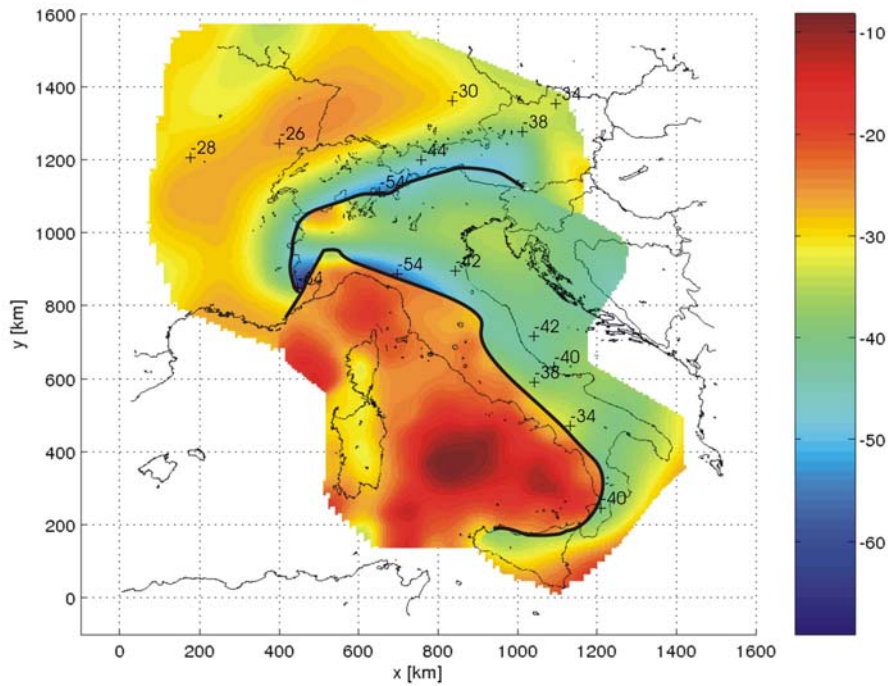


a.)

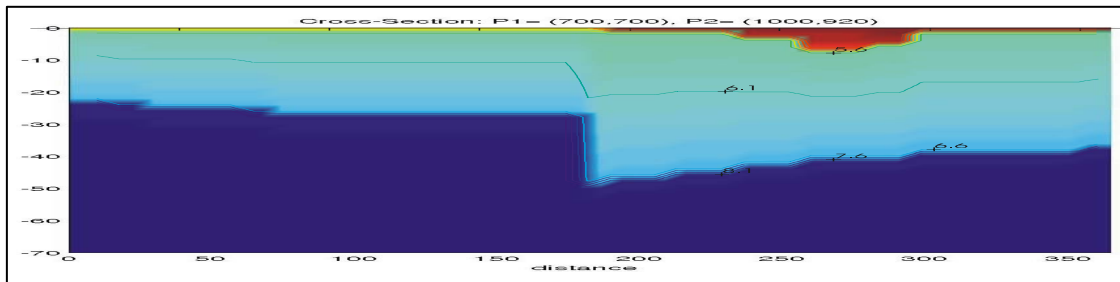


b.)

Figure 3. a.) Map showing the seismic stations selected for the RF study. The circle dimension scales with the number of data available for each station. The triangles are selected stations from temporary experiments. b.) Example showing a profile of 1D Vs models across the southern Apennines.

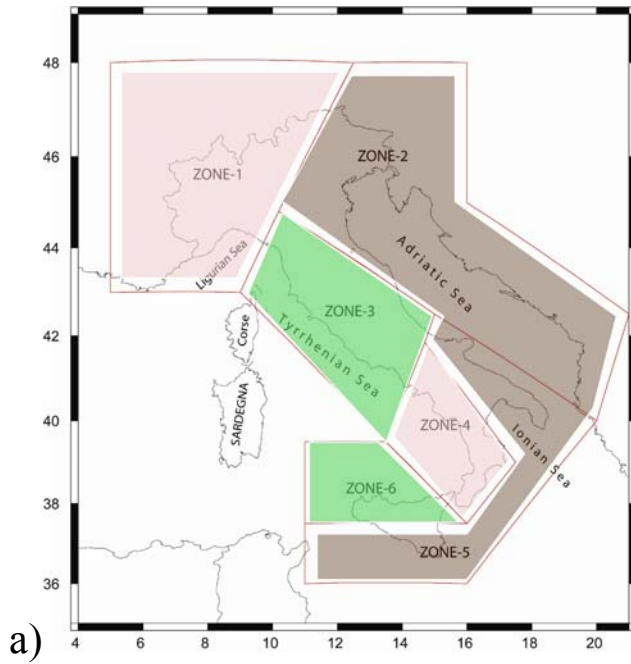


a.)

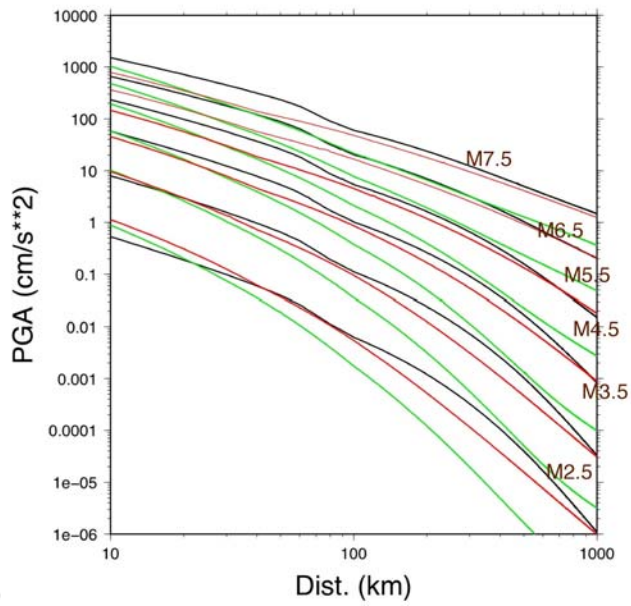


b.)

Figure 4. a.) The Moho depth underneath Italy. b) Example of the 3D P-wave velocity model, including the Moho discontinuity, along a SW-NE vertical section from Elba Island to the Adriatic Sea.

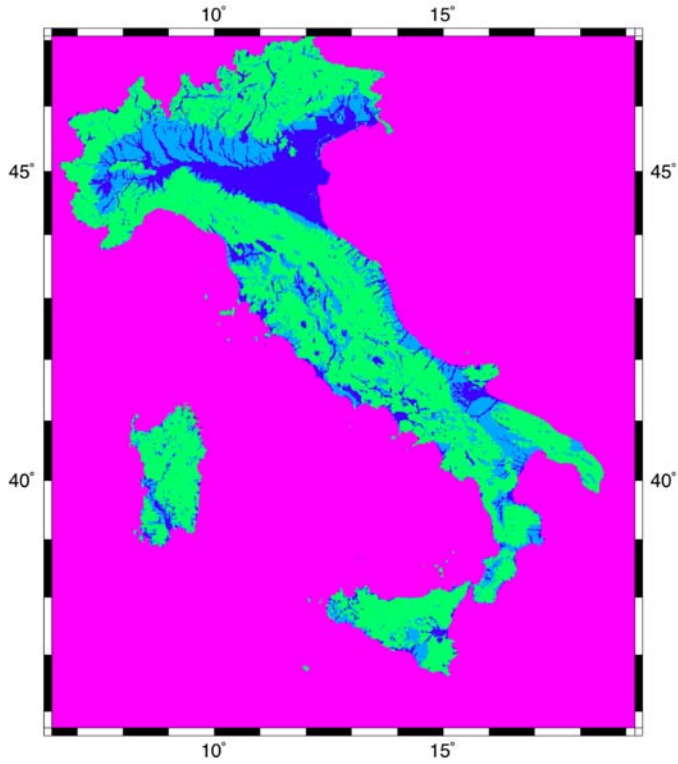


a)

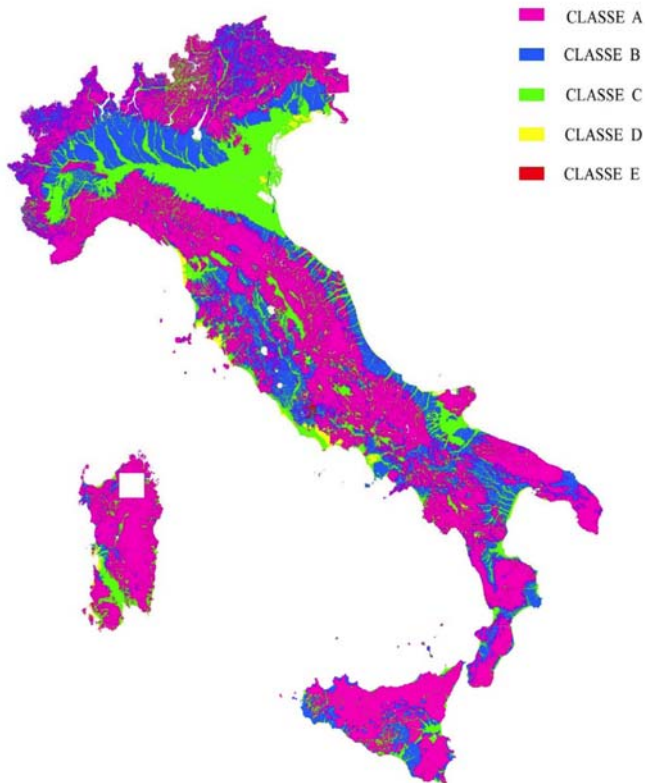


b.)

Figure 5. Attenuation relations used in the implementation of ShakeMap at INGV. a.) Regionalization of the attenuation relations. b) attenuation relations expressed as PGA.

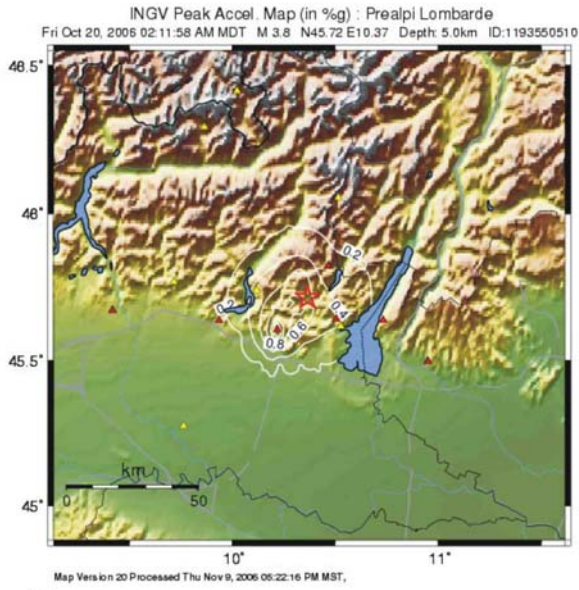


a.)

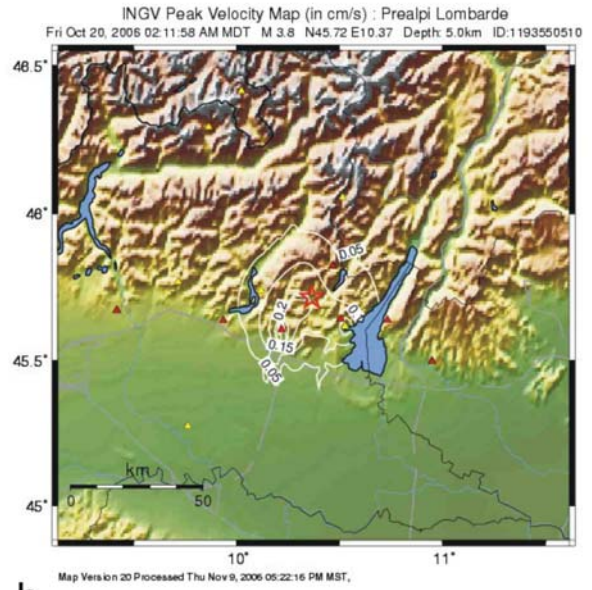


b.)

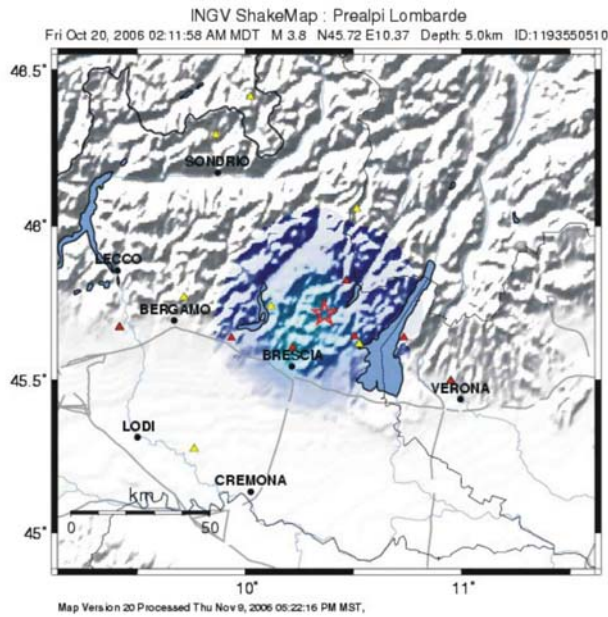
Figure 6. V_{S30} site classification. a.) preliminary site classification with velocities subdivided into three groups (rock=1000, stiff = 700 and soft = 350 m/s). b.) final site classification based on geology and compliant with the EuroCode8 (A=1000, B=600, C=300, D=150 and E=250 m/s).



a.

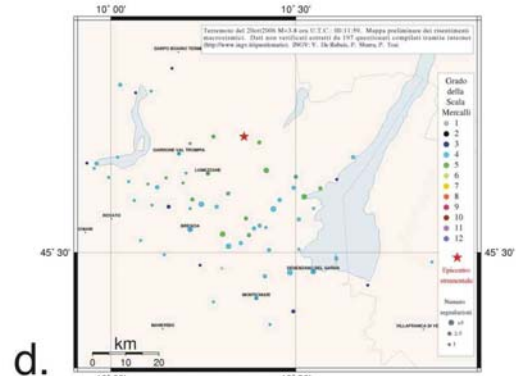


b.

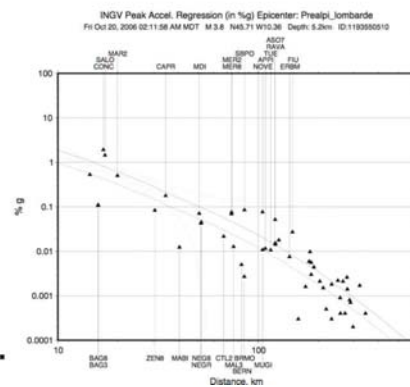


c.

PERCEIVED SHAKING	Not felt	Weak	Light	Moderate	Strong	Very strong	Severe	Violent	Extreme
POTENTIAL DAMAGE	none	none	none	Very light	Light	Moderate	Moderate/Heavy	Heavy	Very Heavy
PEAK ACC (%g)	<.17	.17-1.4	1.4-3.9	3.9-9.2	9.2-18	18-34	34-65	65-124	>124
PEAK VEL (cm/s)	<0.1	0.1-1.1	1.1-3.4	3.4-8.1	8.1-18	18-31	31-60	60-116	>116
THEYMETEORICAL INTENSITY	I	II-III	IV	V	VI	VII	VIII	IX	X+

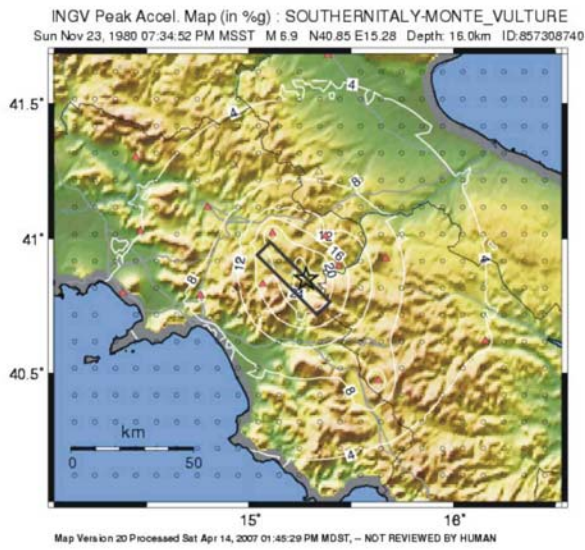


d.

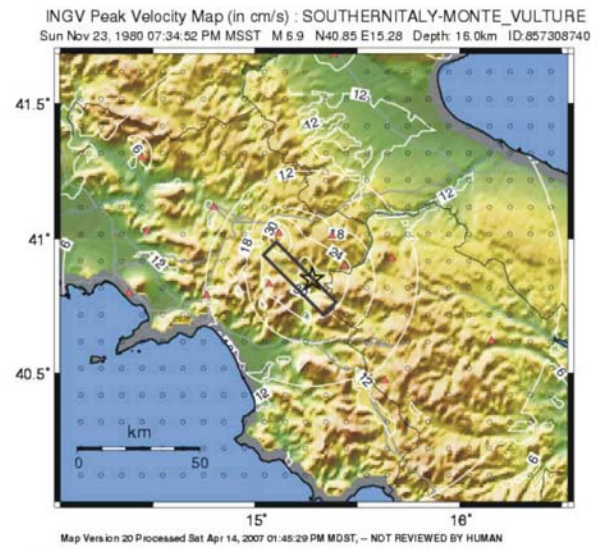


e.

Figure 7. Shakemaps and macroseismic intensity maps determined for the October 20, 2006, M3.8 earthquake that occurred near Brescia (Northern Italy). a.) PGA; b.) PGV; c.) MII. d.) macroseismic intensity determined from web questionnaire. e.) plot generated with *plotreg* where The red solid curve indicates the PGA attenuation for a M3.8 earthquake whereas the green one is adjusted for the “bias” depending on the actual observed data.



a.

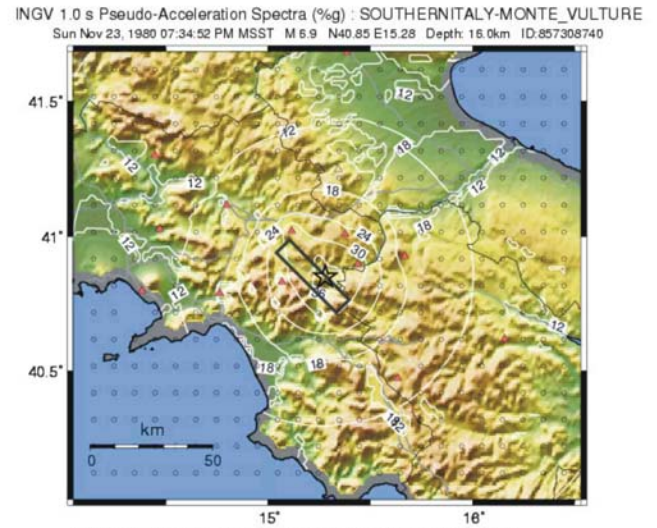


b.



c.

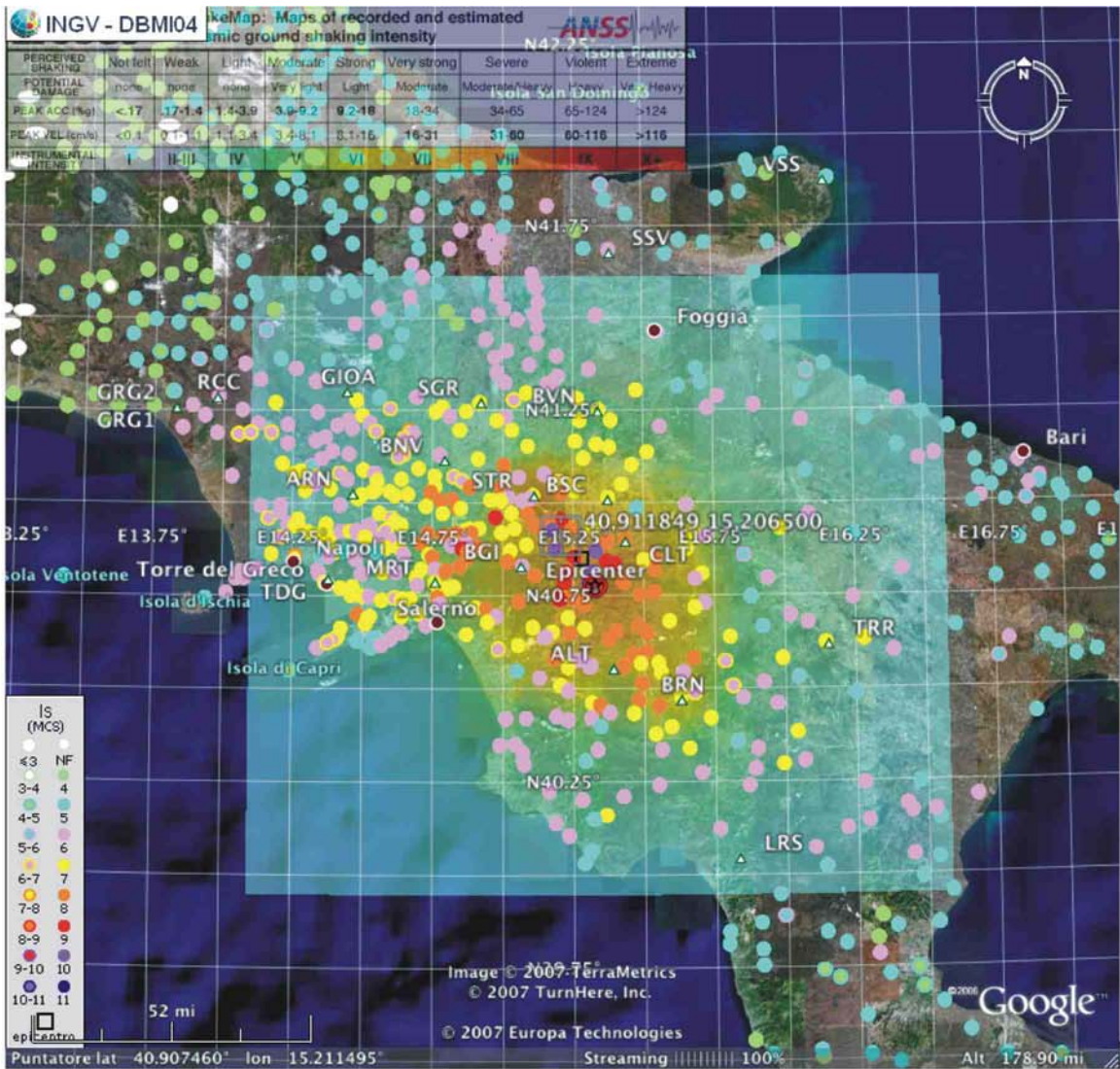
NOTE: These are automated maps based on instrumental response spectra, and may not be appropriate for comparison with design spectral values.



d.

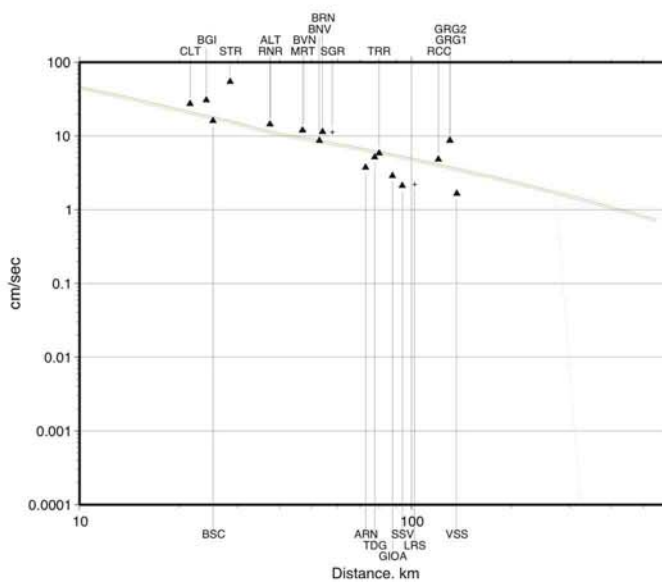
NOTE: These are automated maps based on instrumental response spectra, and may not be appropriate for comparison with design spectral values.

Figure 8. Shakemaps for the November, 23, 1980, Irpinia-Vulture earthquake M6.9. a.) PGA; b.) PGV; c.) Spectral acceleration 5% damping at 0.3 s period; d.) Spectral acceleration 5% damping at 1.0 s period;



a.

INGV Peak Velocity Regression (in cm/s) Epicenter: SOUTHERNITALY-MONTE_VULTURE
Sun Nov 23, 1980 07:34:52 PM MSST M 6.9 N40.85 W15.28 Depth: 16.0km ID:857308740



b.

Figure 9. a.) Comparison between instrumental and macroseismic intensities. b.) plot generated with *plotreg* to show the fit of the PGV data to the regression relation adopted.

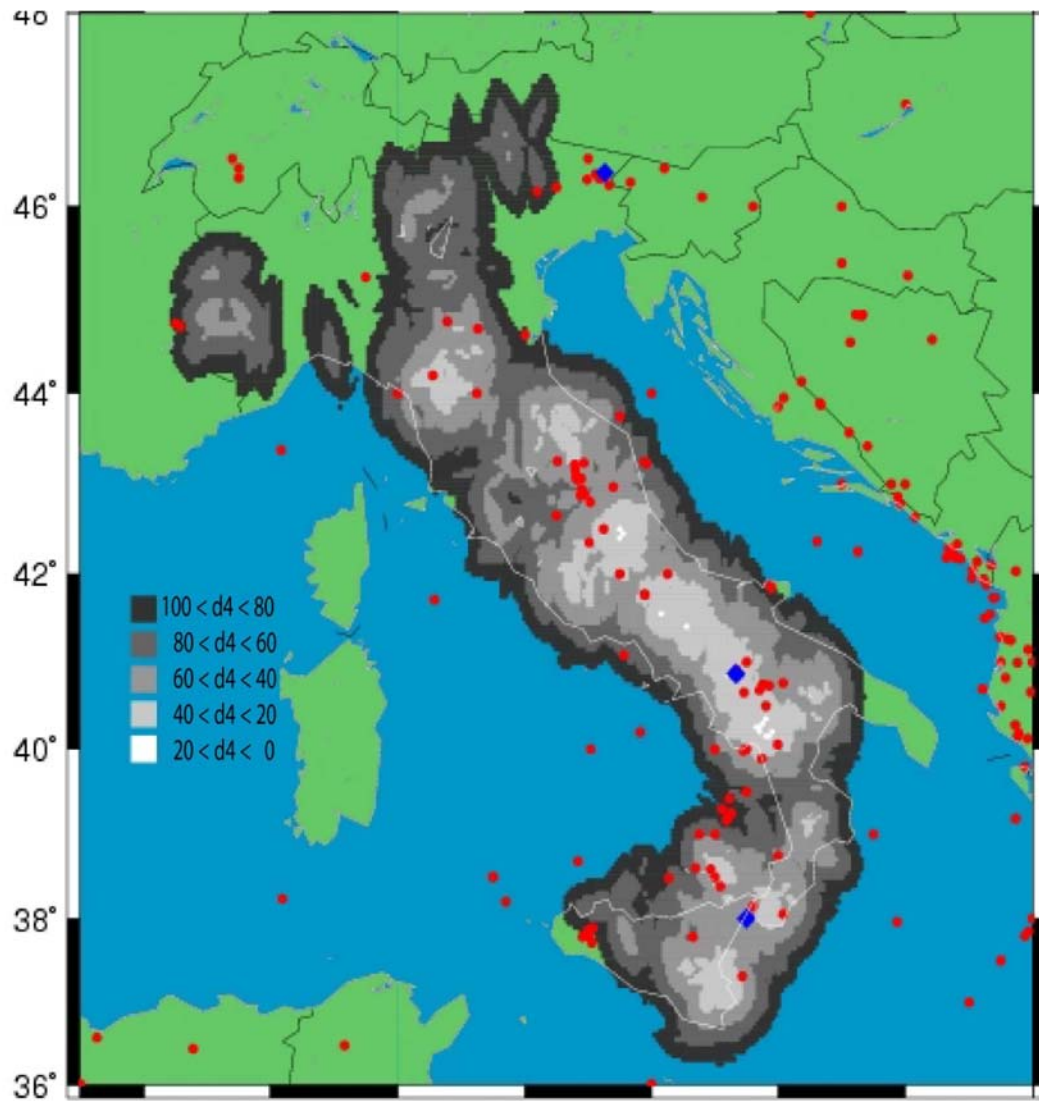
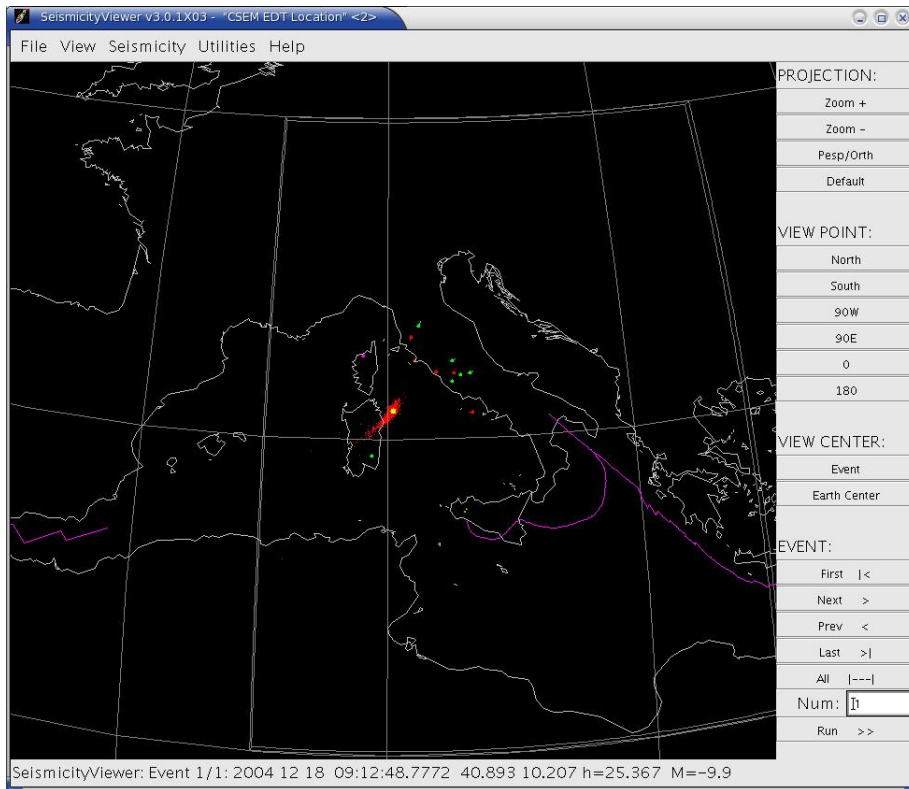
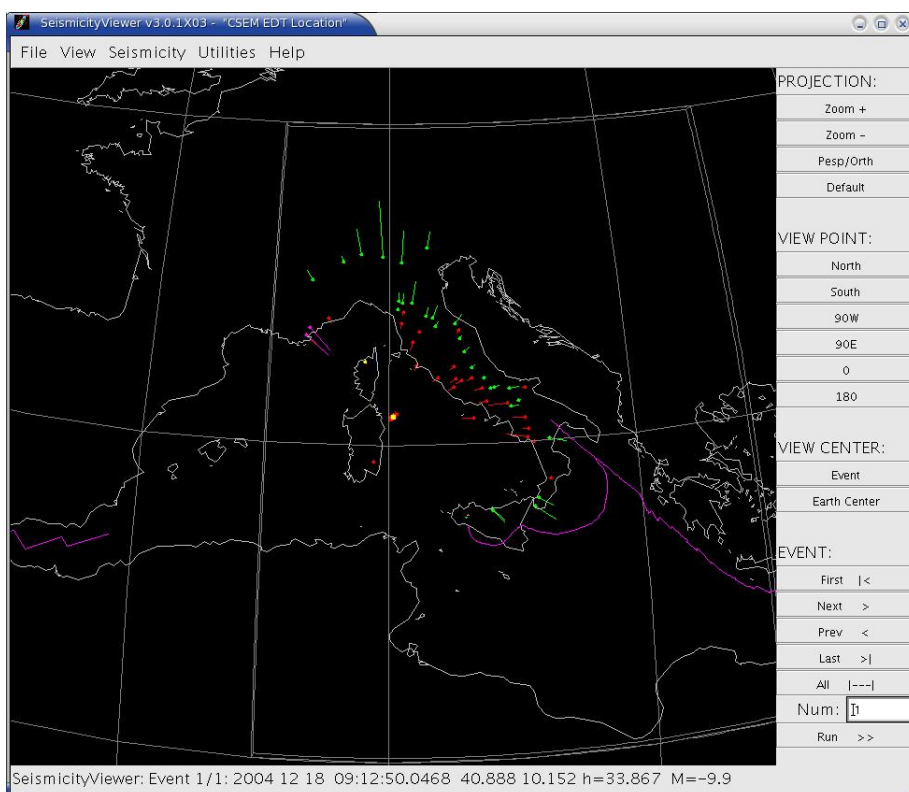


Figure 10. Map of the Italian territory showing the potential for early warning using ElarmS. White and light grey color areas indicate places where ElarmS would be capable to provide early warning determinations of location and magnitude within a few seconds.

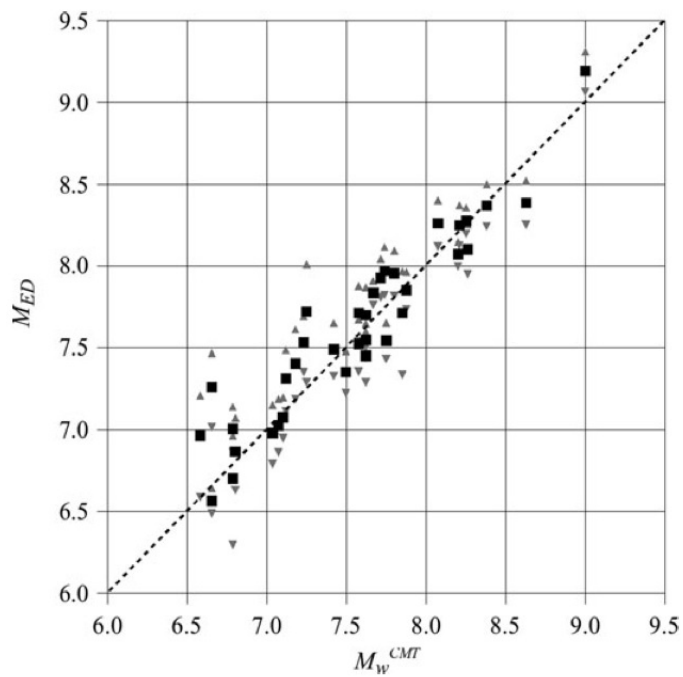


a.)

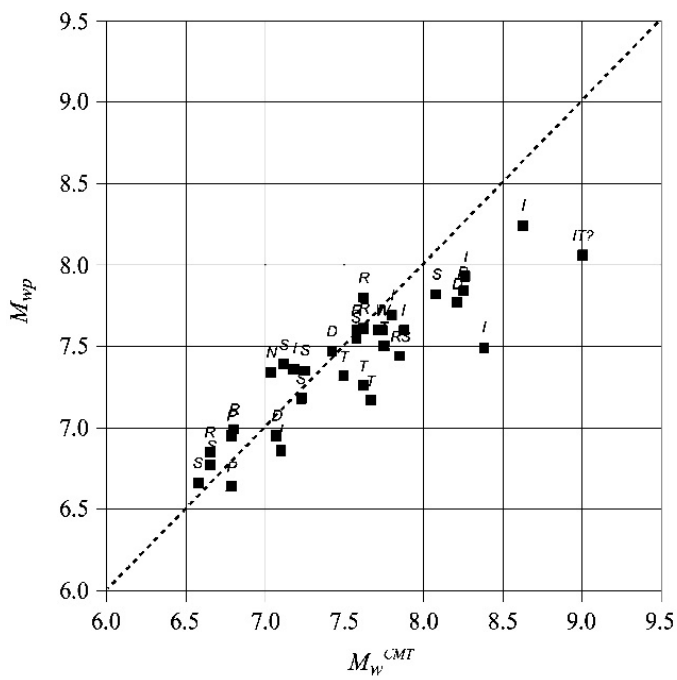


b)

Figure 11. Example of earthquake location obtained from the application of the program NLL. The event occurred near Olbia in Sardinia where very few stations are present. a.) location using the first stations recording the event only on the Tyrrhenian side of the Italian peninsula. It is clear the effect that fewer stations have on the location probability density function shown as a cloud of red points. b) Location with the complete set of stations that have recorded the event.



a.)

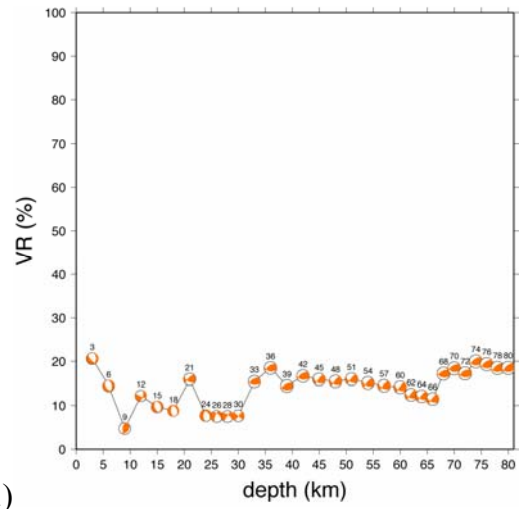


b.)

Figure 12. a.) Comparison of the performance of M_{ED} versus M_{CMT} . b.) Comparison of the performance of M_{wp} versus M_{CMT} . It is clear that M_{wp} saturates around M8 whereas M_{ED} does not. (from Lomax et al., in press).

QuickTime™ e un
decompressore TIFF (Uncompressed)
sono necessari per visualizzare quest'immagine.

a.)



b.)

QuickTime™ e un
decompressore TIFF (Uncompressed)
sono necessari per visualizzare quest'immagine.

c.)

Figure 13. (a) automatic moment tensor solution for the Monti Sibillini earthquake; (b) depth versus variance reduction plot. This plot allows to understand how the depth selected if stable; c.) reviewed moment tensor solution.

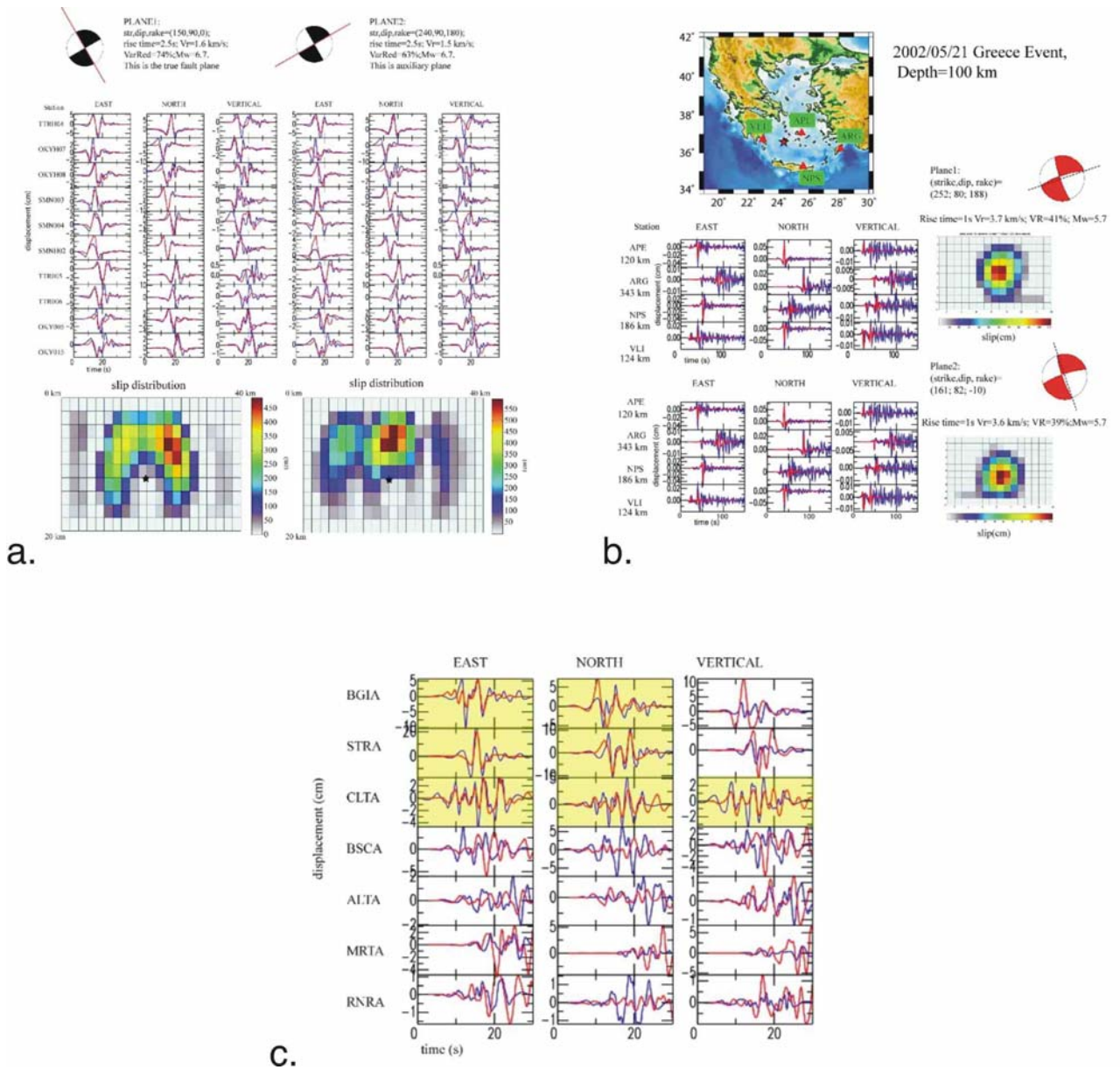


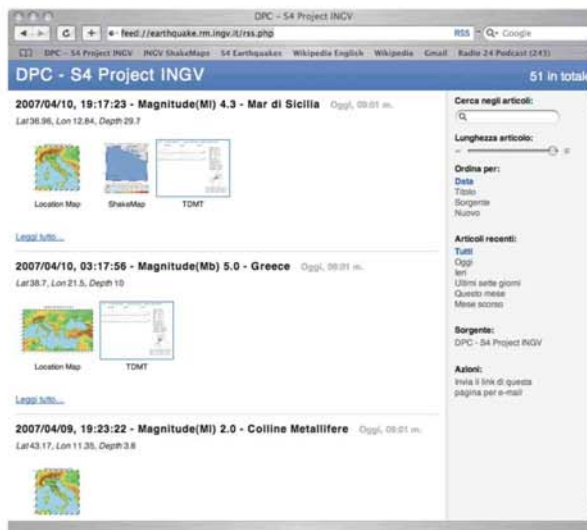
Figure 14. a.) Kinematic inversion of the 2000 Western Tottori earthquake; comparison of strong motion (blue lines) with synthetic waveforms (red lines) for both planes (left fault plane, right auxiliary plane). Bottom panels show the slip distribution of the two planes. b.) Kinematic inversion of the 2002 Greece earthquake; comparison of strong motion (blue lines) with synthetic waveforms (red lines) for both planes. c.) Kinematic inversion of the 1980 Irpinia earthquake; comparison of strong motion (blue lines) with synthetic waveforms (red lines) for both planes



a.



b.



c.



d.

Figure 14. Screenshots of the project web portal developed during the project. a.) Page showing the earthquake locations using the software GoogleMap; b.) INGV ShakeMap page; c.) RSS access to the information within the portal; d.) index of the Time Domain Moment Tensors for the $M > 3.5$ earthquakes.



Progetto S4: “Stima dello scuotimento in tempo reale o quasi reale per terremoti significativi in territorio nazionale”

UR 2 - Coordinatrice: Laura Scognamiglio, Aybige Akinci (1 anno)

TASK 2: (Responsabile Salvatore Barba)

ANALYSIS OF CRUSTAL RHEOLOGY IN PENINSULAR ITALY AND SICILY

Scope of the work is to define the first-order resistance of the crust. We compute the maximum deviatoric stress and the expected rheological behaviour (brittle vs. ductile behaviour) at depth by means of rheological profiles (Ranalli and Murphy, 1987). We compute 40 1-D rheological profiles, or strength envelopes, along DSS and Crop seismic profiles (Figure 1; for the details, see INGV Internal Report n. 4502, 27/11/2006). We used the Coulomb-Navier criterion to describe the brittle behaviour and the Power Law Creep to represent plastic flow.

To compute the rheological profiles we need to define crustal stratification, temperature, gross composition, tectonic regime, and strain rate. Such data have been derived as in the following:

- Depth of the main interfaces in the crust and allowed velocity ranges come from DSS and/or CROP profiles. We used such a parameterization to define strata velocity from tomography (Di Stefano et al., 2005), allowing a tolerance of 2 km in the depth of the interfaces. Practically, 15 km tomography cells have been linearly projected onto seismic profiles geometries allowing for some tolerance in both the geometry and the final velocity range. As main strata, we considered sedimentary covers, intermediate crust, lower crust, and upper mantle.
- Temperature has been computed assuming stationary uniform vertical conduction of the heat (Dragoni et al., 1996) and using regional or local heat flow data (Pasquale et al., 1997; Della Vedova et al., 2001).
- Based on the projected velocities and computed temperatures at depth, we choose the possible composition for each layer in each of 40 points by means of tabulated literature data (Rudnick and Fountain, 1995, Christensen and Mooney, 2005). We related the composition to density, friction coefficient, fluid pressure and creep parameters according to Ranalli (1995) and list in table 1 all the relevant information.
- Tectonic regime comes from ZS9 seismic zonation (Meletti and Valensise, 2004) and, for Umbria and Sicily, from Lavecchia et al. (in preparation).
- Regional and local strain rate, based on long-term (~100 y) triangulation and short-term GPS data, have been derived by Hunstad et al. (2003) and Serpelloni et al. (2005).

From Coulomb-Navier criterion and Power Law Creep (Ranalli and Murphy, 1987) we compute the yield strength profiles at depth. All the needed parameters are shown in Table 2.

References:

- Christensen M.I., Mooney W.D. **Seismic velocity structure and composition of the continental crust - a global view.** *J. Geophys. Res.*, 100 (B6), 9761-9788, 1995.
- Della Vedova B., Bellani S., Pellis G., Squarci P. **Deep temperatures and surface heat flow distribution.** In: **Anatomy of an orogen, The Apennines and adjacent Mediterranean basins**, (Vai G.B., Martini I.P. Editors), *Kluwer Acad. Publ., Dordrecht, The Netherlands*, pp. 65-76 + 2 plates, 2001.
- Di Stefano R., Aldersons F., Kissling E., Baccheschi P., Chiarabba C., Giardini D. **Automatic seismic phase picking and consistent observation error assessment: application to the Italian seismicity.** *Geophys. J. Int.*, 165 (1), 121-134, 2006.
- Hunstad I., Selvaggi G., D'Agostino N., England P., Clarke P., Pierozzi M. **Geodetic strain in peninsular Italy between 1875 and 2001.** *Geophys. Res. Lett.*, 30 (4), 1181, 2003.
- INGV Internal Report n. 4502, **Definizione di profili reologici 1D come confronto per modelli crostali**, 27/11/2006.

Meletti C. and Valensise G. (a cura di). **Zonazione sismogenetica ZS9** – App. 2 al rapporto conclusivo, <http://zonesismiche.mi.ingv.it/>, 2004. Accessed on 30 June 2007.

Ranalli G., Murphy D.C. **Rheological stratification of the lithosphere**. *Tectonophysics*, 132 (4): 281-295, 1987.

Ranalli G. **Rheology of the Earth**. *Kluwer Academic Publishers*, 1995

Pasquale V., Verdoya M., Chiozzi P., Ranalli G. **Rheology and seismotectonic regime in the northern central Mediterranean**. *Tectonophysics*, 270 (3-4), 239-257, 1997.

Rudnick R.L, Fountain D.M. **Nature and composition of the continental-crust - a lower crustal perspective**. *Rev. Geophys.*, 33 (3), 267-309, 1995.

Serpelloni E., Anzidei M., Baldi P., Casula G., Galvani A. **Crustal velocity and strain-rate fields in Italy and surrounding regions: new results from the analysis of permanent and non-permanent GPS networks**. *Geophys. J. Int.*, 161 (3), 861-880, 2005.

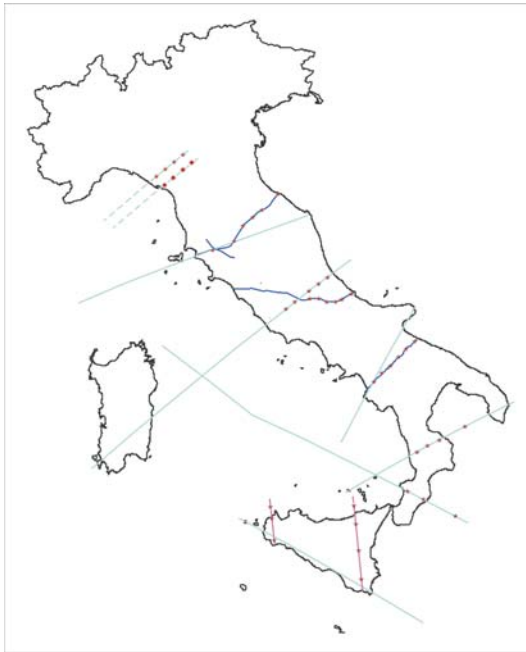


Figure 1 - Locations of the rheological 1-D profiles (stars) and CROP-DSS lines.

Layer	Lithology	Code	Density (kg/m ³)	A (MPa ⁿ /s)	n	E (kJ/mol)
UC	Solnhofen limestone	SOL	2500	1E-0.12 (s ⁻¹)	/	197
UC	Solnhofen limestone	SOL	2500	2.5E+3	4.7	297
IC	DRY QUARTZITE	QZd	2620	6.7E-6	2.4	156
IC	WET QUARTZITE	QZw	2620	3.2E-4	2.3	154
IC	GRANITE	GR	2750	1.8E-9	3.2	123
IC	WET GRANITE	GRw	2750	2.0E-4	1.9	137
IC	QUARTZ-DIORITE	QZD	2750	1.3E-3	2.4	219
IC	WET QUARTZ -DIORITE	QZDw	2750	3.16E-2	2.4	212
LC	FELSIC GRANULITE	GRF	2706	8.0E-3	3.1	243
LC	MAFIC GRANULITE	GRM	3038	1.4E+4	4.2	445
LC	DIABASE	DIA	2850	2.0E-4	3.4	260
LC	ANORTHOSITE	AN	2850	3.2E-4	3.2	238
UM	WET PERIDOTITE	PW	3250	2.0E+3	4.0	471
UM	DRY PERIDOTITE	PD	3250	2.5E+4	3.5	532

Table 1 - Assumed rheologies, density, and creep parameters A, n, and E. The code indexes table 2 results. UC, IC, LC, UM: upper-intermediate-lower crust and upper mantle.

Name	lon	lat	Hf (mW/m ²)	hr (km)	Strain rate (10 ⁻¹⁵) (s ⁻¹)	Zs9	Kinematics (Zs9)	Used Kinematics	Bottom of interfaces (km)				Rheologies
									UC	2	IC	LC	
pt 1 Lun	10.0020	44.1000	70	8	0.786 (G)	916	NF		7		16	34	SOL-QZD-GRF-PW
pt 2 Lun	10.2268	44.2372	60	8	0.786 (G)	915	NF		9		18	37	SOL-GR o QZD-DIA-PW
pt 3 Lun	10.4527	44.3739	50	8	0.786 (G)	913	UNK	NF	9		19	37	SOL-GR o QZD-GRF-PW
pt 4 Lun	10.6708	44.5050	40	8	1.3-15 (G)	913	UNK	TF	7		19	36	SOL-GR o QZD-AN-PW
pt 1 Lun I	9.7950	44.2589	70	8	0.786 (G)	916	NF		8		15	32	SOL-GR o QZD-QZd-PW
pt 2 Lun I	10.0301	44.4008	60	8	0.786 (G)	915	NF		9		18	38	SOL-GR o QZD-QZd-PW
pt 3 Lun I	10.2409	44.5275	50	8	0.786 (G)	913	UNK	NF	9		17	37	SOL-GR o QZD-GR-PW
pt 4 Lun I	10.4570	44.6549	40	8	1.3 -15 (G)	913	UNK	TF	9		18	37	SOL-GR o QZD-GR-PW
pt 1 Crop03	11.1968	42.9170	110	8	0.18 (H)	921	NF		2		14	21	SOL-GR-DIA-PW
pt 2 Crop03	11.7484	43.1227	110	8	0.18 (H)	921	NF		4		15	26	SOL-GR-DIA-PW
pt 3 Crop03	11.9604	43.3890	70	8	1.6 (H)	920	NF		4.5		15	26	SOL-GR-DIA-PW
pt 4 Crop03	12.2412	43.5536	50	8	1.6 (H)	919	NF		8		21	38	SOL-GR o QZD-DIA-PW
pt 5 Crop03	12.4579	43.6699	40	8	1.6/ 1.3 -15 (G)	918	UNK	NF/TF	10		26	45	SOL-GR o QZD-DIA-PW
pt 6 Crop03	12.7643	43.9065	40	8	1.3 -15 (G)	917	TF		10		19	35.5	SOL-GR-DIA-PW
pt 1 Crop11	13.5873	42.0321	45	10	1.8 (H)	923	NF		18	25	38	44	SOL-QZD-GRM-PW
pt 2 Crop11	13.8028	42.0412	40	10	1.8 (H)	923	NF		16	22	34	42	SOL-QZD-GRM-PW
pt 3 Crop11	14.0041	41.9840	40	8	1.8 (H)	923	NF		14	19	32	39	SOL-QZD-GRM-PW
Crop11	14.2166	41.9792	40	8	1.8 (H)	918	UNK	TF	12	16	29	37	SOL-QZD-GRM-PW
pt 5 Crop11	14.3826	42.0295	35	8	1.27 (H)	ND (917)	OUT	TF	10	15	27	35	SOL-QZD-GRM-PW
pt 6 Crop11	14.6189	42.1294	35	8	1.27 (H)	ND (917)	OUT	TF	9	13	25	35	SOL-QZD-AN-PW
pt 1 Crop04	15.1673	40.5260	40	10	0.76 (H)	ND (927)	OUT	NF	8		22	28	SOL-GR o QZD-GRF o DIA-PW
pt 2 Crop04	15.3622	40.6801	40	8	3.21 (H)	927	NF		9		20	39	SOL-GR o QZD-GRF o DIA-PW
pt 3 Crop04	15.5777	40.8216	40	8	3.21 (H)	ND (927)	OUT	NF	6		18	32	SOL-QZD-GRF o DIA-PW
pt 4 Crop04	15.7780	40.9720	45	8	0.1 (G)	925	SS		8		18	29	SOL-QZD-AN-PW
pt 5 Crop04	15.9673	41.1183	45	8	0.1 (G)	925	SS		10		28	36	SOL-QZD-AN-PW
pt 6 Crop04	16.1842	41.2653	45	8	0.1 (G)	925	SS		9		27	33	SOL-QZD-AN-PW
pt 1 Calabria	16.2270	39.2512	60	7	0.825 (S)	929	NF		9		22		SOL-QZD o DIA-PW
pt 2 mid Calabria	16.4893	39.3579	60	7	0.825 (S)	929	NF		7		24		SOL-QZD o DIA-PW
pt 2 Calabria	16.7833	39.4710	50	7	0.444 (S)	930	UNK	NF	5	21-25	35		SOL-QZD o DIA-PW
pt 2 bis Calabria	17.4284	39.7196	50	7	0.444 (S)	ND	OUT	TF	3		15	30	SOL-GR o QZD-DIA-PW
pt 3 Calabria	15.9946	38.5381	50	7	0.825 (S)	929	NF		7		17		SOL-QZD-PW
pt 4 Calabria	16.3967	38.3864	50	7	0.444 (S)	930	UNK	NF	5		18	36	SOL-GR o QZD-DIA-PW
pt 4 bis Calabria	17.1803	38.0830	50	8	0.444 (S)	ND	OUT	SS	9		27	32	SOL-QZD-DIA-PW
pt 1 Sicily	12.6109	38.2486	50	8	0.63 (S)	ND	OUT	TF	9		18	28	SOL-QZD-GRM-PW
pt 2 Sicily	12.6583	38.0588	50	10	0.1 -1 (S)	ND	OUT	TF	9		24	34	SOL-QZD-GRM-PW
pt 3 Sicily	12.7201	37.6489	80	10	0.1 -1 (S)	ND	OUT	TF	10		24	33	SOL-GR o QZD-GRM-PW
pt 4 Sicily	14.6899	38.2736	80	8	0.63 (S)	933	TF		6		15	24	SOL-GR o QZD-DIA-PW
pt 5 Sicily	14.7314	37.9451	50	10	0.1 - 1 (S)	ND	OUT	NF	12		23	38	SOL-QZD-DIA-PW
pt 6 Sicily	14.7935	37.4560	70	10	0.1 - 1 (S)	ND	OUT	TF	10		20	32	SOL-GR o QZD-GRM-PW
pt 7 Sicily	14.8628	36.9394	70	10	0.1 - 1 (S)	935	SS		10		22	32	SOL-GR o QZD-GRM-PW

Table 2 – Resulting parameters for rheological profile construction. Profile locations, heat flow (hf), characteristic depth

for radioactive heat productivity (hr), strain rate (S = Serpelloni et al., 2005; H = Hunstad et al., 2003; G=Lavecchia et al. (personal communication); ZS9 area code; ZS9 kinematics and used kinematics if undetermined (UNK) by ZS9 or outside (OUT) from the zonation (NF Normal, TF Thrust, SS Strike slip); depth of interfaces; code for rheological parameters (see table 1).

HIGH FREQUENCY WAVE PROPAGATION IN THE ITALIAN PENINSULA

Robert Herrmann and Luca Malagnini examined the newly available broadband digital data sets for use in structure and source studies. Digital data from the Rete Sismica Nazionale (RSN) and from the CAT/SCAN experiment were used.

Source studies:

Moment tensor inversion of the data from two earthquakes within the CAT/SCAN network were obtained using the Western US generic velocity model (used because of the availability of precomputed Green's functions and the approximate similarity of the upper crustal velocity model., c.f., http://www.eas.slu.edu/Earthquake_Center/MECH.NA/20070625023226/index.html). The objective was the determination of moment magnitude for the calibration of a high-frequency ground motion scaling model being developed for the region by Akinci and D'Amico. The source parameters determined are as follow:

<i>Event</i>	<i>Lat</i>	<i>Lon</i>	<i>Depth</i>	<i>Strike</i>	<i>Dip</i>	<i>Rake</i>	<i>Mw</i>
20040224052126	15.43	40.72	12	170	40	-35	4.05
20040903000412	15.68	40.70	10	190	85	45	4.42

Care was taken in selecting the earthquakes for study so that the use of a 1-D velocity model would be appropriate. Nearby earthquakes in the sea were not considered. The inversion focused in modeling the broadband ground velocity in the 0.02 – 0.10 Hz band in order to provide tighter constraints on the source depth and also to challenge the validity of the model. The broadband waveform fits indicate the appropriateness of the upper crustal velocity structure to this part of the peninsula, an initial step in the routine determination of source parameters. Future efforts can focus on the use of the use of the RSN data stream to characterize smaller earthquakes.

Shallow crustal studies:

Digital waveforms from the RSN satellite telemetered broadband seismic network were used in an initial determination of the inter-station Green's function through the cross-correlation of ground noise. Two months of digital were used. Because of the available inter-station distances, focus was made on the 0.05 – 1 Hz frequency band. The network digital data were prepared by deconvolving the instrument responses to permit the use of all stations and by down-sampling to a 20Hz sample rate to speed the processing. Inter-station Green's functions were estimated for each of the 1278 station pairs; the computations completed in 35 days on the new Sparc (talismano) computer. This initial study demonstrated the promise of the technique. We learned that we should consider the 0.02 – 1 Hz frequency band since there seems to be adequate long period signal related to mid-crustal structure. The interpretation of the observed Green's function as simple surface-wave propagation is affected by scattering of the signal for many of the station pairs. For a few paths, selection of the fundamental mode group velocity is easy. However, in order to interpret all of the inter-station Green's functions, the expected dispersion for typical crustal profiles must be understood on the basis of other work on the three-dimensional nature of the crust.

Future work:

Success in moment tensor inversion for earthquakes with $M < 4$ requires well calibrated local models of the upper crust shear-wave velocity. Routine attempts at moment tensor inversion permits a test of velocity models derived from refraction and receiver function studies. Rapid access to the complete waveform data archive is required for the development of this capability.

The use of the cross-correlation technique for determining inter-station Green's functions is promising, but a systematic study using at least 12 months of data is required to evaluate the assumed symmetry and the seasonal variation of the noise sources in addition to increasing the signal in the noise correlation stack.

Sufficient data sets now exist, e.g., waveform from local moment tensor inversion, initial inter-station Green's functions and receiver function analysis to begin to evaluate candidate models for local crustal structure.

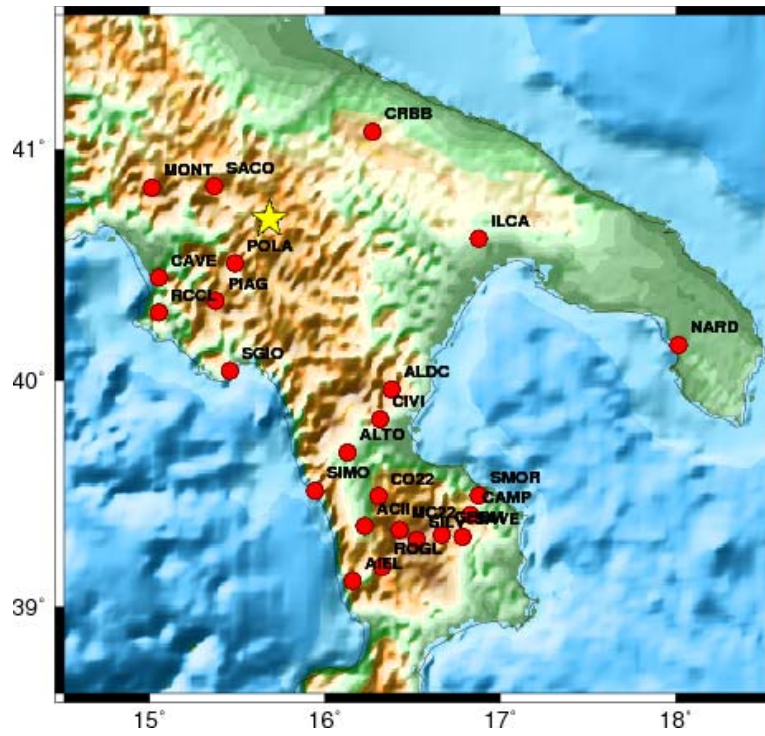


Fig. 1. Location of stations used for the moment tensor inversion of the 20040903000412 earthquake.

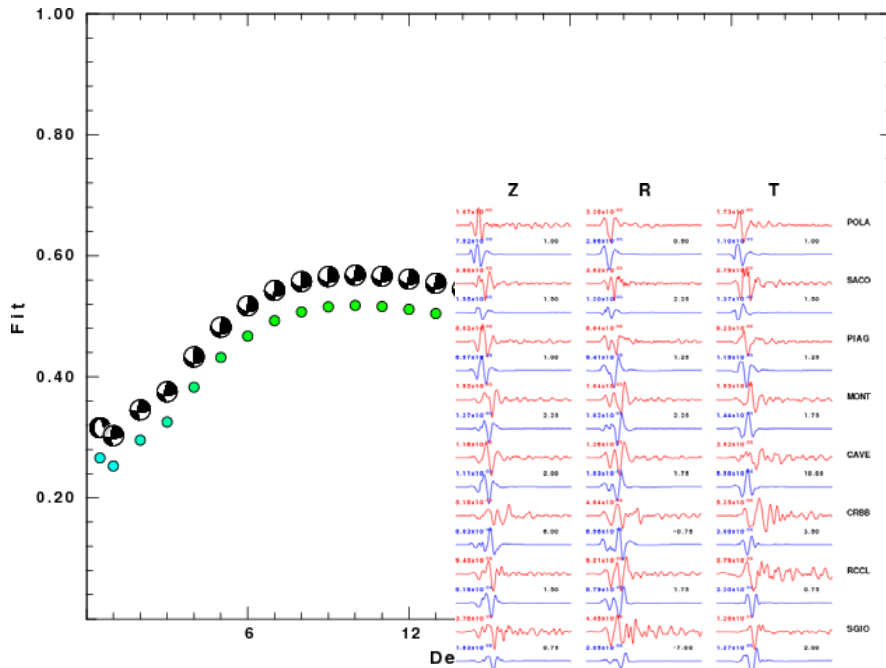


Fig. 2. Goodness of fit and best foc for 20040903000412 earthquake.

depth for the

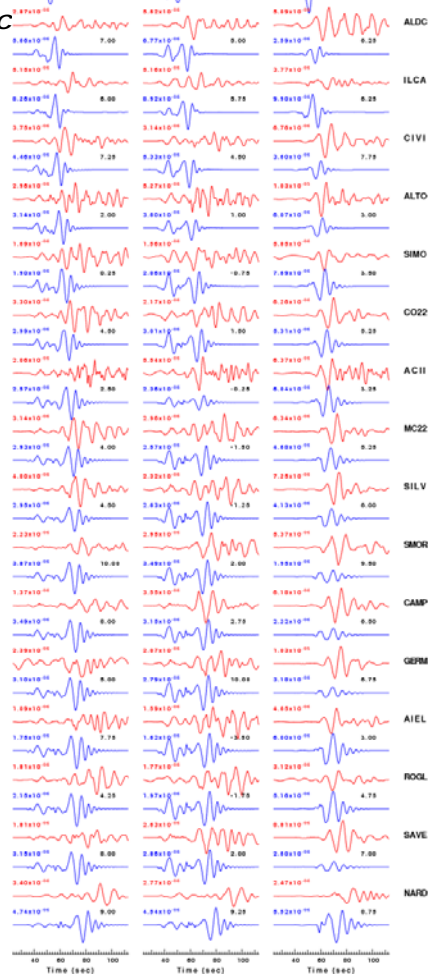


Fig. 3. Comparison of observed (red) and predicted (blue) waveforms for the 20040903000412 earthquake. Each trace pair is plotted at the same scale. Traces are ground velocity (m/sec) filtered into the 0.02 - 0.10 Hz band.

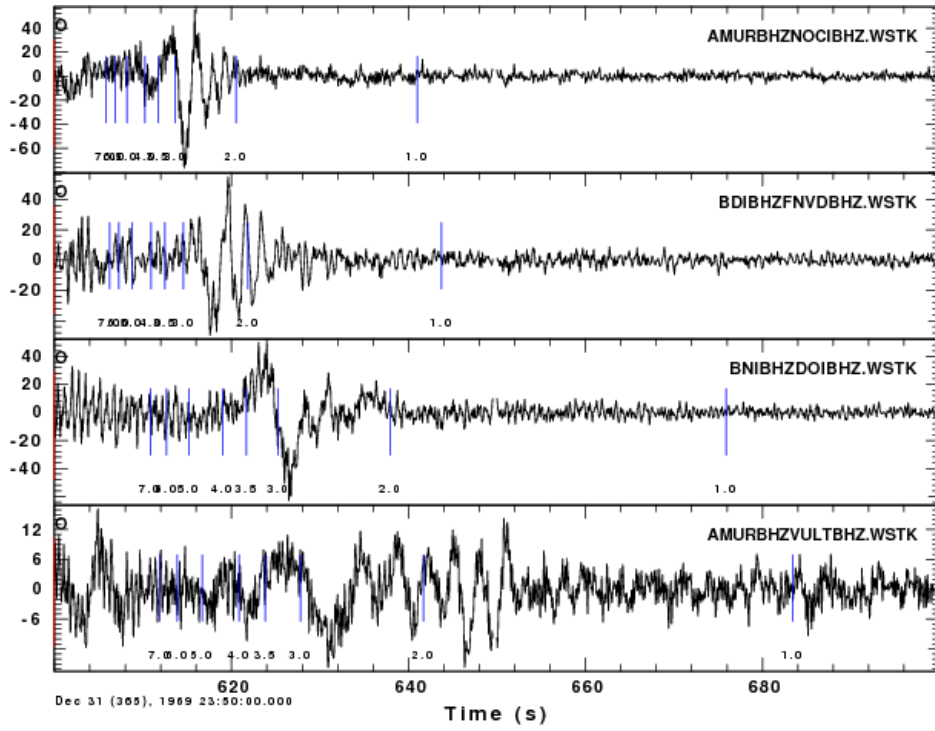


Fig. 4. Interstation Green's functions from the cross-correlation of ground noise. All traces start at zero lag. The tics indicate signal group velocities.

TASK 3: (Responsabile: Valerio De Rubeis)

COLLECTION AND ELABORATION OF MACROSEISMIC DATA THROUGH INTERNET (2005-2006)

We have developed a method to collect and elaborate information on effects of an earthquake based on M.C.S. (Mercalli, Cancani, Sieberg) scale. These informations come from people living on the area affected by the quakes, with access to internet, through an on-line questionnaire. Questions derive directly from the macroseismic scale. It is required that the questionnaire compiler has information on group of people around his/her living place, to report damages and effect of such a group. Generally this group is sized as a small town or village.

Through the use of statistical methods, to each questionnaire is associated a macroseismic degree. It is also possible to recognize unreliable questionnaire, due to errors in compilation.

Resulting maps obtained through this procedure are available to the site:

<http://www.ingv.it/~roma/attivita/pererischio/macrosismica/macros/campi/effettirecenti/lista.html>

REAL TIME AUTOMATED METHODS DEVELOPMENT FOR THE DEFINITION OF MACROSEISMIC FIELD MAPS (2006-2007)

Starting from January 2007, the macroseismic questionnaire has been deeply modified both for kind of questions and for elaboration methods. It is available at the web address: <http://terremoto.rm.ingv.it>.

An important difference with the previous method is that now the questionnaire is directed to single persons, having adapted the M.C.S. and E.M.S. macroseismic scales.

Considering the experience gathered with the old questionnaire (on line since 1997), we can show that people induced an overestimation of the damages, when compiling a questionnaire. This was due to the fact that old questions were referring to whole groups of people feelings and reported by the compiler (the compiler was considered expert and able to test large area effects). For this reason original Mercalli effects were set and considered as averaged over large people groups. It is clear that a single internet questionnaire compiler has an intuitive estimation of effects and damages over a large area, often driven by fear and emotive reasons. To overcome this effect we have modified the original M.C.S. and E.M.S. macroseismic scales into the new W.M.C.S. and W.E.M.S. macroseismic scales: the letter W indicates the web origin of information.

The statistical methods used to analyze the questionnaires have been adapted to the new scales and the filters to detect errors in compilation have been strengthened.

Starting from the end of June a completely automated procedure is running. For every earthquake, each single questionnaire can be recorded after compilation. It is analyzed and a degree for each of the two web macroseismic scales is assigned. If it passes the reliability tests it constitutes information that it will be displayed into macroseismic maps. Such maps are rescaled to fit all data into a range due to the earthquake magnitude. This procedure is activated in real time and the graphical results, along with data listings, are available to a dedicated web page (<http://terremoto.rm.ingv.it/index.php?page=list>). In particular produced maps represent: felt intensities into W.M.C.S. scale, felt intensities into W.E.M.S. scale, and felt sound effects. These three maps are in jpg format. The first one (W.M.C.S. scale intensities) is also offered into kmz format: it can be visualized with the Google Earth program. This allows a variable representation scale and each intensity point has additional information such as the number of questionnaires that produced that value. Values presented into geographic maps are also available into ASCII format for

downloading.

Obtained data, although produced by people with no specific technical experience, give a good and reasonable representation of macroseismic intensities in real time. A large number of information can be collected, processed and stored including data from events with low magnitude. This class of events did not receive attention prior the activation of this automated system for cost reasons.

In conclusions the whole procedure allows in real time the collection, analysis and visualization of effects on people and urban structures from earthquakes. Regarding high magnitude events the method complete in real time the information obtained by specialized personnel. For low-medium magnitude events the method is the sole source of information.

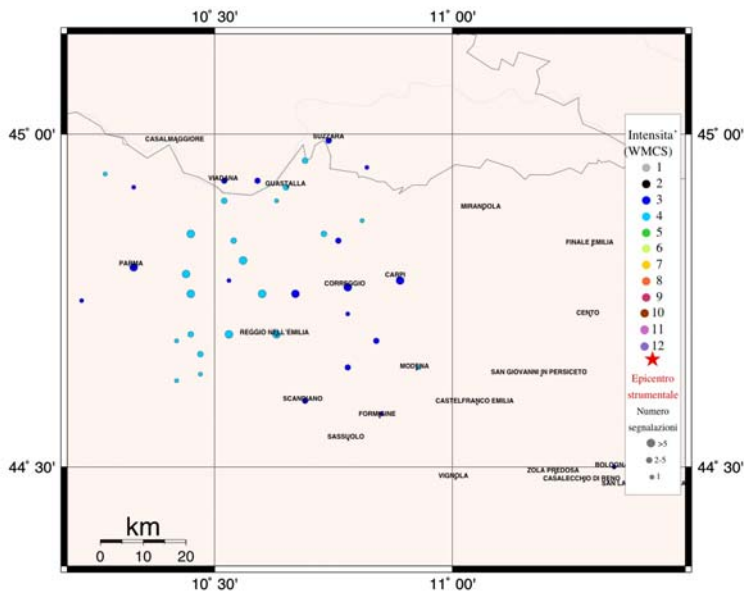


Figure 1: Earthquake of May 9 2007, $M_l=4.0$, deep=27.2 km, U.T.C. time: 06:03:50. Preliminary map of macroseismic intensities in WMCS scale. 334 compiled questionnaires at the web address: <http://terremoto.rm.ingv.it>.

TASK 4: Regional ground motion scaling (Responsabile: Laura Scognamiglio, INGV)

Aim of the research carried out by this Task was: i) to understand whether techniques based on the analysis of weak-motion seismic recordings could be used to predict the ground motion induced by larger events; ii) to compare the reliability of the ground motion predictions for moderate events based on weak-motion and strong-motion equations; iii) to extend our weak-motion techniques in order to isolate the seismic source for the precise, automatic estimate of the “absolute” moment-rate spectra of the events recorded by the investigated regional networks. A “calibration” of the techniques’ potential has been carried out on data from the extended San Francisco Bay Area, and similar studies have been developed in Central and in Southern Italy.

GROUND MOTION EXCITATION/ATTENUATION MODEL FOR SAN FRANCISCO REGION

By using small-to-moderate-sized earthquakes located within ~200 km of San Francisco, we characterize the scaling of the ground motions for frequencies ranging between 0.25 and 20 Hz, obtaining results for geometric spreading, $Q(f)$, and site parameters using the methods of Mayeda et al. (2005) and Malagnini et al. (2004). The results of the analysis show that, throughout the Bay Area, the average regional attenuation of the ground motion can be modeled with a bilinear geometric spreading function with a 30 km crossover distance, coupled to an anelastic function, where: $Q(f) = 180 f^{0.42}$. A body-wave geometric spreading, $g(r) = r^{-1.0}$, is used at short hypocentral distances ($r < 30$ km), whereas $g(r) = r^{-0.6}$ fits the attenuation of the spectral amplitudes at hypocentral distances beyond the crossover.

The frequency-dependent site effects at 12 of the Berkeley Digital Seismic Network (BDSN) stations were evaluated in an absolute sense using coda-derived source spectra.

Our results show: i) the absolute site response for frequencies ranging between 0.3 Hz and 2.0 Hz correlate with

independent estimates of the local magnitude residuals (dM_L) for each of the stations; ii) moment-magnitudes (M_W) derived from our path and site-corrected spectra are in excellent agreement with those independently derived using full-waveform modeling as well as coda-derived source spectra; iii) our weak-motion-based relationships can be used to predict motions region-wide for the Loma Prieta earthquake, well above the maximum magnitude spanned by our data set, on a completely different set of stations. Results compare well with measurements taken at specific NEHRP site classes; iv) an empirical, magnitude-dependent scaling is necessary for the Brune stress parameter in order to match the large magnitude spectral accelerations and peak ground velocities with our weak-motion-based model; v) moderate earthquakes are better predicted by our model than by strong-motion-based predictive equations.

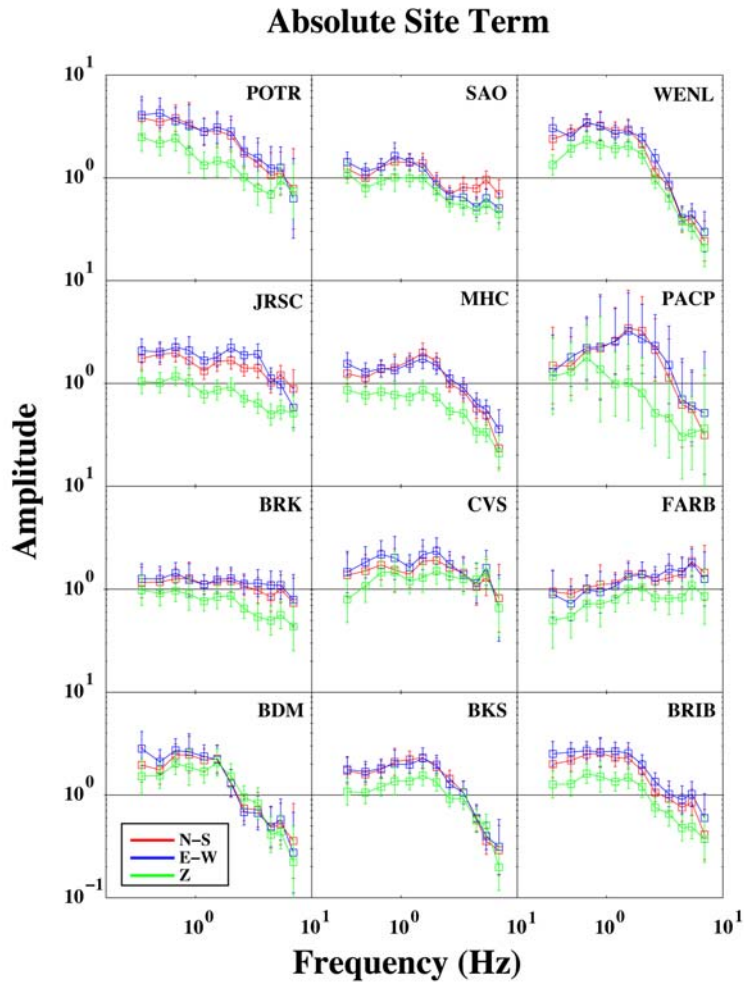


Figure 1. Absolute site terms for stations BDM, BKS, BRIB, BRK, CVS, FARB, JRSC, MHC, POTR, SAO, WENL, and PACP (N-S component, red, E-W component, blue, vertical, green).

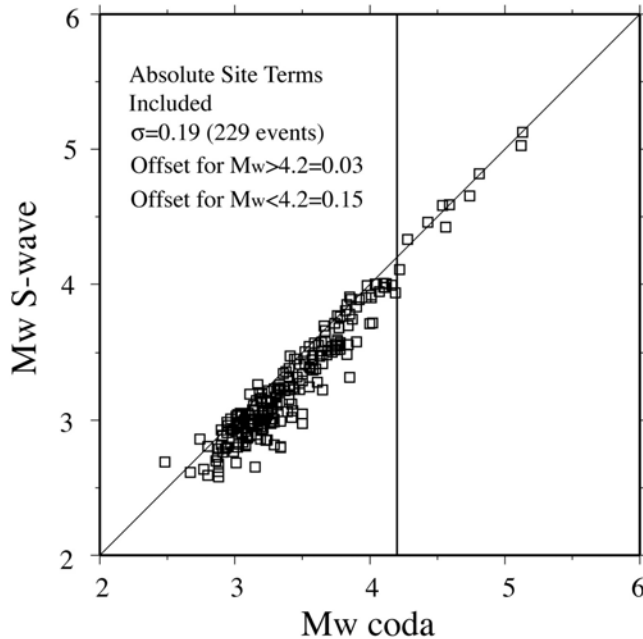


Figure 3: The results shown above were obtained using the code developed by Luca Malagnini (published in Bodin et al., 2004) for the automatic computation of the moment magnitude, given $g(r)$, $Q(f)$, κ_0 , and $T(r)$ obtained from the regional study on excitation and attenuation of the ground motion. The attenuation model is described in Malagnini et al. (2007). Other parameters in the code are also listed in the paper. Duration used is the one at 1.75 Hz ($T=\text{const.}=7$ sec for $r < 70$ km; $T=0.01*r$ for $r > 70$ km, r in km). The coda-wave moment magnitudes represented our reference estimates. Y-axis: automatically obtained S-wave M_w 's, computed by correcting the observed spectra for the regional attenuation (path and absolute site terms), X-axis: "ground-truth", coda-based M_w 's, computed by Mayeda et al (2005). A residual adjustment of 0.03 magnitude units would be needed to perfectly match (in an L-1 sense), the ground-truth values. For smaller magnitudes ($M_w < 4.2$), scatter is larger and a residual adjustment of 0.15 magnitude units is found.

GROUND MOTION EXCITATION/ATTENUATION MODEL IN CENTRAL APENNINES

We provide a complete characterization of the ground motion in the Central Apennine region, in the frequency range 0.25 - 22.5 Hz, by using 705 moderate size earthquake recorded in 1991-2002 period, by 23 three-component digital stations run by *Servizio Sismico Nazionale (SSN)*. We used only crustal events (shallower than 30 km), with local magnitudes ranging from 2.0 to 5.1, and epicentral distances between 10 and 155 km.

Following the regression technique described in Malagnini et al. (2000), we modeled the 1-D regional propagation characteristics by using the anelastic attenuation function $Q(f) = 100 f^{0.40}$, coupled with a bilinear geometrical spreading with 40 km cross-over distance defined as: $g(r) = r^{-1.0}$ for $r < 40$ km, and $g(r) = r^{-0.5}$ for $r \geq 40$ km. For 478 earthquakes, recorded at 12 of the 23 stations, we have computed moment-rate source spectra, moment magnitude, seismic moment, and radiated energy, using the coda envelopes method developed by Mayeda and Walter (1996) and later modified by Mayeda et al. (2003). Figure 1 shows the moment-rate spectra evaluated for 11 calibration events, for which we had previously determined RCMT moment magnitude.

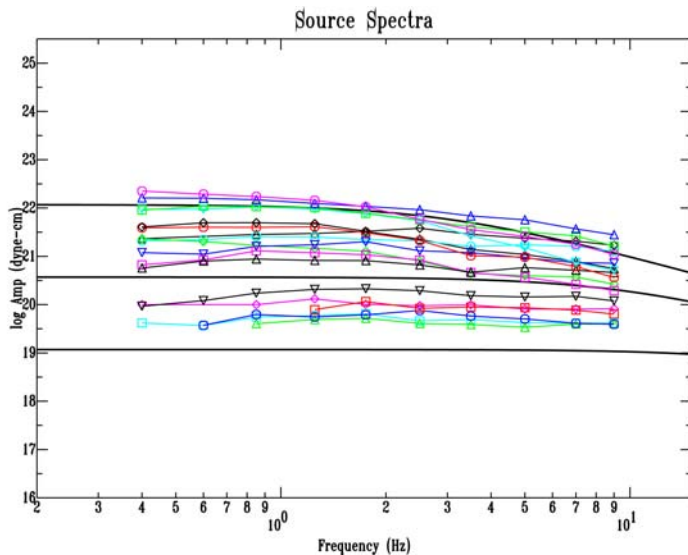


Figure 1: Moment rate spectra for the 11 events used in the calibration. For these earthquakes we already had M_w from the RCMT catalogue.

Starting from the coda derived source terms, and the calibrated regional attenuation model for Central Apennine, we were able to get an estimate of the absolute site response. The source terms were propagated at the reference distance of 40 km through the geometric/anelastic attenuation function, and deconvolved from the observed data amplitudes to evaluate the absolute behavior at the 12 sites used. We consider this response as absolute because the source terms are not affected by any specific site term, in the same way as the propagation path.

In order to test our spectral attenuation model, we have compared the moment magnitude computed by correcting the observed spectra for the path and the absolute site responses, with those obtained from the coda study, that represent our reference estimates (Fig. 2). The match between the magnitudes is good. This result supports the capability of this methodology to characterize the regional ground-motion, estimate the absolute site response for sites included in the seismic network and to provide the ingredient for an automatic moment magnitude computing tool.

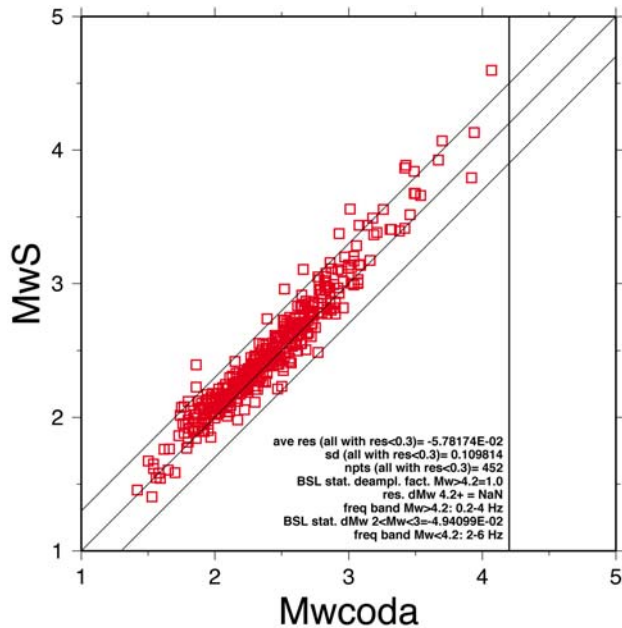


Figure 2: Comparison between coda-wave moment magnitudes, and automatically computed S-waves moment magnitudes.

GROUND MOTION SCALING IN CALABRIAN ARC

We provide a description of the ground-motion characteristics in southern Italy. We used seismic recordings coming

from two different projects: the SAPTEX (Southern Apennines Tomography Experiment) and the CAT/SCAN (Calabria Apennine Tyrrhenian – Subduction Collision Accretion Network). Under the CAT/SCAN project, 40 portable digital broadband seismographs were deployed throughout southern Italy by Lamont-Doherty Earth Observatory, Istituto Nazionale di Geofisica e Vulcanologia (INGV), and University of Calabria, while 26 SAPTEX stations were deployed in the same area by INGV only. We used about 10.000 records from 307 earthquakes registered from January 2002 to October 2005. The magnitude of the events ranges between 2.5 and 4.7, whereas the epicentral distances are comprised between few kilometers and about 280 km. By using the approach described in Malagnini et al. (2000), we have estimate a predictive relationship that included the source excitation terms, an attenuation operator and site effect terms. We have found that the propagation term could be described trough the following anelastic attenuation function $Q(f) = 140(f/f_{ref})^{0.30}$, where $f_{ref} = 1\text{Hz}$, coupled with geometrical spreading function $g(r) = r^{-1.0}$ for $1 < r < 60$ km, $g(r) = r^{-0.5}$ for $r > 60$ km. Excitation terms are modelled by using a Brune spectral model with a magnitude-dependent stress parameter, and a station-dependent attenuation.

Following Boore's (1996) implementation of the stochastic ground motion model, by using a set of programs called Stochastic Model Simulation (SMSIM), we predicted the absolute level of the ground shaking. Figure 1 shows the comparison among the results evaluated during our studies and the attenuation relationships obtained by Sabetta and Pugliese (1996), and Ambraseys et al. (1996) for magnitude 4.0, 5.0 and 6.0. We compared the obtained values of Peak Ground Acceleration with values of PGA for events with magnitude between 4.0 and 5.0.

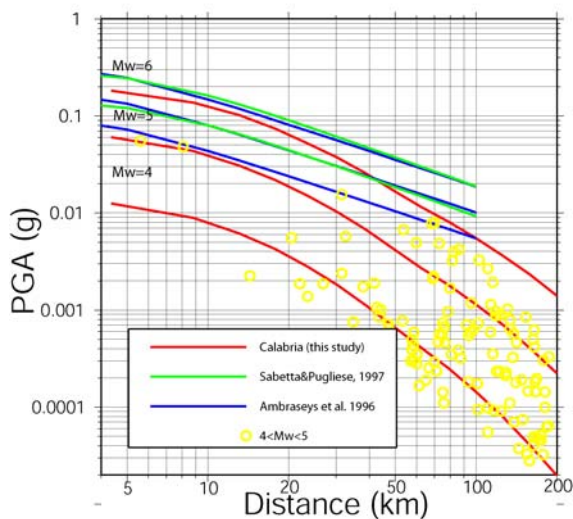


Figure 1: Peak Ground Acceleration (PGA, in units of g) observed for the events in the data-base with magnitude ranging from 4.0 to 5.0 (yellow circle), compared with prediction curves computed with the ground motion parameters developed in this study (red curves). Green's prediction curves are from Sabetta and Pugliese (1996), while blue curves are from Ambraseys et al. (1996).

DATABASE COLLECTED FOR NORTHERN SICILY

We have collected waveforms from 392 earthquakes recorded in Sicily by seven three-component digital stations (INGV Seismic Network, and Mednet network) located in the region from October 2005 to May 2007. These events have magnitude ranging from $M_I=1.0$ to $M_I=4.2$, epicentral distances comprised between few kilometers to about 300 km, and they have maximum depth around 50 km. Each waveforms has been corrected for the instrumental response and examined to eliminate those having spurious transients, doubles events or low signal to noise ratio.

References:

Ambraseys, N. N., K. A. Simpson, and J. J. Bommer (1996), **Prediction of horizontal response spectra in Europe**, *Earthquake Eng. Struct. Dyn.*, 25, 371-400.

- Boore, D. M. (1996). **SMSIM: Fortran programs for simulating ground motion from earthquakes, version 1.0**, *Geol. Surv. Open-File Report 96-80A*, 73pp.
- Malagnini, L. and R.B. Herrmann (2000). **Ground-Motion Scaling in the Region of the 1997 Umbria-Marche Earthquake (Italy)**, *Bull. Seism. Soc. Am.*, 90, 1041-1051.
- Mayeda, K., A. Hofstetter, J. O'Boyle and W. R. Walter (2003). **Stable and Transportable Regional Magnitudes Based on Coda-Derived Moment-Rate Spectra**, *Bull. Seism. Soc. Am.*, 93, 224-239.
- Sabetta, F. and A. Pugliese (1996). **Estimation of response spectra and simulation of nonstationary earthquake ground motion**, *Bull. Seism. Soc. Am.*, 86,337-352.

TASK 5: Stima degli effetti di sito alle stazioni di registrazione ed utilizzo di GIS esistente (classificazione del territorio nazionale tipo Eurocode) (Responsabile: G. Milana, INGV-Roma1).

SITE CHARACTERIZATIONS ACTIVITIES

The activities on site characterization topic were concentrated in three areas in Central Italy: Valmontone (RM), Barisciano (AQ) and Castelli (TE). The first site was selected for testing low cost techniques for measuring shear waves velocities in a site where lots of geotechnical and geophysical testing were already performed. The other two sites were selected since they host seismic stations of the regional Abruzzo seismic network, operating since early nineties (De Luca et al., 2000), used for applying the absolute site effect techniques proposed by Malagnini et alii (2004).

Investigation techniques were: microtremor H/V analysis and surface waves analysis performed using both single station and multichannel seismic array with both active and passive energy sources. The receiver function approach was also applied to Castelli site where many recorded local seismic events were available.

Valmontone test site was investigated performing microtremor analysis using a three component digital station RefTek 130 equipped with extended band seismic sensors Lennartz LE3d-5s. Data were recorded in a few hour daily time window close to the point where cross hole measurement were performed. Array measurements were based on a 48 channel linear deployment with 4.5 Hz vertical component geophones of 1.5 meters spaced and active (8 mm gun) source and on a cross array based on 72 geophones. The extension of the area did not allow a longer deployment giving some limitation on the investigated depth. Active data were recorded on 2 seconds time windows with a sampling rate of 0.125 ms, while passive data were recorded on 30 seconds time windows with a sampling rate of 2 ms. The joined use of active and passive sources improves the quality of data since active sources give better information on high frequencies, while passive sources allow to enlarge the frequency range towards lower values and, consequently, towards higher investigation depth. The use of a 2D array with passive source is essential to resolve the ambiguity between apparent and real velocities estimation, always present in 1D array techniques applied on passive data.

The same analysis was applied to Barisciano site using a 100 channels deployment with spacing of 3 and 5 meters due to the high depth of the bedrock in the area. In Barisciano site, due to bigger extension and complexity of the investigated sedimentary basin, an extensive campaign of microtremor acquisition and analysis was performed to better describe the bedrock geometry.

Due to logistic and morphological difficulties Castelli site was only investigated by microtremor and receiver function techniques.

Final results and considerations

Valmontone test site confirms that a combined use of microtremor, MASW and NASW approach is able to reproduce the results obtained by geotechnical investigation. As already known the array geometry gives a strong constrain on investigated depth that cannot be greater than 1/4 – 1/6 of the deployment length. Using passive source and refraction microtremor techniques it is very easy to obtain unrealistic information trying to extend the dispersion curve picking in the low frequency range.

Figure 1 shows the comparison between cross-hole shear waves velocities measurements, array dispersion curve inversion for three velocity models with the same residuals, and microtremor analysis. Again the agreement between different techniques is fairly good if we take into consideration the limited extension of the array, due to logistic difficulties.

For Barisciano site microtremor analysis can allow to describe the behavior of the bedrock that is located at depth greater than 150 meters. In this case surface waves techniques are not particularly useful due to the presence of an important velocity inversion, inferred by geological literature data and from cross hole measurements that describe a gravel layer thicker than 42 meters with shear waves velocities of about 800-1000 m/s.

Castelli site also present a velocity inversion at a 25 meters depth, derived from cross hole measurements, also in this case surface waves techniques are not particularly useful. Microtremor data are not easily understood in terms of simple 1D response but are in very good agreement with receiver function results. This site would need further investigations.

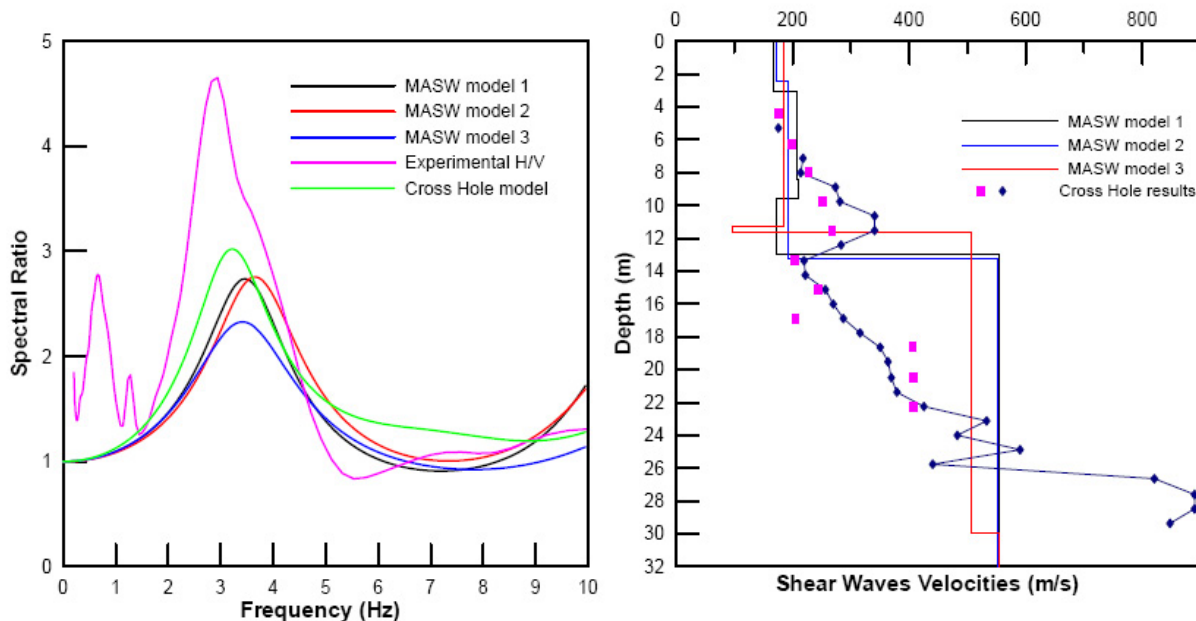


Figure1: Surface analyses for Valmontone site. (A) Comparison between MASW models, H/V ratio, and Cross-hole data. (B) Comparison between shear waves velocity measured by Cross-hole and MASW models.

NATIONAL SEISMIC NETWORK (RSNC) SITES ANALYSIS

Site response for the RSNC was often considered not important since the majority of recording sites is located on rock sites condition. This approach is only partially true because, for network geometry reasons, some of the station must be located on geological conditions that can induce site amplification. Also for rock sites the effect of highly fractured rock can produce amplification. The capability of continuously recording seismic signals for all the RSNC sites makes quite easy the use of microtremor data for a first estimate of possible seismic amplification; in fact even if it is not obvious to correlate H/V to seismic amplification it is also established that hard rock site often show a unitary H/V ratio and a marked depletion from the unit can indicate the presence o site effect to be better investigated with more details also using more complex techniques..

In our analysis almost 80 RSNC sites were analyzed by extracting few 1 hour time windows recorded at night time in absence of strong cultural noise. For all the recorded signals H/V ratios were evaluated using the recommendation given by Sesame Project (2001-2004). As expected many of the analyzed sites show a very flat almost unitary H/V ratio, according to sites characteristics; it is possible, anyway, to find at least 10-15 sites with an anomalous behavior. Some of these features in H/V ratios can be easily explained in terms of local geology, as for the SBPO (San Benedetto Po) station, located on the deep sediments of Po plain, or for CLTB (Caltabellotta) station installed on a very sharp hill crest. Some other anomalies are quite surprising only considering surface geology or site topography. As an example of these unclear response is possible to mention the MURB (Monte Urbino) station located on a hill not too steep on outcropping rock. As a first trial receiver function approach was applied to many seismic events recorded at the 15 anomalous stations of the RSNC. The obtained results show a substantial agreement between the two approaches showing that the two techniques give similar values of the H/V ratio, this observation must be further investigated on

new studies due to the lack of theoretical background to explain such behavior. In the future such simple preliminary analysis can be extended on all the new site recently installed on the RSNC, some extra investigation and more detailed analysis are necessary both to better understand the origin of amplification factors and to translate them in corrective factors to be implemented in the Shake Map procedures.

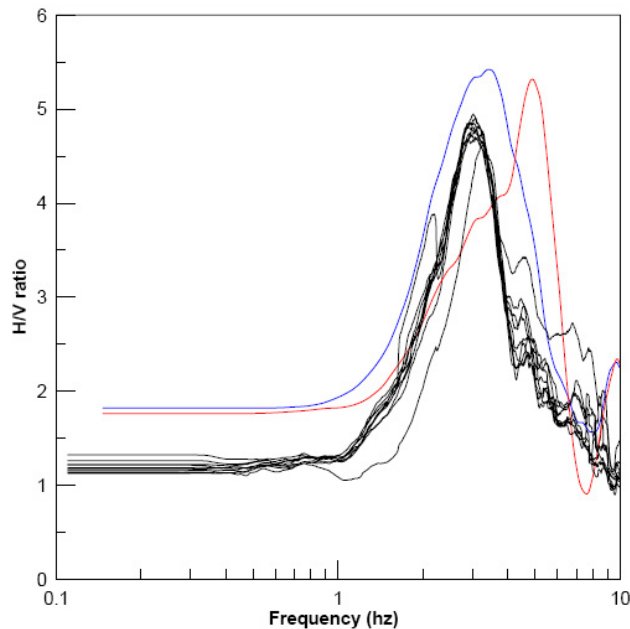


Figure 2: Comparison between H/V ratios for seismic noise (black lines), and seismic events N-S components (blue curves), and E-W components (red curves)

References:

De Luca G., Scarpa R., Filippi L., Gorini A., Marcucci S., Marsan P., Milana G., Zambonelli E., 2000 - **A detailed analysis of two seismic sequences in Abruzzo, Central Apennines, Italy.** *Journal of Seismology*, Vol. 4, n. 1, January 2000.

Malagnini L., Mayeda K., Akinci A., Bragato P.L., 2004 - **Estimating Absolute Site Effects,** *Bulletin of the Seismological Society of America*; August 2004; v. 94; no. 4; p. 1343-1352.

Sesame Project, 2001-2004 - <http://sesame-fp5.obs.ujf-grenoble.fr/index.htm>

PUBLISHED PAPERS

The following published, or submitted papers have been supported by this *UR*.

William R. Walter, Kevin Mayeda, Luca Malagnini, and Laura Scognamiglio. **Regional body-wave attenuation using a coda source normalization method: Application to MEDNET records of earthquakes in Italy.** *Geophys. Res. Lett.*, May 2007, Vol. 34, No. 10.

Kevin Mayeda, Luca Malagnini, and William R. Walter. **A new spectral ratio method using narrow band coda envelopes: Evidence for non-self-similarity in the Hector Mine sequence.** *Geophys. Res. Lett.*, June 2007, Vol. 34, No. 11.

Luca Malagnini, Kevin Mayeda, Robert Uhrhammer, Aybige Akinci, and Robert B. Herrmann. **A Regional Ground-Motion Excitation/Attenuation Model for the San Francisco Region.** *Bull. Seism. Soc. Am.*, June 2007; **97**: 843 - 862.

Sean R. Ford, Douglas S. Dreger, Kevin Mayeda, William R. Walter, Luca Malagnini, and William S. Phillips. **Regional Attenuation in Northern California: A Comparison of Five 1-D Q Methods.** *Bull. Seim. Soc. Am.* (2007), submitted.

INGV-DPC Project S4 - Real- and quasi real-time ground motion estimates of significant earthquakes in the Italian region.

Research Unit S4/03

Responsible:

Enrico Priolo, OGS-CRS Udine

2.1 Achievement of Project Deliverables

The Research Unit 3-OGS was involved in Tasks 1, 2, 3 and 5 of the Project S4. During the two years project, the most of the programmed activity has been realized. Some changes have been introduced in the light of the comment of the Revision Committee, who suggested giving priority to the full implementation of basic applicative products. In particular, we didn't implement the directivity effects in ground motion estimations (Task 3), because it is not a standard feature of the ShakeMap program. In Task 5, we carefully evaluated the impact of site classification and H/V spectral ratios on the reduction of the uncertainty associated to ground motion relations, omitting the full geophysical characterization of the recording sites with other, more sophisticated and time-consuming techniques.

As main goals achieved within the project:

1. we designed and implemented a low-cost accelerometric network in a test area (Task 1);
2. we defined 1D structural models for the NE Italy (Task 2);
3. we installed and customized for NE Italy the ShakeMap software (Task 3)
4. we implemented and tuned the moment tensor computation in near real time for local and regional seismicity recorded by the CRS broad band network (Task 3);
5. we analyzed and modeled a number of seismic sequences occurred in NE Italy to estimate general relations that could be used for predicting the space/time behavior of future sequences (Task 3);
6. we proved, through cluster analysis on European data, that site effects contribute up to 33% of the standard deviation of ground motion relations for PGA; we also proved the inadequacy of the current soil classification criteria to reduce such uncertainty (Task 5).

All the analyses and main results obtained are extensively described and discussed in papers submitted for publication and technical reports.

For the Task 1, in order to increase the number of observation points and to produce detailed shake maps, we proposed the implementation of low-cost accelerometric stations with real-time connection to the Department Centro di Ricerche Sismologiche (CRS) of the OGS at Udine and the Centro Nazionale Terremoti (CNT) of the INGV in Rome. Among the different solutions available we chose the low-cost accelerograph IA-1 developed by GeoSIG in collaboration with the Geological Survey of Canada. The device is equipped with a single-board computer with the Linux O.S. and Ethernet port, a 16-bit A/D converter and a MEMS three-component accelerometer. The sensor has full scale 4g, noise floor 0.5mg and it is suitable for recording earthquakes of magnitude greater than 3 at epicentral distances up to 40 km. For data transmission to the CRS we considered both the costs and the requirements for reliable transmission in case of earthquake. We chose spread-spectrum radio links which guarantees full IP connectivity at 2 Mbps. The overall cost per station is about 3,000 € fairly divided between the accelerograph and the transmission system.

We developed a prototype network in the urban area of Tolmezzo, a small town of about 10,000 inhabitants 50 km north of Udine (NE Italy). Tolmezzo is located in an important seismic area (e.g., it was hit by the 1976 Friuli earthquake with maximum MCS intensity VIII) and the site effects were recently studied within the project SISMOVALP (EU program INTERREG IIIB "Alpine Space"). Furthermore, the area is partially covered by the backbone of the spread-spectrum radio

network developed by OGS in Friuli-Venezia Giulia. Two sensors are currently installed and fully operative by the Hospital and the swimming pool, both in rooms at the basement of low structures.

The acquisition schema designed for the network is shown in Fig. 1. Each accelerograph produces standard files in miniSEED format for both continuous and event recording with data sampled at 100 sps. The files are transferred to the Antelope data acquisition system running at CRS through an IP connection using the program for remote copy “scp”. Here, the data are processed for use with the ShakeMap program and forwarded to INGV/CNT using the “seedlink” protocol (data transmission to other data centers through the orb2rb Antelope protocol is also available).

According to the project, for Task2 we performed a seismic zonation of NE Italy into 6 areas by taking into account results from tomographic inversion as well as other geophysical and geological data available from the literature (Bressan, 2005). For each zone we defined a mono dimensional layered model between 0 and 35/40 km depth, depending on the Moho location, for which we estimated the P wave velocity (V_p), the ratio V_p/V_s , the density and the quality factor Q_p and Q_s , all parameters that are used in the Task 3 for the computation of the Green functions.

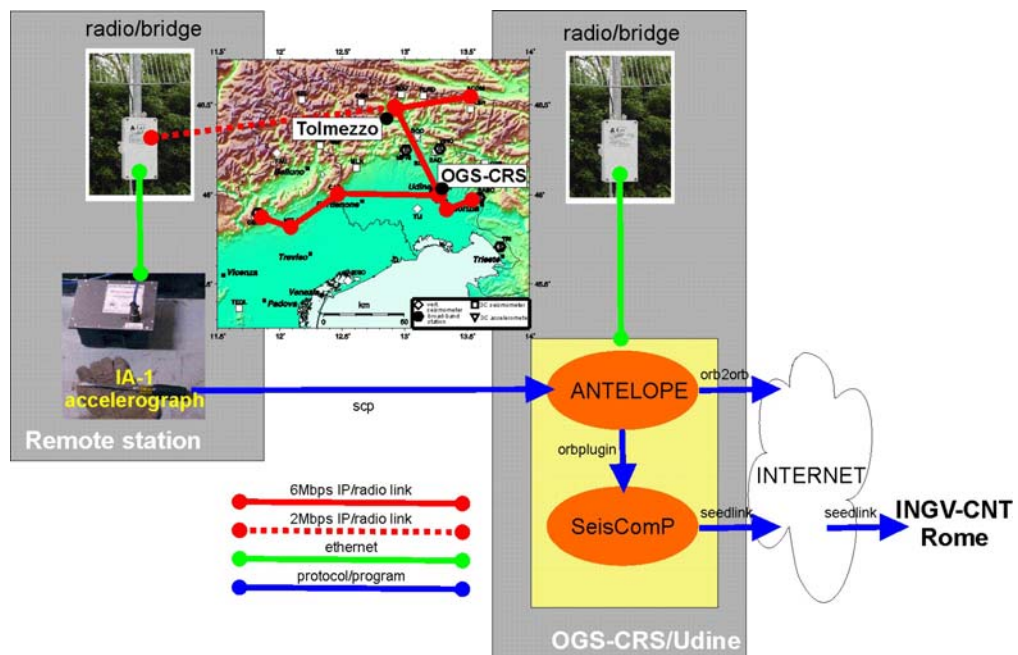


Figure 1. Acquisition schema of the low-cost accelerometric network implemented at Tolmezzo.

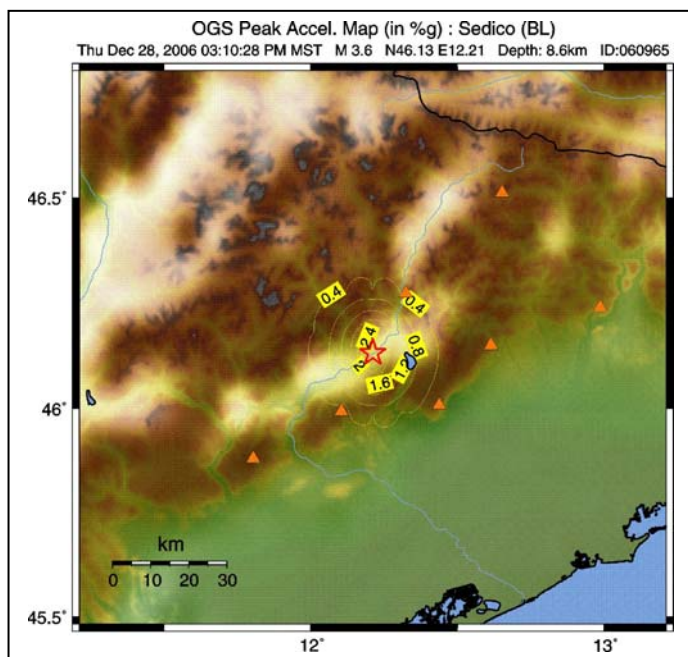


Figure 2. Example of shake map produced for a recent earthquake in Veneto.

For the Task 3 we installed and tested the program ShakeMap for various events recently occurred in NE Italy (Fig. 2) as well as for synthetic data simulated by waveform modeling for scenario and historical earthquakes (e.g., 1936 Cansiglio earthquake, M 5.8). We implemented the available regional ground motion relations and interfaced the software to the Antelope system acquiring data from the broad band, short period and accelerometric stations managed by OGS.

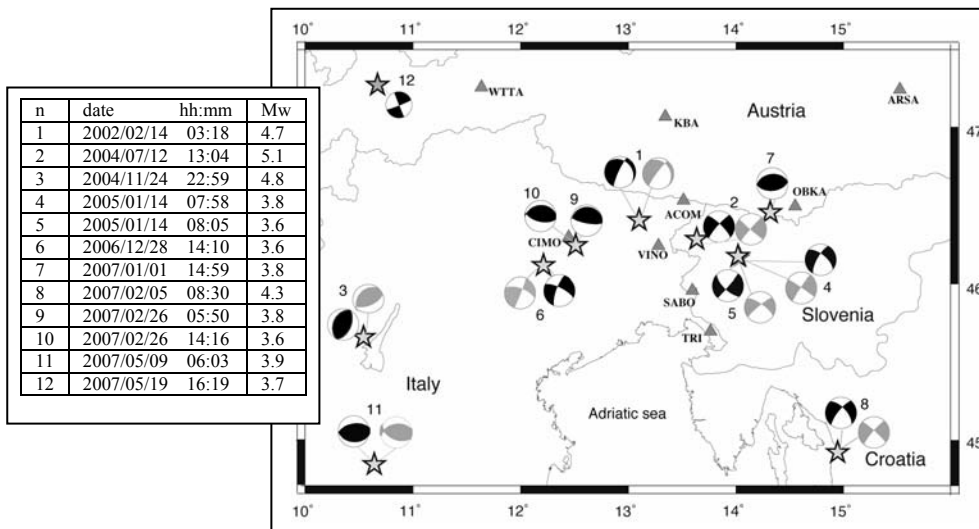


Figure 3. Map of earthquakes (stars) and focal mechanisms (black beach balls) retrieved (Saraò, 2007). For the same event a focal mechanism retrieved by other means (grey beach balls) is plotted when available. Events 1,2,3,4,5 are compared with the SED moment tensor solutions, event 6 is compared with fault plane solutions by polarity inversion (Bressan 2007, personal communication), event 8 and 11 are compared with MedNet CMT solutions.

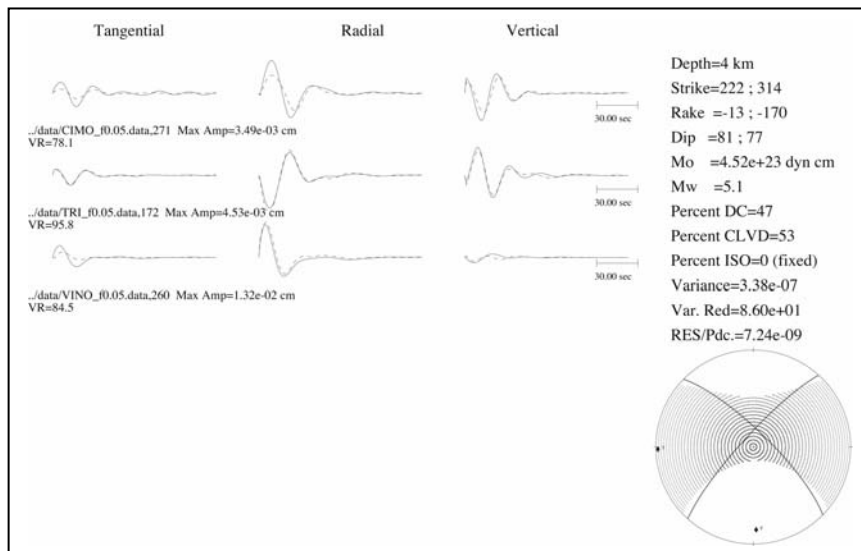


Figure 4. Moment tensor solution for event n. 2 as reported in Table 1. The corresponding waveform fit between real (solid line) and synthetic (dashed line) data is also plotted (Saraò, 2007).

For the Task 3 we also implemented, tested and tuned for NE Italy the seismic moment tensor (MT) inverse code developed by Dreger and chosen for the S4 project. We computed the MT for all the events with MD ≥ 3.6 occurring in the Friuli Venezia Giulia and surrounding area. Several tests, using synthetic and real data, have been performed (some of them in collaboration with INGV) to check the sensitivity of solutions to the number of stations and their geometry relative to the event. We considered 6 broad band stations managed by CRS and, when possible, those of the Austrian network. Our tests, described in details in a technical report (Saraò, 2007), revealed that even one-station solutions prove quite effective in many cases though the minimum number of stations

depends on the epicenter position and on the source radiation pattern. Moreover, the best double couple and the M_w are quite robust although the resolution depth is not always well constrained. In Fig. 3 we show our results. For each event we inverted displacement data filtered from 50 to 20 s ($3.6 < M < 5.0$) and 100 to 20 s ($M > 5.0$). The Green functions were computed using the 1D models determined for Task 2. Due to the restricted region and the simple structural model, the Green functions can be quickly estimated at run time for each earthquake, so that we avoided creating a storage data set. The focal mechanisms obtained are plotted in Fig. 3 together to (when available) the focal mechanisms obtained by other means. In Fig. 4 an example of complete moment tensor solution is given.

Finally, for the Task 3 using data from 8 seismic sequences occurred in Friuli-Venezia Giulia and western Slovenia in the last 30 years (mainshock magnitude between 3.7 and 5.6), we estimated the average parameters of some statistical models (both original and from the literature) that describe the space-time behaviour of the aftershock occurrence (Gentili 2006; Gentili and Bressan 2007). Such models can be used to predict the behaviour of future seismic sequences after the occurrence of the mainshock. From this point of view, the more interesting and original result is the estimation of a linear relation between the Brune stress drop of the mainshock and the magnitude difference between the mainshock and the largest aftershock (Fig. 5). Such correlation was established using few data points and for a narrow magnitude range, therefore at now we cannot extrapolate a general behaviour. Nonetheless, it constitutes an interesting starting point for further investigation.

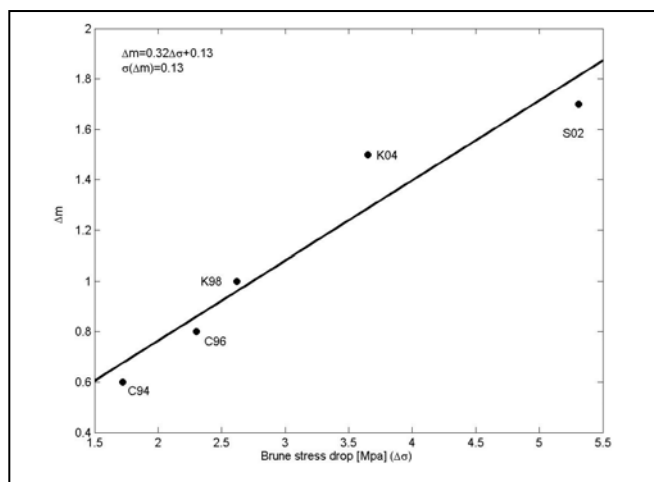


Figure 5. Relation between the Brune stress drop of the mainshock and the magnitude difference between the mainshock and the largest aftershock estimated for some seismic sequences in NE Italy (Gentili and Bressan, 2007).

The objectives of the Task 5 have been partially revised after that the geophysical investigations on the accelerometric sites that recorded strong earthquakes in Italy have been moved to the new project S6, not involving OGS. We have focused our efforts on the estimation of the maximum reduction of the standard deviation σ associated to ground motion relations obtainable either by site classification or using the H/V spectral ratios (HVSRS) computed from microtremors.

The introduction of a soil classification in a ground motion relation is often unsatisfactory, because it has only a marginal effect on σ . We have investigated on the subject by analyzing the residual from a ground motion relation for 399 values of PGA in the strong motion range (magnitude between 5 and 7.6) collected at 142 sites in Europe and the Middle East (Bragato, 2007). By applying cluster analysis to the residual we have found that site effects contribute to 33% of the total σ , a proportion that is much higher of what found by Lee et al. (1998) in California. Furthermore, there is the theoretical possibility of reducing by σ by 23% using only 3 categories. On the other hand the available geological classification into 3 soil categories according to V_{s30} (soft soil, stiff soil and rock) gives no reduction of σ , a result similar to what found in USA for

analogous soil classifications (e.g., Lee and Anderson, 2000). The main conclusion of the work is that in Europe site classification could help to reduce σ but the current classification is inadequate, so that alternative, better classification schemas should be developed. We have assessed the possibility of characterizing site effects in ground motion relations using HVSRs from noise recordings. For the analysis we recorded noise and computed the spectral ratios for 9 accelerometric stations active during the 1976 Friuli seismic sequence (Barnaba et al., 2006). For each station we computed the average ratio between 1 and 8 Hz (HVS1-8). With the exception of one station (BUI), which experienced liquefaction effects, HVS1-8 is well correlated ($R=0.78$) with the average station residuals of $\log(\text{PGA})$ computed for a ground motion relation valid for the area (Fig. 6).

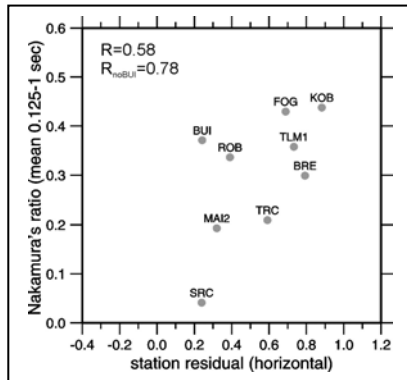


Figure 6. Correlation between the average station residual from ground motion relation (PGA) and the logarithm of the average HVSRs between 1 and 8 Hz computed from noise recordings at the accelerometric stations of the 1976 Friuli sequence (Barnaba et al., 2006).

Using the available PGA values and excluding station BUI, we have estimated the ground motion relation

$$\log(\text{PGA}) = c_1 + c_2 M + c_3 \log(r) + c_4 \text{HVS1-8}$$

for three magnitude classes (4-5, 5-6 and >5.8 , including 67, 37 and 22 observations, respectively) and compared the resulting σ with that obtained without site correction. We found that the inclusion of the HVSR term has maximum effect at low magnitudes, where σ reduces by 23%, is useful at intermediate magnitudes (reduction of σ by 14%), while the impact is scarce for magnitude greater than 5.8 (reduction by 8%). Though the data are too scarce to draw firm conclusions, the analysis gives a useful indication about the range of applicability of the technique.

One of the sites with high amplification (Tolmezzo/Ambiesta dam, TLM1 in Figure 6) was studied into detail in the framework of the SEISMOVALP project cited above. The study (Barnaba et al., 2007) includes spectral analysis of the 1976 strong motion recordings, near-surface S-wave profiling by surface wave analysis and the azimuthal analysis of HVSRs. The results attribute the observed amplification to the relief and its interaction with the nearby dam-reservoir system.

References

- Barnaba C., Bragato P.L. and Romanelli M., 2006. Acquisizione ed elaborazioni H/V di misure di rumore ambientale nei siti della Rete Temporanea ENEL-ENEA del 1976-77, OGS report Rel. OGS 2006/67-CRS 12.
- Barnaba C., Priolo E., Vuan A. and Romanelli M., 2006. Site effect of the strong-motion site at Tolmezzo-Ambiesta dam in northeastern Italy, Bull.Seism.Soc.Am. 97, 339-346.
- Bragato P.L., 2007. Optimal site classification for empirical ground-motion relations, submitted to Bull.Seism.Soc.Am.
- Bressan G., 2005. Modelli di velocità 1D dell'Italia nord-orientale, OGS report Rel. OGS 2005/20-CRS 5.
- Gentili, S., 2006. Identificazione delle sequenze di aftershock nelle Alpi nord-orientali, OGS report Rel. OGS 2006/71-CRS 15.

- Gentili S. and Bressan G., 2007. The aftershock sequences in the Friuli - Venezia Giulia region and western Slovenia in the last thirty years. OGS report Rel. OGS 2007/16-CRS 5.
- Lee, Y., Zeng Y. and Anderson J.G., 1998. A simple strategy to examine the sources of errors in attenuation relations, Bull. Seism. Soc. Am. 88, 291-296.
- Lee, Y., and Anderson J.G., 2000. Potential for improving ground-motion relations in southern California by incorporating various site parameters, Bull. Seism. Soc. Am. 90, S170–186.
- Saraò A., 2007. Feasibility study of automatic moment tensor determination at CRS. OGS report Rel. OGS 2007/60-CRS 16.

2.2 Specific problems which have delayed progress

2.3 Relevant publications which have arisen directly from this project

Publications JCR

Bragato P.L., 2007. Optimal site classification for empirical ground-motion relations. Submitted to Bull.Seism.Soc.Am.

Abstracts/conference presentations

Gentili, S., Bressan, G., 2007. PI, RI, and RTL: three earthquakes forecasting methods applied to moderate earthquakes in the northeastern Italy and western Slovenia areas". Presented at: 5th International Workshop On Statistical Seismology: Physical And Stochastic Modelling Of Earthquake Occurrence And Forecasting (Poster) EMFCSC, Erice - Sicily (Italy), 31 May - 6 June, 2007.

Progetto S4 - STIMA DELLO SCUOTIMENTO IN TEMPO REALE E QUASI-REALE PER TERREMOTI SISGNIFICATIVI IN TERRITORIO NAZIONALE

Responsabili: Luca Malagnini (INGV-ROMA) e Daniele Spallarossa (Unige)

Achievement of Project Deliverables

Following the list deliverables listed in the approved project, the research unit (RU) has achieved the following applicative deliverables:

- Updating of the seismic network (i.e. real time transmission system)
- Prototype implementation of the USGS-ShakeMap package at Dip.Te.Ris..
- Prototype of web site accessible at <http://www.dipteris.unige.it/geofisica/AutoLoc.php> where earthquake locations, and ground motion maps (PGA, PGV, instrumental intensity) are published.
- Implementation of fully non-linear earthquake, global search methods for earthquake location.

In addition, the main research achievements obtained by the RU during the project are: Three-dimensional velocity model for the South-western Alps and Northern Apennines.

In detail, the RU has been involved in Tasks 1, 2, 3 and partly in 5 of the approved project. Here it follows a description of the work done and the results obtained in each task during the two year project. Other deliverables are listed in the reports of the individual tasks.

TASK 1

In the framework of task 1, Dip.Te.Ris updated the seismic network of NorthWestern Italy (RSNI network) improving the potentiality of real time seismic monitoring. Modern high quality seismic instruments have been installed (i.e. analogical 1C stations have been replaced by digital Nanometrics Taurus equipped with 3C sensors: Trillium 40s or Trillium 240s) and high velocity digital transmission systems have been used (i. e. RUPA network or Satellite system) with the aim to transfer and to process seismic data by real time procedures. Figure 1 shows the current configuration of the network. The Dip.Te.Ris. manages three kinds of seismic stations:

- Digital stations equipped with 3-component sensors connected in real time to the seismological laboratory of the Dip.Te.Ris by using RUPA or Satellite/RSP connection. (Red triangles, figure 1)
- Digital stations equipped with 3-component sensors using a “Dial-up” transmission system. Recordings are transferred to the Dip.Te.Ris. Processing Centre every two hours using modem transmission system Telecom or GSM (mobile phones). The system automatically calls the stations to get information on the seismicity occurred in the last two hours. In case of strong event it is possible “to force” the callings to the dial-up stations in order to dispose of the recordings within 10-15 minutes (blue triangles, figure 1).
- Analogical stations equipped with 1-component sensors connected in real time to the seismological laboratory through CDA connections (green triangles, figure 1).

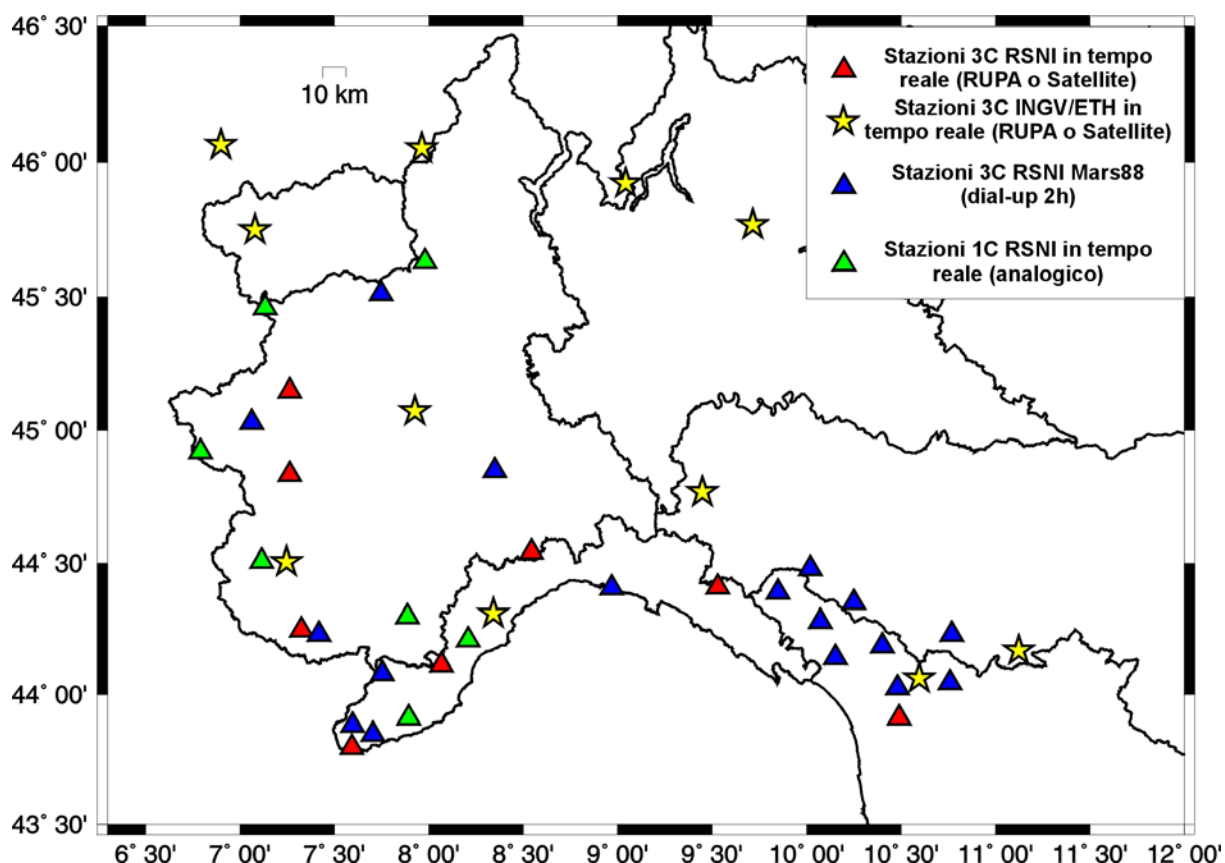


Figure 1: Actual configuration of the RSNi network (triangles) and of the INGV and ETH stations that are included in the automatic location procedure described in the following paragraphs.

The updating of analogical 1-component stations (green triangles in fig.1) into digital ones equipped with 3C broad-band sensors and with a real time connection system based on RUPA or Satellite (RSP) connection provided by INGV have been almost completed. Besides the transmission system, the existing 1C station instrumentations have been substituted by 3C broad-band TRILLIUM 40 coupled with high resolution acquisition systems (TAURUS, Nanometrics). At the moment, all real time digital 3C stations (red triangles in fig. 1) are shared with the INGV. At the same time, some INGV stations with the same instrumental characteristics (yellow symbols in fig.1), transmit on real time to the Dip. Te. Ris, allowing for a fast and efficient data exchange. It is important to highlight that within this Task of the DPC S4 Project, not only the procedure useful to guarantee a real time connection among the most RSNi stations has been developed, but also the one to share, in real time, information with INGV.

TASK 2

Recently the use of tomographic inversion methods has allowed us to accurately define both 1D and 2D models for South-Western Alps and Northern Apennines. The tomographic study covers an area of about 380 x 460 km extending in latitude from about 43° N to 46°N 50' and in longitude from 6° E to 12° E. 3958 local events have been used for a total of 59.781 P phase first arrivals and 44.863 S phase first arrivals.

Vp and Vs 3D velocity models have been obtained for the area under study. Since the P velocity distribution was widely studied in the past, we mainly focus our attention in discussing S-velocity model and Vp/Vs ratio.

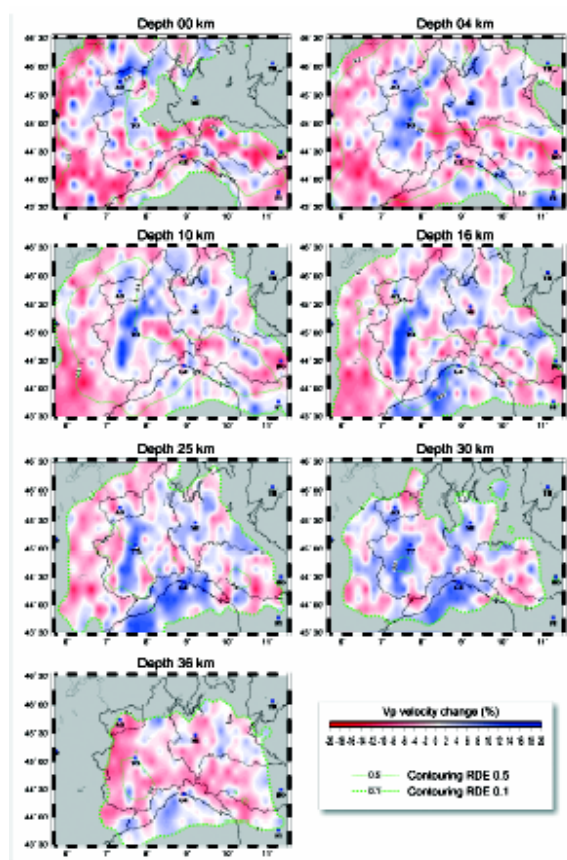


Figure 2: Velocity model expressed as variation from the average velocity of each layer.

TASK 3

The aim of this task is the development of automatic procedure for phase picking and for event location. Considering the technological and instrumental updating of the RSNi network, allowing real time transmission (e.g. via satellite and/or RUPA connection) of data recorded by 3C stations (Broad-band and short period) to the CED, automatic picking and location procedure have been strongly improved. During the first stage, data from real time stations (1C and 3C) were processed using a two-step automatic picking. The first step implies the P and S detection through the APK algorithm (sac2000), based on Allen (1978) procedure. This method works on pre-processed signals considering “fixed” band-pass filters carefully calibrated for each station on the base of a trial-and-error procedure. The second stage implies the use of the re-picking algorithm “Mannekenpix 1.7” (Alderson, 2004). This algorithm allows the improvement of the automatic detection of the P phase obtained by the previous picking. In the case of 3C stations, the P phase arrival time is searched analyzing the vertical component, while the S phase one considering the two horizontal components and averaging the S arrival times observed.

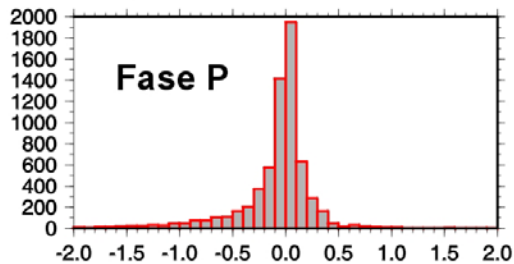
Afterwards, the automatic picking procedure was improved using a “variable” band-pass filter for the pre-processing of data. This filter based on the S/N ratio allow to define, for each event and station, a variable frequency band where P and S phases are particularly evident and consequently detectable from the STA/LTA analysis computed by the APK algorithm.

More recently, a new procedure has been developed by applying a method based on the seismic signal envelope and on the Akaike Information Criterion (AIC). The P- and S-phase arrival time is detected selecting the minimum of the AIC function (Sleeman and Eck, 1999). In detail the steps are:

- Event detection
- Creation of a directory containing the SAC format waveforms transmitted on real time from the RSNi and INGV networks (by using stations shown in fig 1 as red and green triangles and yellow stars).
- Preliminary signal filtering (BP 2.5 – 15 Hz) and envelope using a threshold of 0.16 (vertical component).
- Computation of the AIC function on the previously selected window and recognition of P arrival time as minimum of AIC function.
- Pick validation based on S/N ratio analysis
- Preliminary location based on the validated picks (only P phases) using the Hypoellipse code (Lahr, 1979).
- Validation of the location quality.

- Definition of the theoretical S arrival times through a simplified velocity model and selection, for each station, of a time window around the theoretical S arrival time.
- Computation of the AIC function on the window selected in the previous step and recognition of S arrival time as minimum of AIC function
- Pick validation based on S/N ratio

Picking APK + Mannenkepix



Picking AIC

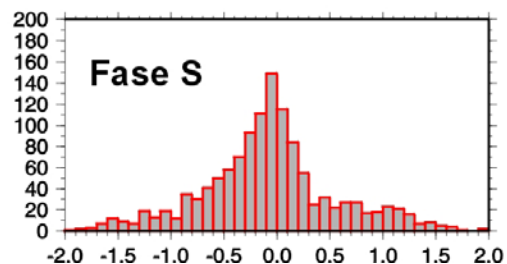
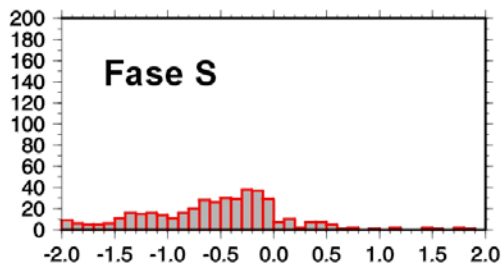
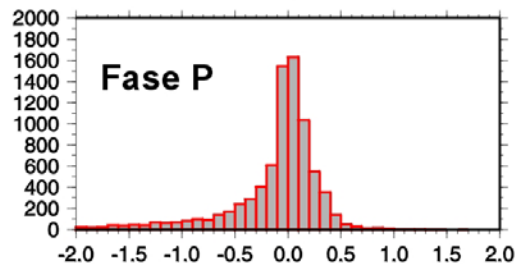


Figure 3: Differences between automatically and manual detected P arrival times (upper panels) and between automatically and manual detected S arrival times (lower panels). Right panels show results obtained using the AIC based procedure, while the left ones using the APK based procedure.

It is worth noting that the APK based procedure is more selective, while the AIC allows the detection of a larger number of S arrival time.

On the base of automatic picks, the event location is calculated by Hypoellipse code (Lahr, 1979) using different 1D velocity models calibrated for the area monitored by the RSNI network (Spallarossa et al., 2001). Recently NonLinLoc method (Lomax et al., 2002, Lomax et al., 2001) have been introduced and tested. This method is applied using the 3D velocity model coming from tomographic inversion described in Task 2.

In the following figures a comparison among automatic locations obtained using the two different automatic picking procedures and the two location procedures is shown.

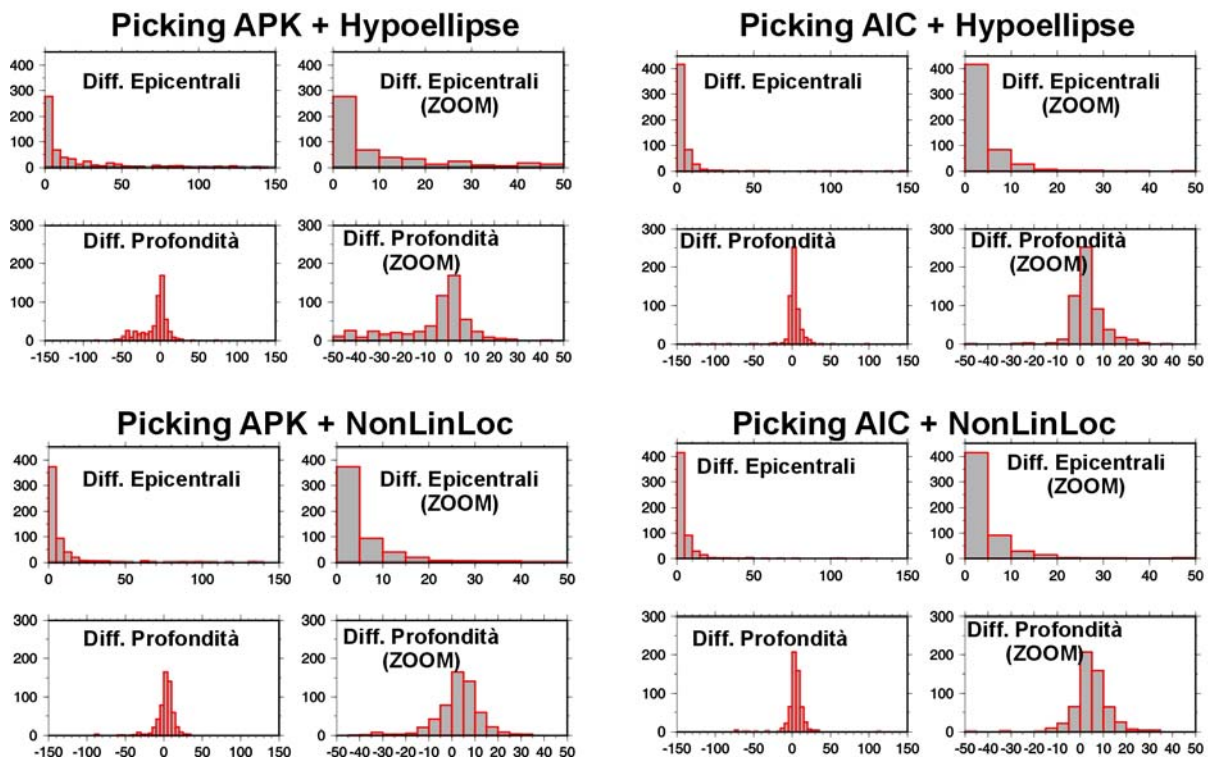


Figure 4: Differences between automatic and manual locations.

For the time being, the automatic location procedure working at Dip.Te.Ris. is based on:

- AIC based picking
- Hypoellipse code

It is important to highlight that the location procedure is extremely robust in recognising “false” events (as verified through a different tests), as anthropical or natural noise. In those cases the S/N-based validation systems of the automatic picking procedure allow the identification of “false” events.

Regarding the magnitude computation, at the moment, the code developed by the Dip.Te.Ris. and applied in Spallarossa et al. (2002) is used. It allows to automatically compute MI values for the North-western Italy seismicity. Recently the method has been updated by calibrating the relationship parameters using a dataset of 7000 events recorded from 1998 to 2006 by 29 stations (25.000 Wood-Anderson amplitudes; max magnitude 5.1).

Finally the Dip.Te.Ris. developed an automatic moment magnitude computation based on the methodology proposed by Mayeda et al. 2003. A set of correction parameters to be used in the automatic procedure have been carefully calibrated for the real time 3C stations of the RSNI, ETH and INGV within the North-western Alps and Northern Apennine. Previous works (Morasca et al., 2005a, Morasca et al. 2005b) calibrated such parameters for few of these stations and using two slightly different methodology, consequently it was necessary to re-calibrate the parameters using

all real time stations and exactly the same methodology for the Northwestern Alps and Northern Apennines.

The automatic procedure is based on the coda waves analysis that allows to obtain stable amplitude measurements compared to the more commonly used direct waves amplitudes. In fact coda waves are less influenced by random effects and radiation pattern reducing the scattering in the source and path terms. In general the coda-based magnitudes are roughly a factor of 3 to 4 more stable than any direct phase measurement. This means that a single station coda measurement could be enough for a good quality Mw definition. Another advantage of the method is in the extension of Mw estimates to significantly smaller events which could not otherwise be waveform modelled. Figure 5 shows an example of automatic Mw computation based on the coda waves analysis for three large events. Notice that although the large scatter for the event of Salo' due to the location external to the network, the Mw value is comparable to the one obtained by MedNet and SED.

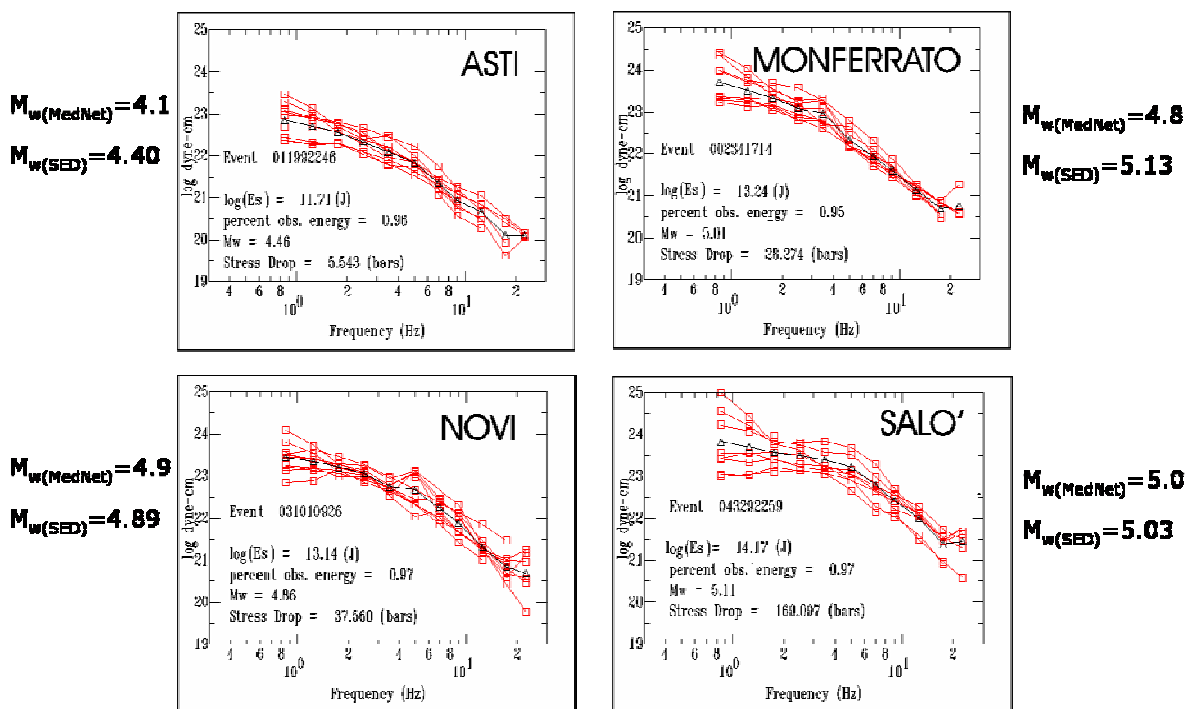


Figure 5: Example of automatically derived source spectra used for the Mw computation. Red curves are station source spectra, while black curves are the averages over all stations. The automatic Mw is derived on the base of the average spectra.

Once hypocentral coordinates and magnitude are automatically defined for an event, another automatic procedure is applied in order to validate the obtained parameters. This method, based on the evaluation of the parameters associated to the location quality (i.e. GAP, number of phases, ERH, ERZ, rms) and on the magnitude value, allows a controlled management of further

analysis and divulgation procedure of the data. In detail, for good quality location (i.e. $GAP < 275$, $ERH < 30$ km, $ERZ < 50$ km, $N. fasi > 4$, $rms < 1.0s$) and for events with $Ml > 2.0$ the following procedures are applied:

- Sending of e-mail (to a selected e-mail addresses) including all location parameters and a link to a web page (<http://www.dipteris.unige.it/geofisica/AutoLoc.php>) where the epicentre map, the location string, the PGA and PGV values for each station, the list of towns closer to the epicentre and the automatic arrival times are shown. When also the shake map is computed, it is shown in the same web page, but a password is necessary to see it.
- Sending of an SMS (to a selected phone numbers) including the location string (Hypocentral coordinates, magnitude, the closest town and the quality parameters (ERH, ERZ, GAP,..)).
- Elaboration of the shake and intensity maps using the Shakemap code

Shakemap is a code that allows the elaboration of shake maps (in terms of PGA, PGV, PSA) and intensity maps, combining experimental shake parameters obtained from seismic recordings, calibrated attenuation laws and local amplification information. The automatically determined ground shaking parameters (PGA and PGV values computed at seismic stations) are used to constrain the shake-maps computed on the base of the event characteristics (magnitude, hypocentral coordinates) and of the considered attenuation laws.

Information about the local geology, important for the site effect estimation, are introduced in the code.

Adequate attenuation laws are also introduced by testing attenuation law proposed by Sabetta e Pugliese (1996) for events with $Ml > 4.5$; and the one proposed by Frisenda et al. (2004) for smaller events. Within the end of the project we will introduce a new attenuation law derived by the Dip.Te.Ris. in collaboration with the INGV of Milan and the OGS (Trieste).

Likewise, it was necessary to introduce a law valid for the whole Italian territory for the conversion of the shake parameter PGV in "instrumental" intensity (Faccioli e Cauzzi (2006)).

TASK 5

For all RSNi stations, the H/V spectral ratio have been used for preliminary analysis of site effects; in the framework of this task, the Dip.Te.Ris. has improved the definition of local seismic response of installation sites by a complete classification procedure. For the time being, the classification procedure has been completed only for site showing significant site effects on the ground of H/V analysis and/or station correction parameters computed in calibrating local magnitude scale (Spallarossa et al., 2002),.

The classification procedure can be summarized as follow:

- Geological and stratigraphical analysis (i.e. depth of bedrock, geotechnical characteristics of superficial deposits) of sites where RSNi seismic station are installed and site response estimate
- Detailed geological survey including geophysical measurements (i.e. MASW) and compilation of geological-geomorphological form for each RSNi station
- Geological and geophysical classification of sites where seismic station are installed and definition of a suitable amplification factor concerning site effect (useful for reducing PGA, PGV to rock condition and for computing shaking and intensity maps by Shakemap code)

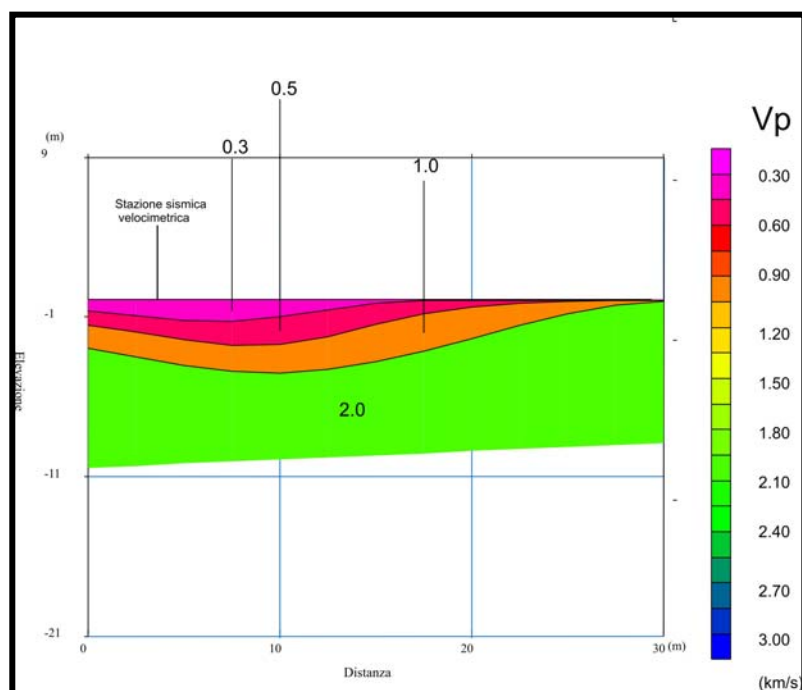


Figure 6: refraction seismic tomography for VINM station (Vinca, Northern Apennines)

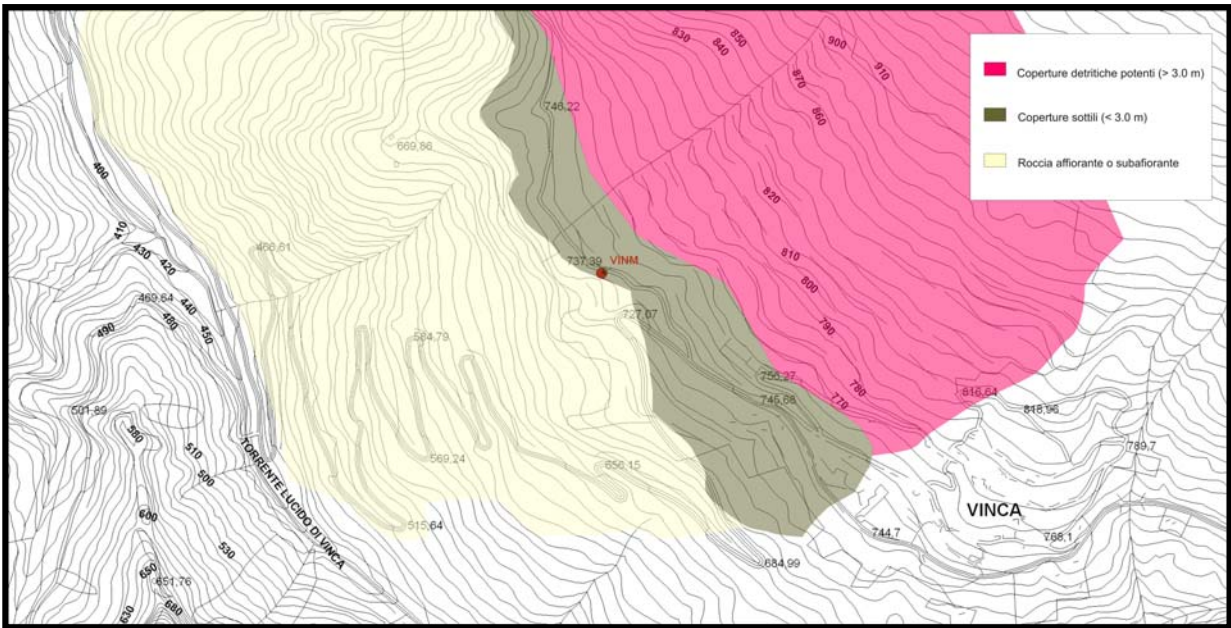


Figure 7: geomorphological map of site of VINM station

Scheda geologico-geomorfologica delle stazioni sismiche della Rete Sismica	
Nome della Stazione	VINM
Localizzazione	Località Vinca –Chiesetta della Madonna - Fivizzano (MS)
Elemento C.T.R.	249060
Latitudine (WGS84)	44N0847
Longitudine (WGS84)	10E0913
quota	710 m.s.l.m.
rilievo in sito	l'area è collocata piede del corpo di frana in prossimità di un salto morfologico; la frana è costituita da materiale proveniente dalla creste rocciose soprastanti e presenta granulometria non classata con trovanti di dimensioni metriche. La frazione granulare prevalente è cementata per la presenza di materiale calcareo come principale costituente della frana
Unità Litologico-Tecnica / Litologia	U.L.T. C1 Detriti e discariche di cava soprastanti la Formazione di Vinca (S.G.I., 1970, Foglio 96 Massa)
morfologia	la frana, che risulta essere quiescente e/o in parte stabilizzata, è collocata in corrispondenza di un gradino morfologico di probabile origine glaciale collocato lungo un versante dall'acclività elevata (superiore a 45°) che diminuisce bruscamente al piede della nicchia di distacco principale del corpo franoso. La presenza di una nicchia così estesa può essere ricondotta a superfici scollamento tettonico che interessano le formazioni geologiche costituenti i versanti soprastanti il corpo di accumulo
distanza dalla prima rottura significativa di pendio	la Chiesetta è ubicata a circa 50 m dal gradino morfologico glaciale ben evidente, in corrispondenza del quale si passa da una pendenza di circa 10°-15° relativa alla frana a valori molto elevati superiori a 50° fino all'alveo del torrente Lucido
presenza di acque superficiali	accumuli franosi come questo, che presentano assente o scarsissima frazione fine interstiziale, hanno un comportamento permeabile per porosità con coefficienti estremamente elevati mentre il basamento roccioso sottostante risulta essere praticamente impermeabile: la presenza di una falda sub superficiale è facilmente ipotizzabile considerato il continuo apporto dal versante roccioso soprastante e la forte presenza di acqua alla base del corpo di frana
presenza di frane	il corpo di frana su cui è ubicata la stazione sismica ha un estensione di alcuni Km ² e su di esso si sviluppa l'intero centro abitato del paese di Vinca; gli spessori massimi sono nell'ordine delle decine di metri mentre in corrispondenza della stazione tali spessori sono ridotti a qualche metro
prove in situ	MASW - Sismica a rifrazione con strumentazione a 24 canali
Vs 30	920
Fenomeni di amplificazione	Dal punto di vista geologico-stratigrafico non sono state individuate le condizioni per la presenza di effetti di sito (Sito Tipo A = roccia) anche se le condizioni morfologiche potrebbero portare a effetti di sito topografici

Figure 8: Form regarding the site classification of VINM station

References

Allen R.V., 1978: Automatic Earthquake recognition and timing from single traces; *Bull. Seism. Soc. Am.*, Vol. 68, No. 5, pp 1521-1532

Lahr J.C., 1979: Hypoellipse: a computer program for determining local earthquake parameters, magnitude, and first motion pattern, U.S. Geol. Surv., Open File Rep. 79-431 pp.

Lomax A., Curtis, A. (2001). Fast, probabilistic earthquake location in 3D models using oct-tree importance sampling, *Geophys. Res. Abstr.*, **3**, 955.

Lomax, A., Virieux, J., Volant, P. and Berge C. (2000). Probabilistic earthquake location in 3D and layered models: introduction of a Metropolis – Gibbs method and comparison with linear locations, in *Advances in Seismic Event Location*, C. H. Thurber and N. Rabinowitz (Editors), Kluwer, Amsterdam, 101-134.

Morasca P., Mayeda K., Malagnini L. and Walter W.R., 2005a: Coda-derived source spectra, moment magnitudes and energy-moment scaling in the Western Alps; *Geophys. J. Int.*, 160 (1), 263-275.

Morasca, P., Mayeda, K., Gök, R., Malagnini, L., Eva C. (2005). A break in self-similarity in the Lunigiana-Garfagnana region (Northern Apennines). *Geophysical Research Letters* Vol. 32, No. 22, L2230110.1029/2005GL024443

Sleeman, R., and T. v. Eck (1999). Robust automatic P-phase picking: an on-line implementation in the analysis of broadband seismogram recordings, *Phys. of the Earth and Planet. Int.*, 113, 265-275.

Spallarossa D., Ferretti G., Bindi D., Augliera P. e Cattaneo M. (2001): Reliability of earthquake location procedures in heterogeneous areas: synthetic tests in the South Western Alps, Italy, *Phys. Earth Plan. Int.*, 123

Spallarossa D., Bindi D., Augliera P. and M. Cattaneo (2002 - a). An MI scale in Northwestern Italy, *Bull. Seism. Soc. Am.* Vol. 92, 2205-2216 pp.

INGV-DPC Project S4

**Stima dello scuotimento in tempo reale o quasi reale per terremoti
significativi in territorio nazionale**

Section 2. Report from individual Research Units

INGV-DPC Project S4 - Stima dello scuotimento in tempo reale o quasi reale per terremoti significativi in territorio nazionale

Research Unit S4/05

Responsible:

Giovanni Costa, Dipartimento di Scienze della Terra, Università di Trieste

2.1 Achievement of Project Deliverables

Task 3

Real-time moment magnitude computation.

An algorithm for the moment magnitude (M_w) estimation has been developed applying the methodology described in Andrews [1986]. This methodology uses the Brune spectrum and the corner frequency and is applied to the S waves. The relative code is written in MATLAB and interfaced with the Antelopeã real-time system installed at DST, hereafter SYSTEM. The code reads the data (waveform, event location, instrumental calibrations, etc.) directly from the SYSTEM and adds two new tables (station M_w and network M_w) to the database. This permits to obtain M_w in real-time for the events localized by the system. At DST a database is maintained in the framework of the project Interreg IIIa Italia/Austria “Reti sismologiche senza frontiere nella Alpi sud orientali” since 2004, and contains the waveforms of the Austria (ZAMG), Slovenia (ARSO) and Friuli Venezia Giulia (DST and OGS) seismological networks. Broadband data and strong motion data relative to about 50 stations, 193 events, 3576 traces, has been analyzed in order to test the code (Fig. 1). The standard deviation of the single station moment magnitude estimates with respect to the average event estimate is rather low and does not depend on distance. The method gives moment magnitude values in very good agreement with independent estimates (moment tensor inversion). For all events the retrieved moment magnitudes are compatible, even for the smallest considered ones, with the local magnitudes given by the SYSTEM. For the Bovec 1998 event, for which there is an independent fault size estimate, the equivalent radius value derived with this method validates our procedure. The procedure is ready to be used in real-time at DST.

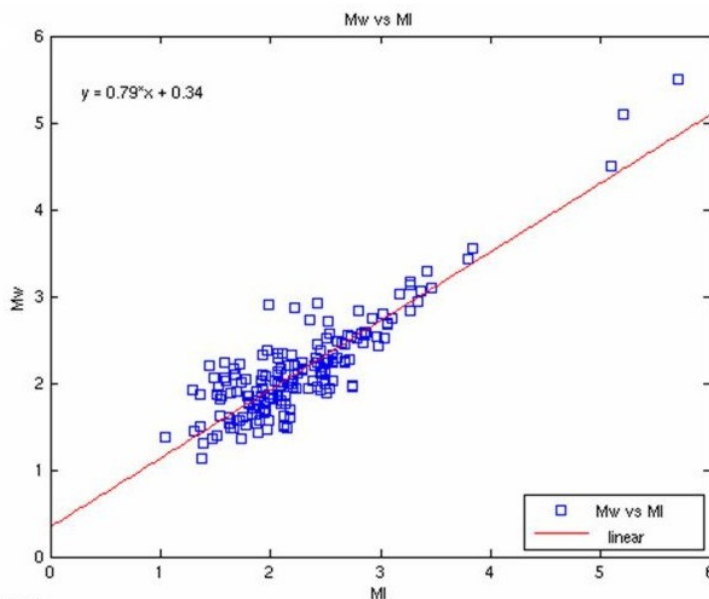


Figure 1

Figure 1. Comparison between local Magnitude (MI) and Moment magnitude (M_w) computed using Andrews (1986) methodology.

In order to compare our methodology with a different approach used by other UR in this project, M_w has been computed for about 143 events ($1.0 \leq M_w \leq 4.0$, hypocentral distance between 20 and 225 km, depths generally less than 15 km) applying the empirical method based on coda envelope amplitude measurements described by Mayeda et al. (2003). The work has been done in cooperation with the UR of DipTeris, University of Genova. Earthquakes distributed throughout the eastern Alps recorded by two broad-band sensors operated by the NE-Italy BroadBand Network have been analyzed. The two stations TRI (Grotta Gigante, Trieste, reference station) and VINO (Villanova delle Grotte, Udine), both located in a natural cave, have been considered. To calibrate the source moment-rate spectra, independent moment magnitudes from long-period waveform modelling for two moderate magnitude events in the region: Bovec 2004, $M_w=5.2$ (Harvard) and Carnia 2002, $M_w=4.7$ (MedNet) have been used. After these two stations calibration M_w has been computed for the complete dataset (Fig. 2).

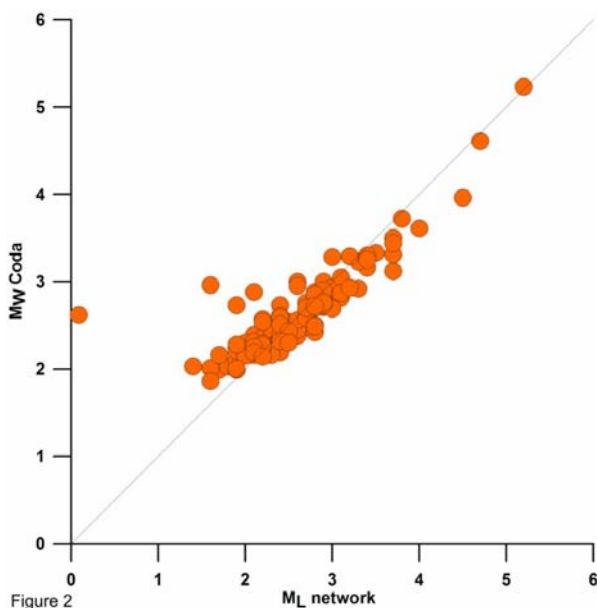


Figure 2. Comparison between local Magnitude (M_L) and coda moment magnitude (M_w) computed using Mayeda et al. (2003) methodology.

Real-time shake-map implementation.

The TriNet “ShakeMap” software (ver 3.0.1, Wald et al., 1999b) has been interfaced with the SYSTEM that produces the waveforms, the location and the ground motion parameters (PGA and PGV), principal inputs for the shaking map generation. These data are extracted and transferred to the “ShakeMap”. Shaking maps have been produced also using Antelope directly, following a very similar procedure. This software has been tested generating the shaking maps related to the 2004 Bovec earthquake. After tested with success this routine, we have decided to concentrate our effort on the more flexible and universally used TriNet software.

The V_{s30} values obtained from the soil topography (global digital elevation model, gtopo30, USGS), from the geological map of Italy provided by the UR of INGV Rome and from the geological map provided by the Geology Department of the University of Trieste for Friuli has been used and the results compared. In this map the region is divided into three different soil types (bedrock, stiff soil and soft soil). The amplification factors are computed from the V_{s30} values at each site at four ranges of input acceleration levels for short periods (0.1-0.5s) and mid periods (0.4-2.0s) from Borchardt (1994). The map has been used for the tests and is actually routinely used for the real-time shake-map computation.

The ground motion relations (PGA; PGV; SA at 0.3, 1.0 and 3.0 s) have been computed (see task 4) using mainly waveforms recorded by the RAF. The intensity used to produce the intensity maps is derived from the ground motion parameters (PGA and PGV) and the definition of MMI

(Wood and Neumann, 1931). Different relations between PGA, PGV and MMI have been selected and shaking maps computed and compared using the relations proposed by Wald et al. (1999a) and Faccioli and Cauzzi (2006). In real-time shake-maps computation the latter relation is routinely used, since it is calibrated on Italian data. However, this kind of “instrumental” intensity has limitations and can be misleading, therefore it is better not to use it in the real-time shake-map context.

In order to test the influence of the number and geometry of the stations on the ground motion estimation, synthetic seismograms have been computed on a regular grid, and a scenario has been generated for the 2004 Bovec earthquake. Shake maps have been produced using the PGA and PGV extracted from the synthetic signals as input, computed in grids with increasing spacing. A Shake map is also computed using as input synthetic values computed only in correspondence of real recording stations. The final results depend strongly on the number of signals used and only if a large number of signals is available the ground motion pattern is accurately reproduced. In the 2004 real case the number of stations was insufficient.

In the Southern Alps area 8 earthquakes with $M \geq 4.5$ occurred in the last 30 years: Friuli (06-05-1976, 20:00, $M_I=6.3$; 11-09-1976, 16:31, $M_I=5.4$; 11-09-1976, 16:35, $M_I=5.7$; 15-09-1976, 03:15, $M_I=6.2$; 15-09-1976, 09:21, $M_I=6.1$), Bovec-Krn (12-04-1998, 10:55, $M_I=5.7$; 12-07-2004, 13:04, $M_I=5.4$) and Carnia (14-02-2002, 03:17, $M_I=5.4$). The related data was used to test our software calibration. The ground motion parameters have been extracted and the related shaking maps produced. Of course, the number of data available is completely different for the different events, very few for Friuli and Bovec-Krn 1998 events, a discrete number for the more recent ones. Consequently, also the accuracy in reproducing the real ground motion pattern changes. A comparison between the shake-maps relative to the main Friuli event computed by our UR and the UR of INGV of Rome, using the same data but in a completely independent way, has been done. The results are in very good agreement and very similar maps have been obtained for PGA, PGV and PSA.

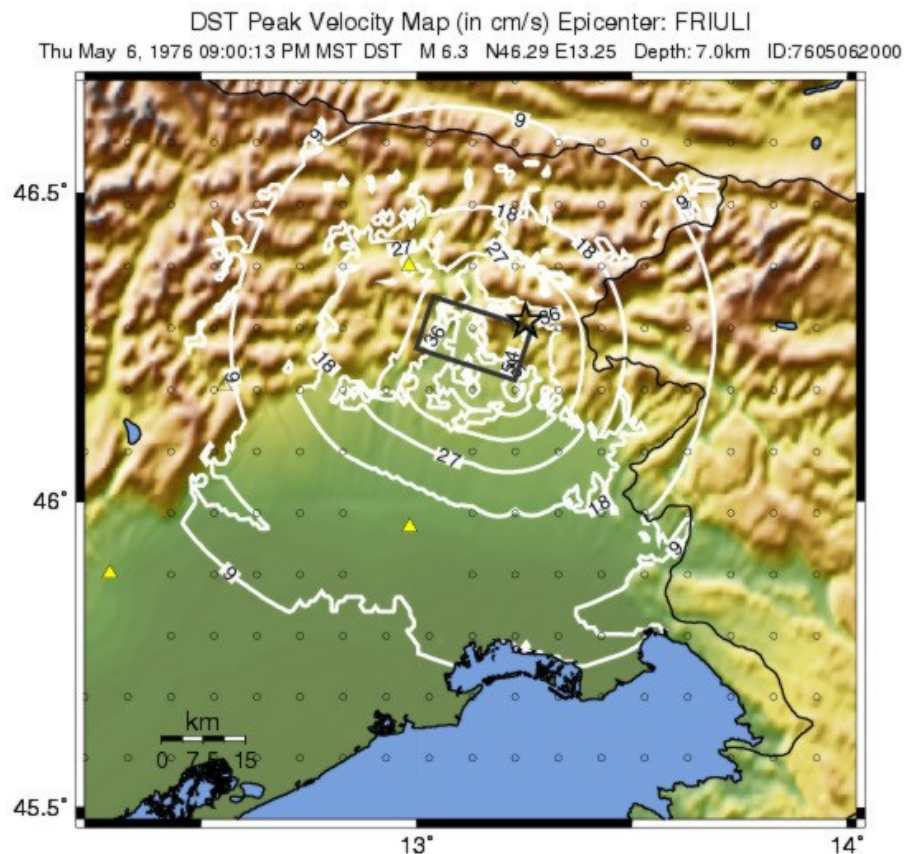


Figure 3. PGV shake map for an extended source model.

A detailed knowledge of the source parameters is required to generate the shaking maps with the finite-fault model and this approach was possible only for two seismic events: the 1976 Friuli (Fig. 3) and the 1998 Bovec earthquakes. The fault dimensions are used only in the source-receiver distance computation. The distance from the fault rupture is adopted. No theoretical information is available on the seismic moment distribution or the directivity effects and therefore only data from recording stations placed near the rupture area can provide us hints on these finite-fault effects. The ground motion profile follows the fault shape but in the near field the ground motion pattern is different if short- or long-period parameters are considered. Of course for the Friuli earthquake the introduction of the finite fault decreases the values of PGA and SA at 0.3 s with respect to the point-source ones, while the estimations of PGV and SA at 1.0 and 3.0 s do not vary much. On the other side the Bovec earthquake has a smaller magnitude and the values of PGA and SA at 0.3 s follow the trend of other parameters and they do not decrease as strongly as in the previous example.

Once the shake-map software has been calibrated and extensively tested, it has been definitively inserted in the real-time system running at DST. At the same time the software was implemented to generate the Web pages of the earthquakes in real-time and to send E-mail messages when new maps are available. Starting from January 2007, shake-maps are computed in real-time for more than 100 events in the Southern Alps area using the data contained in the DST Antelope database (Fig. 4).

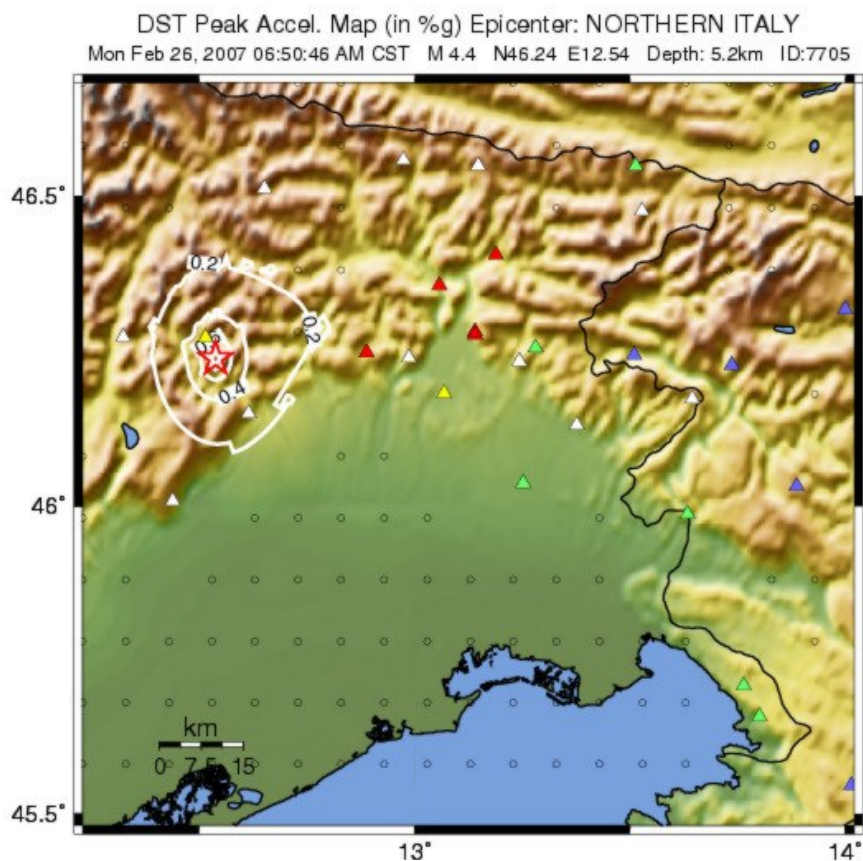


Figure 4. Example of real-time shake map computation.

In order to test the goodness of the actual network configurations, scenarios for some historical earthquakes have been computed. The synthetic seismograms are computed for the receivers placed where the recording stations are or will be installed. Three seismic events occurred during the last century in the Southern Alps area (1936 Cansiglio earthquake, 1976 Friuli earthquake and 1998 Bovec-Krn earthquake) have been considered. The reflectivity model (Kennett, 1981) is used to compute the synthetic seismograms and an average 1-D structural model of the area selected. The

synthetic signals are produced for an upper frequency of 1 Hz, so the ground motion relations have been computed by low-pass filtering the observed data of events with $M \geq 4$. The sources parameters are derived from other studies. The ground motion parameters (PGA and PGV) are extracted from the synthetic signals and used as input file in the ShakeMap software to generate the scenarios (Fig. 5).

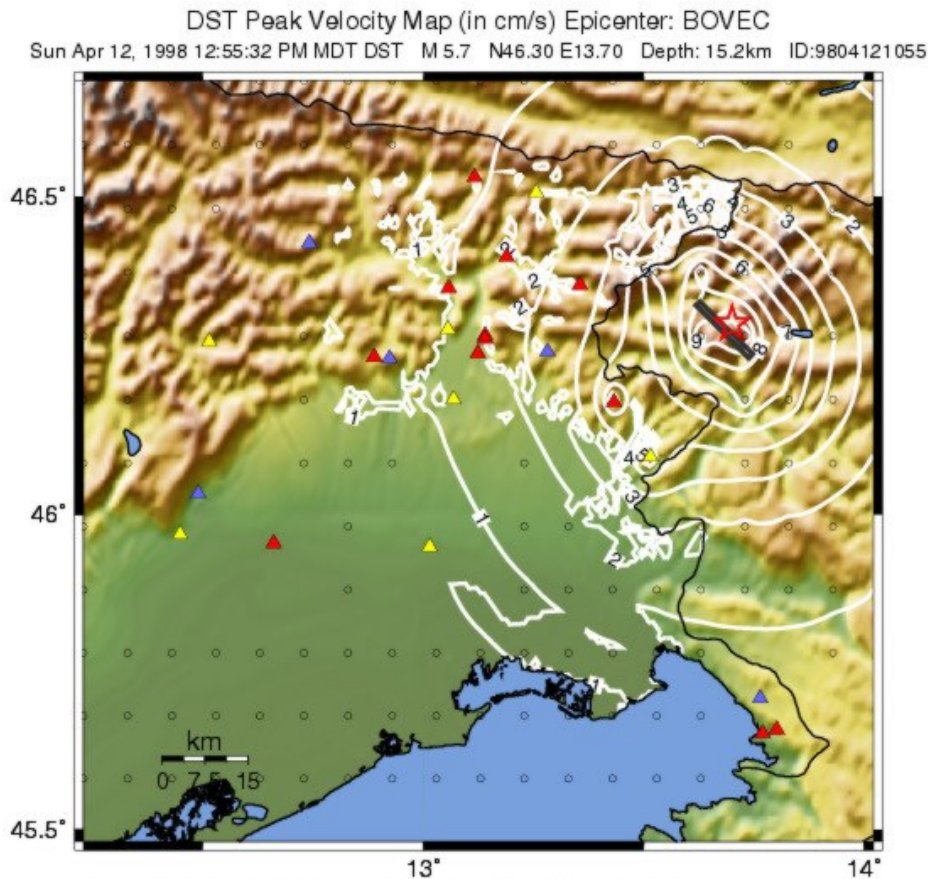


Figure 5. Scenario for PGV (10Hz) in the case of the $M_L=5.7$ Bovec 1998 event (Slovenia).

Task 4

Ground motion relations

The ground motion relations (PGA; PGV; SA at 0.3, 1.0 and 3.0 s) have been computed using mainly waveforms contained in the RAF database. The database, maintained by DST, contains 570 three-component high-quality waveforms related to 362 seismic events occurred in NE Italy, Austria and Slovenia. The magnitude range is $1.0 \leq M \leq 5.6$ and epicentral distances less than 400 km. In this study we consider also several high-magnitude events occurred in the past in NE Italy and Slovenia, their waveforms being taken from the ESD database (Ambraseys et al., 2002). We chose 17 events with $M \geq 4.5$, the strongest one ($M_w=6.5$) being the Friuli May 6, 1976 earthquake.

After an extensive analysis of the catalogues available for this region, the OGS catalogue has been used (location and magnitude) to compute the regression parameters for attenuation relations, because this catalogue has been reviewed. Since OGS does not provide ML for all considered seismic events, linear regressions have been computed between local magnitudes estimated by OGS and ML provided by other catalogues. For the Friuli 1976 sequence the locations and magnitude values have been taken from the ESD database. The attenuation relations have been estimated for PVA and for two different types of PHA (largest component and vectorial addition). The path between the source and receiver does not take into account the event depth and epicentral distances are in the 1-100 km range. Different attenuation models have been considered by selecting different functions of distance and different correction factors, due to magnitude saturation, and dependence

between magnitude and distance; typical statistical parameters (R2, R2-adjusted, t-value, F-value...) valuing the goodness of the model have been computed and residual distribution studied using the R open-source software (www.r-project.org). The final best model is:

$$\log_{10}(PGA) = c_0 + c_1 \cdot M + c_2 \cdot \log_{10}(r) + (c_3 + c_4 \cdot \log_{10}(r)) \cdot M^3 + c_5 \cdot S \pm \sigma$$

with $r = \sqrt{d^2 + h^2}$. The obtained standard deviation values ($\sigma_{PVA}=0.338$, $\sigma_{PHA(lc)}=0.361$, $\sigma_{PHA(va)}=0.359$) are comparable with previous studies (Fig. 6). The PGA dependence on magnitude and distance has been also analyzed for three different ranges ($3.0 \leq MI \leq 4.0$; $4.0 \leq MI \leq 5.0$; $5.0 \leq MI \leq 6.3$).

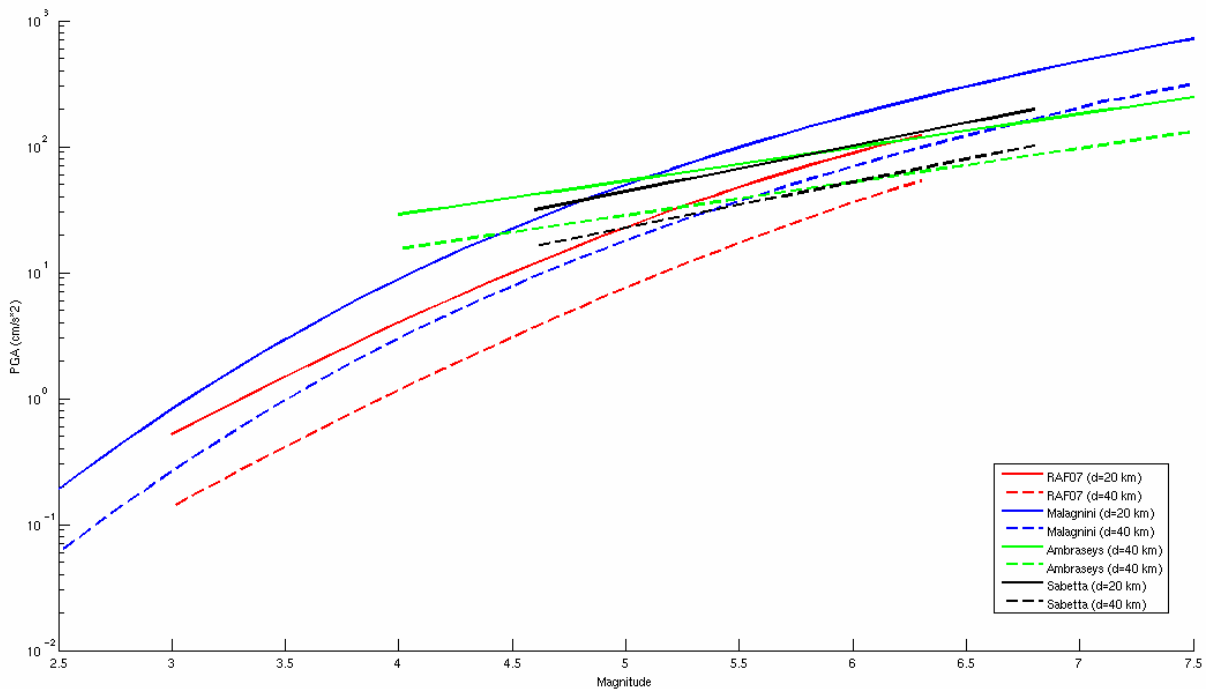


Figure 6. Comparison of different attenuation relations for the largest horizontal magnitude (Malagnini considers the horizontal median).

Empirical attenuation models for amplitude, frequency content and duration parameters of ground motion.

Ground motion relations have been computed for Northern Italy merging observed data recorded by RSNI, RAF, INGV-CNT, INGV-MI, ARSO, SDS-net etc. in the last 30 years (612 waveforms recorded since 1976 with $3.5 < ML < 6.3$, maximum epicentral distance 100 km). The relations are computed for PGA and PGV selecting the vertical and the largest horizontal component. The same relations have been computed also for the acceleration response spectra at the 12 periods ranging between 0.04 s and 2.0 s and for pseudo-velocity response spectra at the 14 periods ranging between 0.04 s and 4.0 s. Arias (Arias, 1970) and Housner intensity (Housner, 1952) and the strong motion duration (Vanmarcke and Lai, 1980) have been also computed and the respective attenuation relationships derived (Fig.7). different magnitude scales have been used: the ML (INGV bulletin or CPTI04 catalogue) and the Mw derived from empirical relations (Gasperini et al., 2004). The sites classification was done considering the EC8 and the geological information of the 1:500.000 Italian Geological Map. Two ground motion models proposed by Sabetta and Pugliese (1987; 1996) and Ambraseys et al. (2005) have been tested and the random effects model (Abrahamson and Youngs, 1992; Joyner and Boore, 1993) has been applied to estimate the

earthquake-to-earthquake and record-to-record components variance. The results have been compared to the models proposed by Sabetta and Pugliese (1987; 1996) and Ambraseys et al. (2005). Our relationships show a better fitting between real and predicted data for $M \geq 5.0$ and for distances > 25 km. Moreover, a considerable improvement is observed for $M \leq 5.0$ (up to one order, for M ranging from 3.5 to 4.5); this result is important since the area under study is mainly characterized by small events ($M \leq 5.0$) produce few damages.

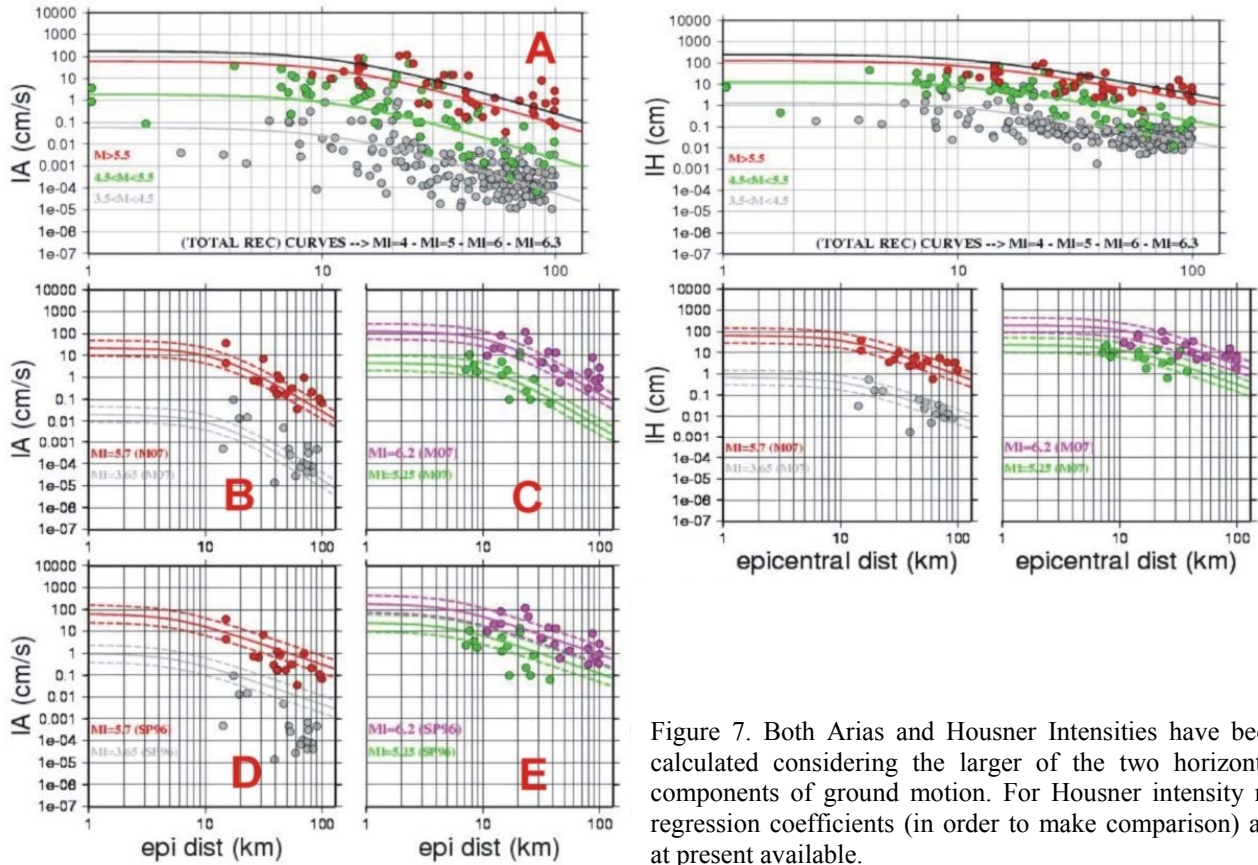


Figure 7. Both Arias and Housner Intensities have been calculated considering the larger of the two horizontal components of ground motion. For Housner intensity no regression coefficients (in order to make comparison) are at present available.

Task 5

Site effect analysis

In order to study the site effects at RAF stations the derived attenuation relations have been used, the mean ratio between recorded and computed (applying our model) PHA calculated for every station with a meaningful number of recordings. Bedrock stations have very similar recorded and computed PGA (MASA, MOGG, PRAD and PAUL); for GEPF, VALL and VINO stations the recorded PGA are lower than the estimated one from attenuation laws (Fig. 8). An unexpected result has been found for CESC: this is a bedrock station placed inside an artificial cave in a mountain area, but the mean ratio indicates that there is an amplification factor of three on the recordings with respect to our estimates from derived attenuation laws. CESC recorded very few data (six registrations only) of earthquakes with $M \geq 3.0$ and this could have resulted in a strong bias.

More detailed analysis have been done for CARC, GESC, GEDE and STOL stations, installed in order to study site effects in particular geological conditions. H/V and reference station method have been used to analyze recorded events and seismic noise. Surface-wave studies have been done in Stolvizza (STOL) and Gemona fan (GESC, GEDE) and extensive noise measurements and analysis performed on the Gemona fan obtaining results in very good agreement with previous gravimetric studies.

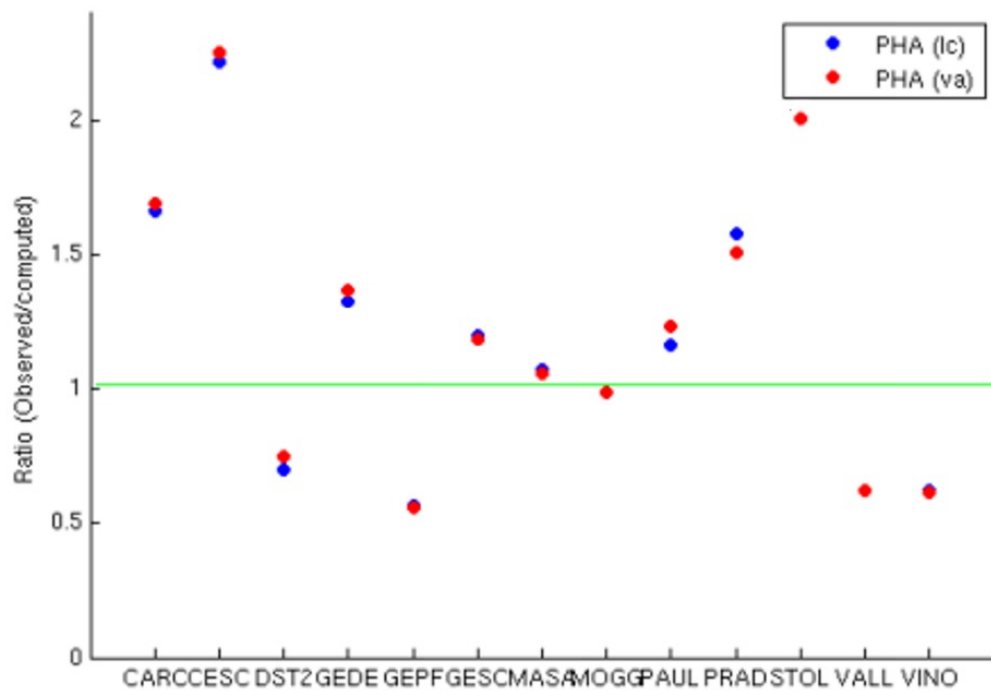


Figure 8. Mean value of the ratio between computed and observed PHA for the stations of the RAF.

Bibliography

- Abrahamson, N.A., Youngs, R.R., (1992). Bull Seism. Soc. Am. 82, 505-510.
- Ambraseys, N.N., Smit, P., Sigbjornsson, R., Suhadolc, P., Margaris, B., (2002). Internet-Site for European Strong-Motion Data, European Commission, Research-Directorate General, Environment and Climate Programme.
- Ambraseys, N.N., Douglas, J., Sarma, S.K., Smit, P.M., (2005). Bull. Earthq. Eng. 3, 1-53.
- Arias, A., (1970). A measure of earthquake intensity. In: Seismic Design of Nuclear Power Plants, R. Hansen (Editor), M.I.T. press, Cambridge.
- Borcherdt, R.D., (1994). Earthquake Spectra 10, 617-654.
- Faccioli, E., Cauzzi, C., (2006). 1st ECEES, Geneva, Switzerland, 3-8 September 2006, Paper n. 569.
- Gasparini, P., Gruppo di lavoro per redazione della mappa di pericolosità sismica prevista dall'ordinanza PCM 3274 del 20 Marzo 2003 (2004). Catalogo dei terremoti CPTI2 - App. 1 al rapporto conclusivo, open file report., 1-29.
- Housner, G.W., (1952). Spectrum intensities of strong-motion earthquakes. In: Proc. Symp. on Earthquake and Blast Effects Structures, C. M. Feigen (editors), Univ. California, Los Angeles, 21-36.
- Joyner, W.B., Boore, D.M., (1993). Bull. Seism. Soc. Am. 83, 469-487.
- Kennett, B.L.N., (1983). Seismic wave propagation in stratified media. Cambridge University press.
- Mayeda, K., Hofstetter, A., O'Boyle, J.L., Walter, W.R., (2003), Bull. Seismol. Soc. Am. 93, 224-239.
- Sabetta, F., Pugliese, A., (1987). Bull. Seism. Soc. Am. 77, 1491-1513.
- Sabetta, F., Pugliese, A., (1996). Bull. Seism. Soc. Am. 86-2, 337-352.
- Vanmarcke, E.H., Lai, S.P., (1980). Bull. Seism. Soc. Am. 70, 1293-1307.
- Wald, D.J., Quitoriano, V., Heaton, T.H., Kanamori, H., (1999a). Earthquake Spectra 15, 557-563.
- Wald, D.J., Quitoriano, V., Heaton, T.H., Kanamori, H., Scrivner, C.W., Worden, C.B., (1999b). Earthquake Spectra 15, 537-555.
- Wood, H., Neumann, O., (1931). Bull. Seismol. Soc. Am. 21, 277-283.

2.3 Specific problems which have delayed progress

None

2.4 Relevant publications which have arisen directly from this project

Publications JCR

Douglas J., Aochi H., Suhadolc P., Costa G. (2007). The importance of crustal structure in explaining the observed uncertainties in ground motion estimation. *Bull. Earthquake Engineering* 5:17-26.

Furlanetto E., Costa G., Suhadolc P., Palmieri F. (2007) Gravimetric characterization of the Gemona (NE Italy) alluvial fan for site estimation, submitted to *Near Surface Geophysics*

Abstracts/conference presentations

Costa G., P. Suhadolc, A. Delise, L. Moratto, E. Furlanetto, F. Fitzko (2006). Estimation of site effects at some stations of the Friuli (NE Italy) Accelerometric Network (RAF). 3rd ESG 2006 International Symposium, Grenoble (France) 30 August-1 September.

Costa G., L. Moratto, D. Sandron, A. Delise, P. Suhadolc (2006). Ground motion attenuation and shaking maps generation in the Southern Alps area. 1st European Conference on Earthquake Engineering and Seismology, Geneva (Switzerland) 3-8 September.

Furlanetto E., Costa G., Palmieri F., Delise A., Suhadolc P. (2006). Gravimetric and microseismic characterization of the Gemona (NE Italy) alluvial fan for site estimation), EGU General assembly, Vienna (Austria) 2-7 April.

Furlanetto E., Costa G., Palmieri F., Delise A., Suhadolc P. (2006) Gravimetric and microseismic characterization of the Gemona (NE Italy) alluvial fan for site estimation, 1st ECEES Geneva (Switzerland) 3-8 September.

Furlanetto E., Costa G., Suhadolc P. (2007) Different approach to evacuate site effects: application to Gemona del Friuli (NE Italy) alluvial fan area. XXIV IUGG, Perugia 2-13 July.

Massa M., Morasca P., Moratto L., Marzorati S., Augliera P., Spallarossa D., Costa G. (2007). Reviewed empirical ground motion attenuation relations for northern Italy using weak and strong motion data. EGU General assembly, Vienna (Austria) 15-20 April.

Moratto L., G. Costa, A. Delise, D. Sandron, P. Suhadolc (2006). Stime dello scuotimento in tempo reale e quasi-reale per terremoti significativi nell'area delle Alpi Sud-Orientali. GNGTS – 25° Convegno Nazionale, Roma 28-30 Novembre.

Moratto L., Costa G., Delise A., Sandron D., Suhadolc P. (2007). Real-Time Shake Maps in Southern Alps area: calibration and validation. XXIV IUGG, Perugia 2-13 July.

Suhadolc P., A. Valori, G. Costa, L. Moratto (2006). Mw estimation for regional seismic events in the Friuli area (NE Italy). 1st ECEES, Geneva (Switzerland) 3-8 September.

Progetto S4 - Stima dello scuotimento in tempo reale e quasi-reale per terremoti significativi in territorio nazionale

UR-6 Coordinatore: Nazzareno Pierdicca (Dipartimento Ingegneria Elettronica-Università La Sapienza di Roma)

Achievement of Project Deliverables

The objective of the unit UR-6, Department of Electronic Engineering, La Sapienza University of Rome, consists in the determination of the damage caused by seismic events in urban areas using remote sensing techniques. These kind of techniques have revealed themselves a suitable monitoring tool for disaster management since they provide a quick detection of land changes in wide areas, especially in remote areas or where the infrastructures are not well developed to ensure the necessary communication exchanges. A limitation for an operational use is the availability of the images in time to manage the crisis. This is a key point for Civil Protections who need a fast and draft overview of the epicentral area, quick information relative to the extension and distribution of damages, and the evaluation of infrastructure (roads, bridges) conditions. A single satellite can provide access time to a specific site in the order of some days. At the moment the use of any type of data (satellites) available and an integration of those data is mandatory to increase the chance to collect information on time. In the near future (years) the implementation of satellite constellations may reduce the access time with the same sensor to 12 hours, as in the case of the Italian COSMO-SkyMed system, based on X-band high resolution (few meters) radars.

For this purpose we have exploited in our research both data provided by active microwave sensors, such as high resolution (tens of meters or less) Synthetic Aperture Radar (SAR), and data from optical sensors working in the visible and infrared bands with spatial resolution ranging from medium (tens of meters) to very high resolution (1 meter or less).

In particular, SAR is widely used in environmental studies due to its characteristics which allow a fairly synoptic view in almost completely weather and time independent conditions, as opposed to optical sensors affected by cloud cover limitations. Multi-temporal observations from SAR can be used to detect urban changes either looking at the image intensity changes, as in the case of optical images, but also taking advantage from the information on the phase of the returned signal. This is specific of the radar technique and in particular of the interferometric SAR (InSAR).

The project activities has been developed following two different guidelines: first of all an analysis of some case studies has been carried out to understand and quantify the sensitivity of the different types of remotely sensed data to urban damages. Successively, based on such experience, few methodologies to generate products with operational applications have been investigated.

We have exploited intensity correlation and the InSAR complex coherence as SAR features to recognize changes on the surface caused by an earthquake. These two features hold different information concerning changes in the scene. The complex coherence is prevalently influenced by the phase difference between radar returns, a distinctive parameter measured by a coherent sensor. It is particularly related to the spatial arrangement of the scatterers within the pixel and thus to their possible displacements. Conversely, the intensity correlation is more related to change in the magnitude of the radar return.

The interaction of the SAR signal with the urban structures has been studied within this project in order to understand the phenomenon that affect the radar backscattering, in addition to surface changes we want to detect. A temporal series of SAR images, concerning the city of Rome, has been analysed for modelling the response of buildings and the influence of urban settlements characteristics on the backscattered signal. In particular, the model takes into account three different effects on SAR coherence in urban unchanged areas: temporal baseline, perpendicular baseline and track orientation

difference between the two interferometric acquisitions. The results of our empirical model are shown in figure 1, which compares measured and modelled complex coherence. Such model has been conceived to correct the above mentioned effects, thus enabling to detect structural changes even from interferometric pairs with different baselines and track orientation.

The potential of medium and very high resolution optical data has been also investigated. Medium resolution images have been used for classifying automatically surface changes in conjunction with SAR data, considering also the comparable pixel dimension. For this purpose we have considered two earthquakes as test beds: Izmit (Turkey) in 1999 and Bam (Iran) in 2003. In the Izmit case the combination of SAR and IRS panchromatic optical data allowed us to apply automatic procedures for damage classification, reaching the 90% of correct classification. In this case, it has also been demonstrated the possibility to significantly improve the results taking advantage of the change detection potential of the InSAR complex coherence combined with optical data, as shown in figure 2, which compares classification accuracy obtained by combining different set of features (optical alone, SAR alone or the integration of both). The correlation with damage level observed in situ has been also demonstrated for the optical change image and SAR intensity correlation when data are aggregated within homogeneous regions (such as blocks of buildings) and this is shown in figure 3. Also for the Bam case study, the combined use of SAR and optical data reached 77% of correct classification, confirming the complementarity of optical and microwave techniques. The apparently lower quality of the Bam result originates from the large spatial baseline of the SAR image pairs and the moderate resolution of the optical data (ASTER satellite with ground resolution of 15 m respect to Izmit case where the collected IRS images with ground resolution of 5 m).

In the Adapazari case, the experience made in the previous cases has been used to test the capability to generate a product useful for civil protection rescue activities. Based on the results of the Izmit and Bam case studies, a procedure to create a damage map has been attempted using only satellite data. The SAR intensity correlation has been used as a unique feature to generate the damage map. Three damage levels (low, medium and high) have been identified, each one corresponding to three thresholds defined on the intensity correlation values. The latter have been calculated within regions extracted from a ground truth map provided by the Kandilli Observatory and Earthquake Research Institute (KOERI) of Turkey. Figure 4 reports the damage map obtained for this case study and the corresponding ground truth map used as reference. Despite the difference on damage levels defined in the two maps (three for the satellite based map and seven for the ground truth one) the satellite map seems to fairly agree with the in situ survey. Once the SAR images will be made available with adequate time delay, the potential of this kind of product is fairly apparent.

Concerning high resolution optical image, they can in principle provide information on collapse of a single building or part of it. However, the information content could be affected by differences in the acquisition time, geometry, and changes in the sight observation angle. The presence of shadows, variation in sun illumination and geometric distortions are critical both for multispectral and panchromatic data, and they may prevent using automatic change detection procedures. Therefore the visual inspection approach is still the most used to produce a realistic and reliable inventory of damages. We had this kind of situation for Al Hoceima (Morocco) and San Giuliano (Italy) earthquakes. Concerning Al Hoceima, the analysis of damages in the urban areas hit by the earthquake was performed using multispectral high resolution (~1 m pan-sharpened) images acquired by the Ikonos satellite. The dataset was composed by one pre- and one

post-seismic scene. Due to the light different looking angle and sun illumination between the two Ikonos acquisitions, geometric and radiometric distortions were present, affecting also buildings and manufactures looking. The damage visual detection was focused on Al Hoceima and Imzourene cities and has demonstrated that the identification of single individual buildings from the available dataset was possible at least by visual interpretation, identifying a couple of damage classes (total collapses and partially damaged structures).

The main limitation for the San Giuliano test case was the absence of any satellite high resolution pre-seismic image. As pre-seismic data an aerial colour photo of the village has been used, whereas one post-seismic high resolution satellite image was available provided by EROS-1A satellite (one meter resolution). Although the two images were very much different, the identification of three different levels of change has been possible. Total collapses and strong damages have been observed even though a large number of false alarms were present (undamaged areas considered as strongly changed). In this case the reason was the lack of homogeneity among data sets and the difference in sun illumination.

Despite of the mentioned problems, high resolution optical data can potentially detect collapse of single buildings. The objective is to develop specific techniques making change detection quick and reliable with respect to simple visual interpretation. The experience gained from San Giuliano and Al Hoceima test cases has provided us with significant guidelines for developing automatic techniques. In particular, it suggested us to extract from the image, before applying any change detection algorithm, all the man made structures to map the potentially damaged area, thus avoiding the false alarms caused by shadow and transitory targets (for example cars), in particularly in those regions where a detailed cartography is not available. To do this it becomes necessary to integrate the spectral information carried out by the images (radiance in different spectral bands) with others features describing the geometry of the objects within the scene. More sophisticated classification algorithms are also needed to manage those information. For this aim, morphology operators have been used to extract features from the original image that give information about the distribution and geometry of the objects, whereas neural network classifiers have been exploited to improve the extraction of urban settlements. The test case for this exercise was the Bam earthquake, using two panchromatic Quickbird images (60 cm of ground resolution) available before and after the event. The results of the automatic change detection procedure are shown in figures 5 and 6, where we can see the potential of this kind of techniques, especially to detect partially damaged structures. In particular, figure 5 represents a possible product where the damage are identified as red areas. Figure 6 shows some details pointing out the capability of the technique to discriminate between shadows and actual settlement changes. This type of product can be conceived as a quick look at the damages, indicating the areas which are worth to better investigate either by image photointerpretation or by carrying out a ground survey, when possible.

We cannot claim to have investigated all possible spectrum of data type, urban settlement conditions and techniques, but the project has provided a quite realistic view of what remote sensing can offer for this application and which methods and sensors worth to be further developed in the future. The experience of this project has been summarized in table 1, where a list of possible damage products are shown, spanning different ground scales and obtainable with different satellite data. Those products can be valuable for managing different phases of the crises, and especially mitigation of the effect in the course of the event and precise inventory of the damage in the post-event phase.

Table 1: Resume of possible earthquake damage detection products derived from remote sensing data

<i>Product</i>	<i>Description</i>	<i>Tools</i>	<i>Scale</i>
Potential damage snapshot	Prompt overview of potentially damaged area (only qualitative)	Medium/high res. OPT & SAR	Medium, tens to hundreds meters
Damage level at district scale	Damage level (i.e., collapse ratio) estimated on homogeneous urban areas	medium/high res. OPT & very-high res. OPT & SAR	District, block of buildings
Collapsed/heavy damaged buildings	Identification of single buildings collapsed or heavily damaged	Very-high res. OPT	Single building

Key publications which have arisen directly from this project

The above overview does not necessarily cover all the activities carried out during the project. A more detailed description is contained in the publications associated to the present study as listed below.

International Journals:

- M. Chini, F. Pacifici, W. J. Emery and N. Pierdicca, "A comparison between statistical and neural network approaches within a common processing scheme for detecting urban changes from high resolution image of Rocky Flats", *Submitted to IEEE Transaction on Geoscience and Remote Sensing*.

- M. Chini, C. Bignami, S. Stramondo, N. Pierdicca, "Uplift and subsidence due to the December 26th, 2004, Indonesian earthquake and tsunami detected by SAR data". *Accepted for publication in the International Journal of Remote Sensing*.

- S. Stramondo, C. Bignami, M. Chini, N. Pierdicca, A. Tertulliani: "The radar and optical remote sensing for damage detection: results from different case studies". *International Journal of Remote Sensing*, Volume 27, N. 20, 20 October, 2006.

Conference proceedings:

- M. Chini, W. J. Emery, F. Pacifici: "Satellite Mapping of the Demolition of the Rocky Flats Nuclear Weapons Plant". *Proc. IEEE/IGARSS 2007, Barcelona (SPAIN), 23 – 27 July, 2007*.

- M. Chini, W. J. Emery, N. Pierdicca: "Land Cover Change Detection of the Demolition of

the Rocky Flats Nuclear Site". *Proc. 4th IEEE GRSS/ISPRS Urban Remote Sensing Joint Event 2007*, Paris, France, 11-13 April, 2007.

- S. Stramondo, C. Bignami, N. Pierdicca, M. Chini: "SAR and optical remote sensing for urban damage detection and mapping: case studies". *Proc. 4th IEEE GRSS/ISPRS Urban Remote Sensing Joint Event 2007*, Paris, France, 11-13 April, 2007.

- S. Stramondo, N. Pierdicca, M. Chini, C. Bignami: "Damage Detection and Surface Effect Mapping by Integrating SAR and Optical Remote Sensing". *Proc. 4th International Workshop on Remote Sensing for Disaster Response*, Magdalene College – Cambridge (UK), 25-27 September, 2006.

- F. Macina, C. Bignami, M. Chini, N. Pierdicca: "Exploiting physical and topographic information within a fuzzy scheme to map flooded area by SAR". *Proc. IEEE/IGARSS 2006*, Denver (COLORADO), July 31- August 04, 2006.

- C. Bignami, M. Chini, N. Pierdicca, S. Stramondo: "Surface Effects of the 2004 Indonesian Earthquake and Tsunami from SAR data". *Proc. FRINGE 2005 Workshop ESA ESRIN*, Frascati (ITALY), 28 November-2 December, 2005.

Presentations at Conferences:

- M. Chini, W. J. Emery, F. Pacifici: "Change mapping in the Rocky Flats area as test bed for damage detection algorithms". *General Assembly of the European Geosciences Union 2007*, Vienna (AUSTRIA), 15 – 20 April, 2007.

- L. Pulvirenti, M. Chini, N. Pierdicca: "Effects of baseline urban texture on SAR image: applications to earthquake damage detection". *General Assembly of the European Geosciences Union 2007*, Vienna (AUSTRIA), 15 – 20 April, 2007.

- C. Bignami, M. Chini, S. Stramondo, N. Pierdicca: "Earthquake urban damage assessment from satellite data". *General Assembly of the European Geosciences Union 2007*, Vienna (AUSTRIA), 15 – 20 April, 2007.

- M. Chini, C. Bignami, S. Stramondo, N. Pierdicca: "The 2004 Indonesian earthquake and tsunami: surface effects from SAR data". *General Assembly of the European Geosciences Union 2006*, Vienna (AUSTRIA), 2-7 April, 2006.

- C. Bignami, M. Chini, N. Pierdicca, S. Stramondo: "Remote sensing techniques for damage assessment in urban area". *Workshop (INGV-OV, IREA-CNR, ESA): Use of Remote Sensing Techniques for Monitoring Volcanoes and Seismogenetic Areas*, Vesuvius Observatory – Naples (ITALY), June 23-24, 2005.

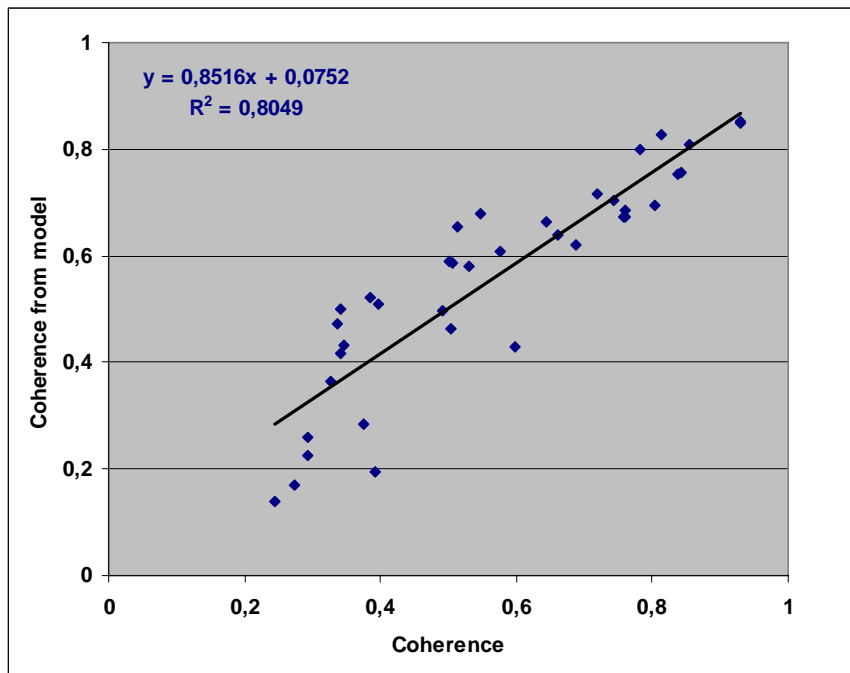


Figura 1: Comparison of InSAR coherence derived from the empirical models as function of spatial and temporal baseline and orbit azimuth angles with coherence derived from the data (ERS image interferometric pairs with different baselines)

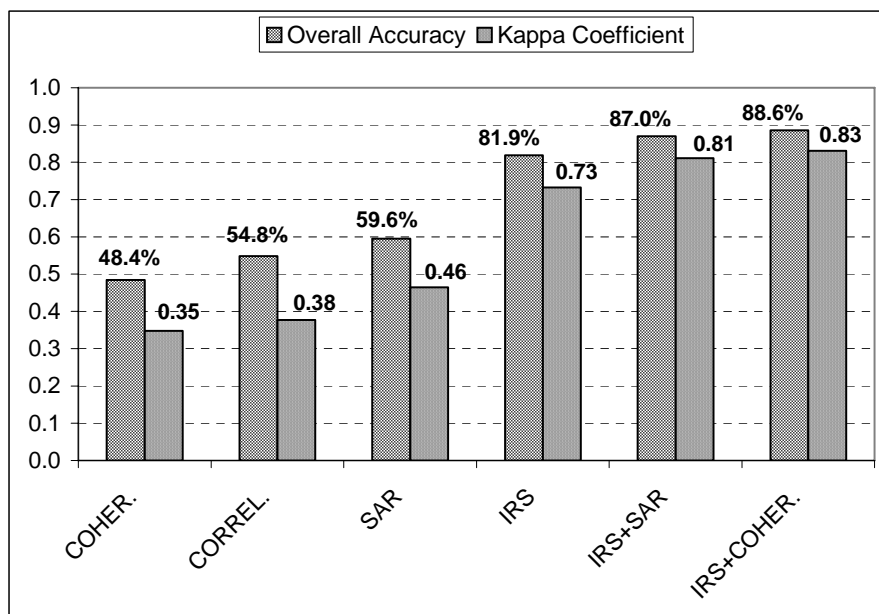


Figura 2: Discrimination accuracy (total error rate and K coefficient) of six different classes of urban changes for the Izmit case study by automatic classification algorithms (Maximum likelihood classifier). The use of optical data (IRS) only, and different combinations of radar features (complex InSAR coherence: COHER; correlation among radar intensity: CORREL, all radar features: SAR) are compared with a combined exploitation of radar and optical features (IRS+SAR and IRS+COHER).

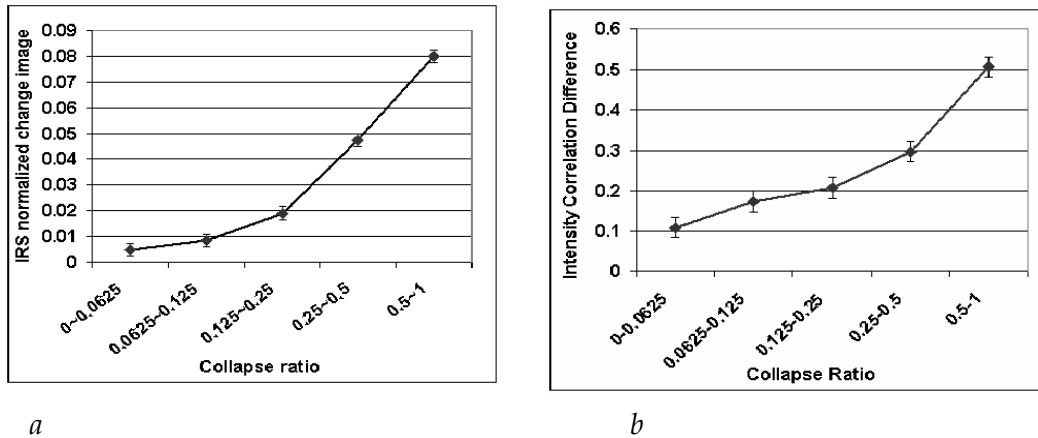


Figure 3: a) IRS normalized change (i.e., difference between pre-seismic and post-seismic images) averaged over the surveyed areas as function of the corresponding collapse ratio; b) Pre-seismic and co-seismic intensity correlation difference averaged over each surveyed area as function of the corresponding collapse ratio.

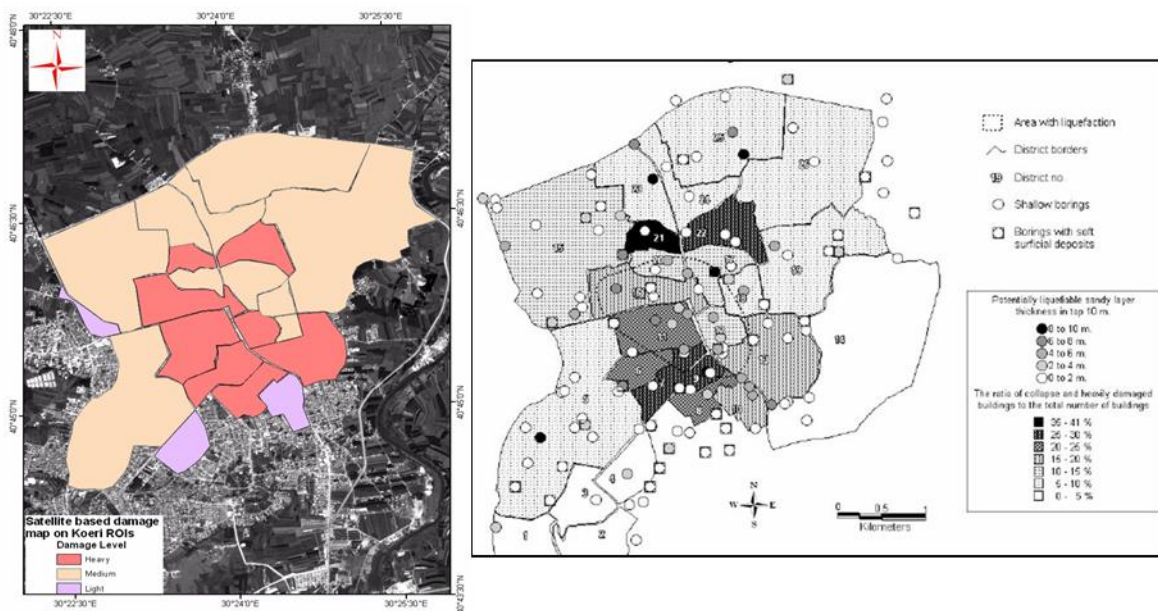


Figure 4: Comparison between the satellite based damage map (left panel) and ground survey damage map (right panel) for the Adapazari case study... Darker colours correspond to heavily damaged areas.

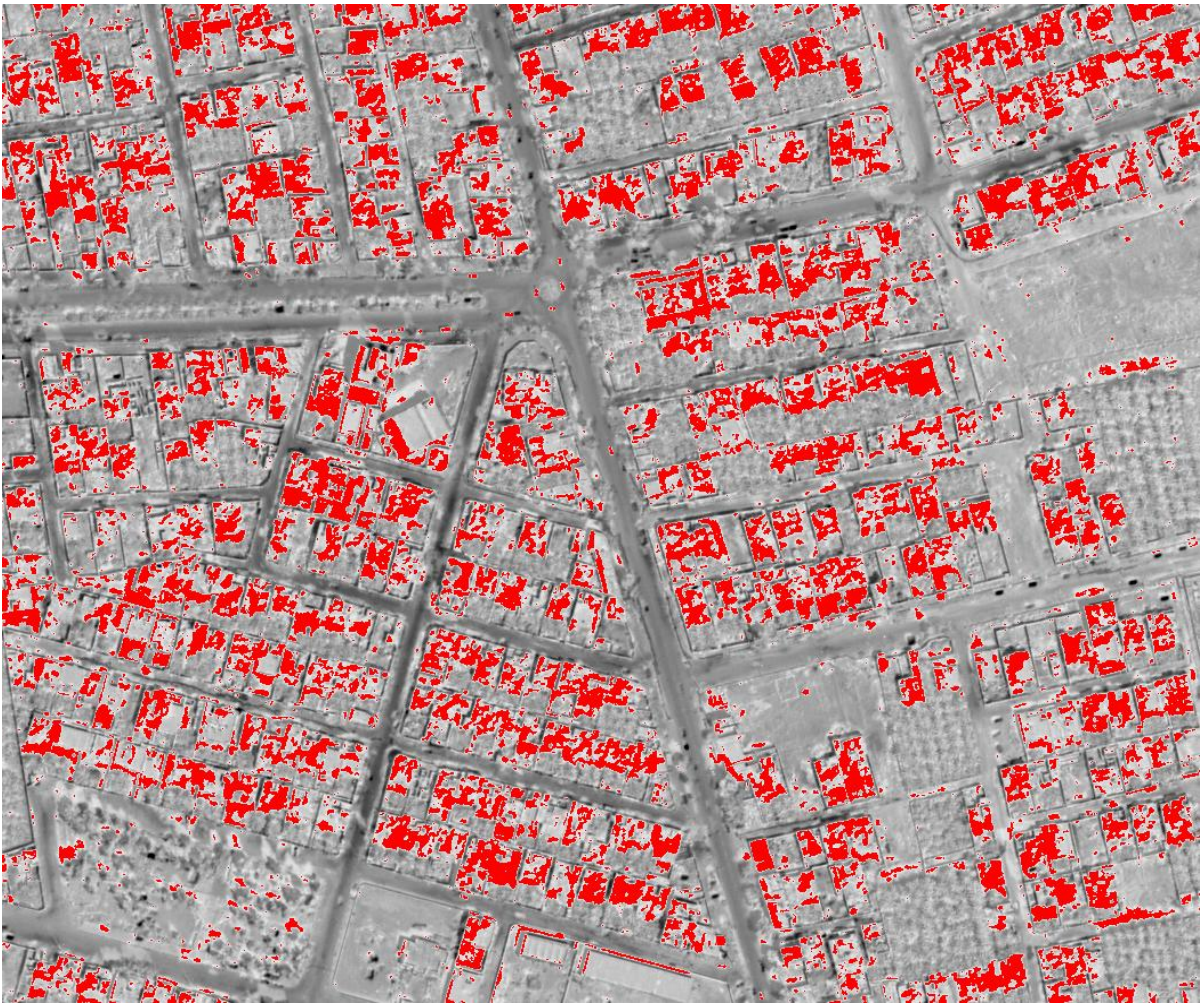


Figure 5: Map of damaged buildings (in red) for the Bam case study derived from a pair of Quickbird images.

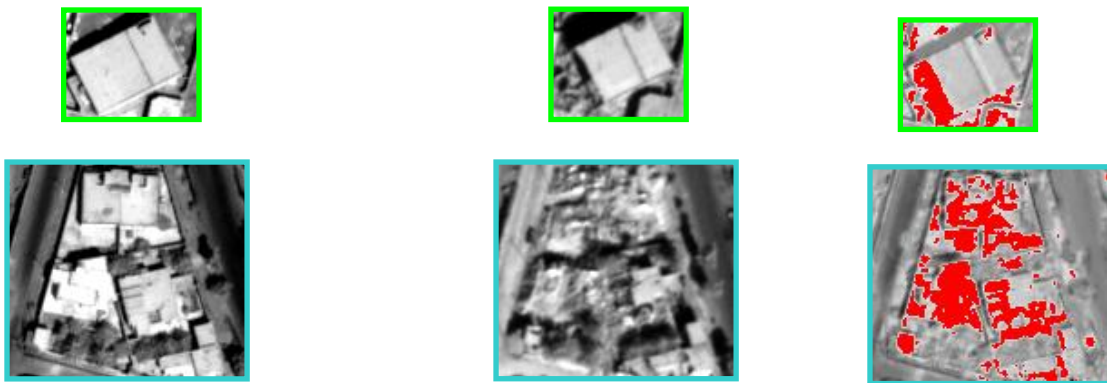


Figure 6: Details of Quickbird images before (left panel) and after (middle panel) the earthquake and the resulting damage map (right panel) where the successful discrimination between shadow and damages can be perceived.

Task S4 UR7 –Research report on the first and second year of the project

Research Unit: RM1.

Responsible:

Prof. Ettore Cardarelli, Dep. ITS “La Sapienza” - Rome

Introduction

We hereby report the activities performed by the Research Unit (UR-Roma1) within the framework of the research project “Stima dello scuotimento in tempo reale e quasi-reale per terremoti significativi in territorio Nazionale”, research unit scientific Prof. Ettore Cardarelli (project coordinators: L. Malagnini e D. Spallarossa), Task 5 –“Stima degli effetti di sito alle stazioni di registrazioni ed utilizzo di GIS esistente”.

The main purposes of the projects are the estimation with rapid numerical techniques of the seismic site response: to do so, particular attention in soil characterization was needed in selected sites.

Our activities for **Task S4** (Convenzione 2004-2006 tra il Dipartimento della Protezione Civile e l'INGV, l'Area di Geofisica del Dipartimento di Idraulica Trasporti e Strade) consisted in two cross-hole surveys located in the municipalities of Barisciano (AQ) and Castelli (TE).

The main task of the geophysical surveys is the elastic characterization of the subsoil at low strain in terms of s-wave and P-wave velocities.

A detailed geophysical characterization of selected sites is needed to validate the proposed approach to evaluate the site response in real time.

With the same purposes this research unit participated in the **Task S6**, using the same field techniques aimed to the elastic near-surface soil characterization in the following sites : Gubbio (PG), Valle dell'Aterno (AQ), Bevagna (PG), Cesena (FC), Durso (BN).

The following measurements have been completed so far: Gubbio, Valle dell'Aterno, Bevagna.

The remaining field surveys will be completed within July 2007. The seismic sources SBS42 and SBS66 used in all the surveys were purchased using funds available

To increase processing productivity a seismic processing software was acquired (Visual_Sunt 10).

A lab equipment comprising ultrasonic probes and an oscilloscope was acquired to test soil samples in order to corroborate field data with independent measurements and is to be delivered within short and it is planned to use it for the remaining investigation sites.

Some people of the research staff will be granted to follow the international meeting “Near surface Geophysics” organized by EAGE in Istanbul (3-6 September 2007).

Here follows the detailed results of the geophysical surveys.

a) Start-up seismic equipment

In order to obtain accurate measurements of S wave velocities in a drilling hole main part of the fund of the project was used to buy a seismic probe source of new generation. Activity developed about this device was organized following the program here described

- December 2005 – Training prof. E. Cardarelli ed ing. M. Cercato in the manufacturing industry (Hannover, Germania)
- Tests on-field (gennaio-febbraio 2005)
- Field survey in Valmontone site (RM)

Site: Barisciano

Two survey were carried out with the aim to evaluate P and S wave velocities.

The geologic formation under investigation consists in calcareous gravel with sandy matrix, with the exception of a thin layer 2m thick at 37 m depth consisting in sandy deposits.

The P-wave survey was performed by seismic transmission tomography, setting 13 receivers downhole in the first hole, 3 geophones on the ground surface and using the other borehole for the shot locations. The horizontal distance between the boreholes at the surface is 8.2 m.

As shown in Fig. 1 the P-wave velocities increase with depth from about 1000 m/s at the surface to about 3000 m. The highest velocities are retrieved between 22m and 37 m depth. Below that depth range appears a velocity inversion, probably due to the presence of sandy deposits at about 38m.

The S-wave survey (performed using 2 m vertical spacing) shows a clear increase of velocity with depth. Particularly below 16 m depth, the s-wave velocity progressively reaching 1300 m/s at 36 m depth. Below this level we have a clear velocity inversion, which is again due to the presence of sand.

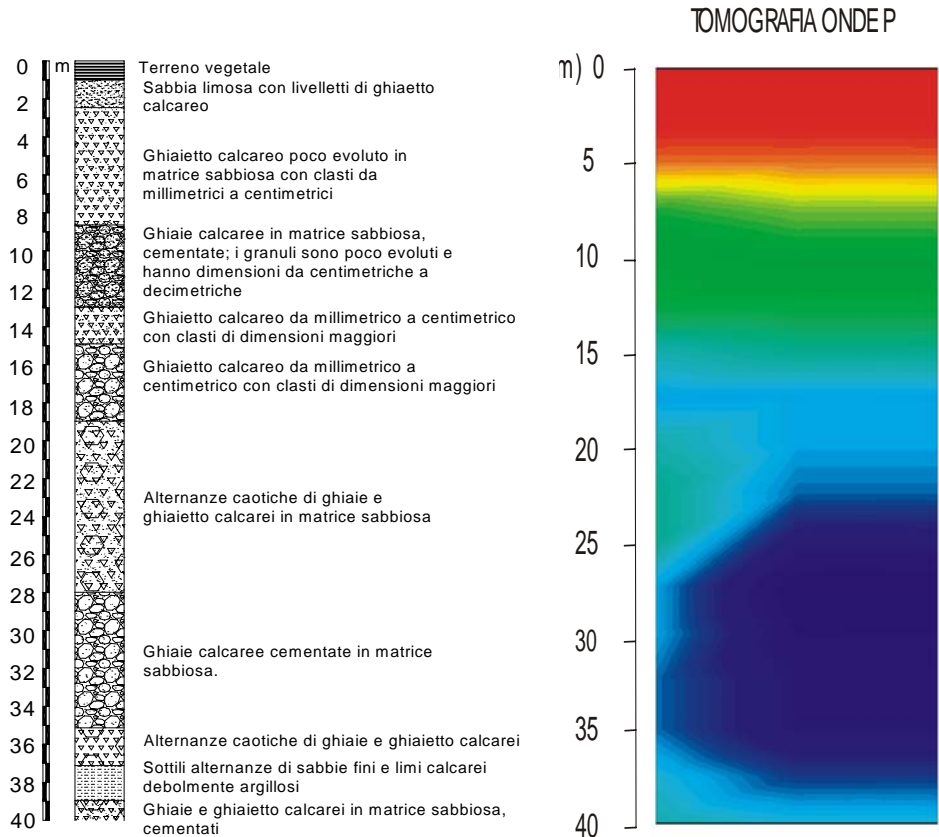


Fig. 1 Seismic tomography (P-wave velocity)

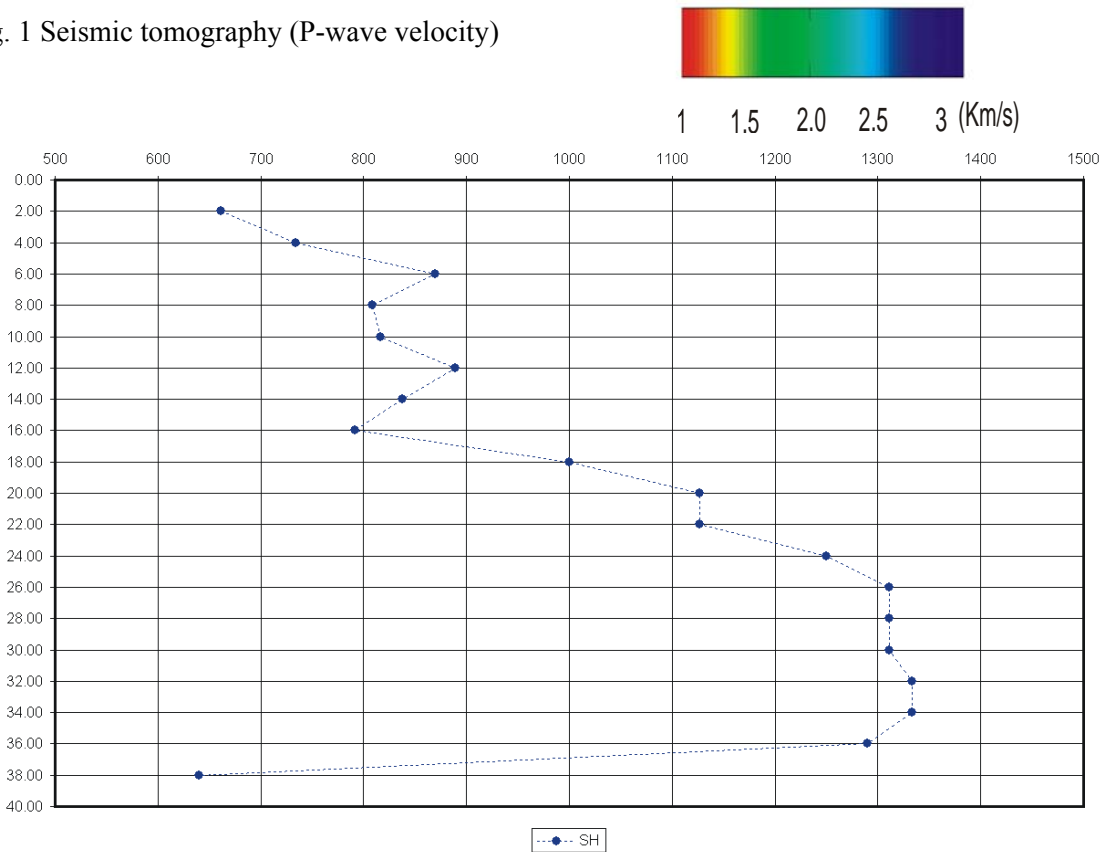


Fig. 2 S-wave profile

Site: Castelli

Using the same approach, we performed a complete P- and S- wave velocity crosshole.

The stratigraphy shows the presence of gravel with sandy matrix down to 25,5 m depth and marly clays seldom interbedded with thin layers of fine gravel down to the maximum investigation depth of 40 m.

We used 16 sensors (13 downhole in borehole S1 and 3 surface receivers between boreholes) and a shot location interval of 2m in borehole 2. Horizontal spacing between boreholes is 7.8 m.

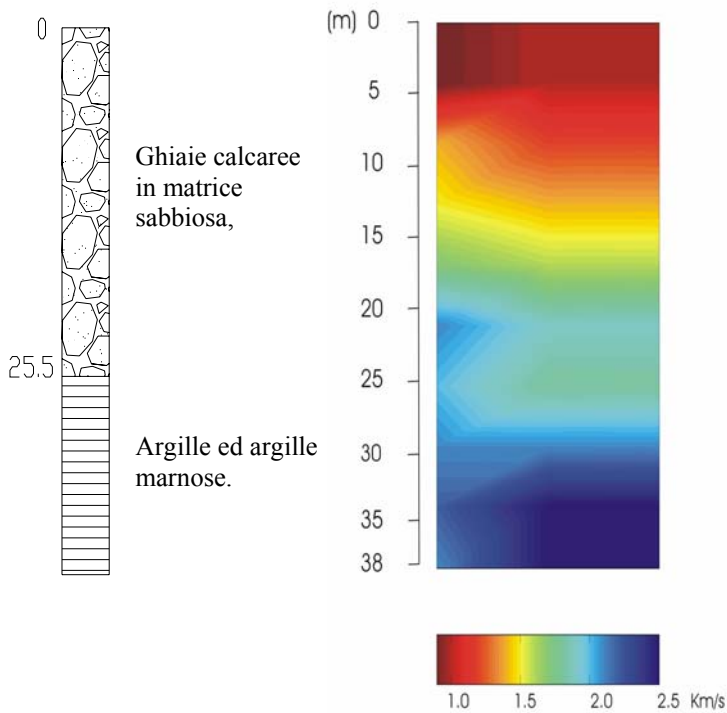


Fig. 3 Seismic P-wave tomography.

As shown in Fig. 3 P-wave velocity values increase progressively with depth, ranging from 1000m/s at the top of the layer stack to about 2500 in the depth interval 25m-38m (bottom hole).

The s-wave velocity profile, (Fig. 4) obtained using 2m vertical spacing, shows depth-increasing velocities. Particularly there is a sharp increase at about 8 m from 500-600 m/s to 800m/s, which is a value that lasts averagely constant down to 24 m depth. Below this level there is a velocity inversion (< 500 m/s) associated to the stratigraphic change from gravel to clayey deposits.

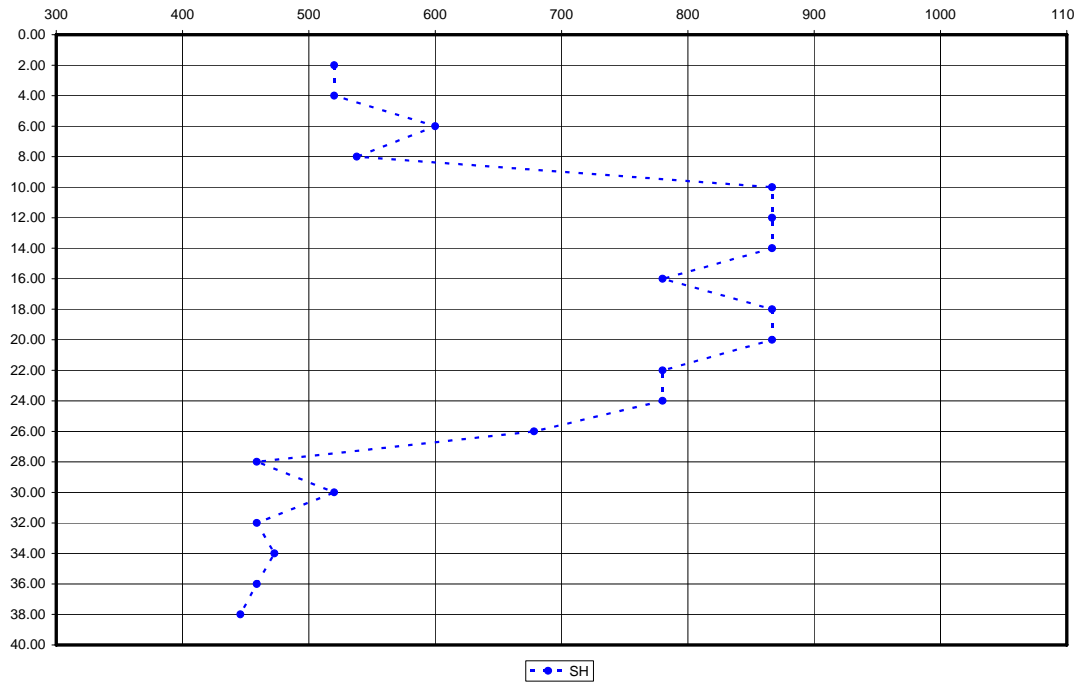


Fig. 4 S-wave profile.

Site: Gubbio (PG)

Introduction

Two downhole field surveys in the municipality of Gubbio (PG) (Task S4) were performed in February 2007. Boreholes are located in two sites: Cabina Enel e Vivaio la Torraccia and labelled as S1 and S2, respectively.

With the seismic source at fixed position(2m b.g.l.), data were acquired ad different receiver positions spaced 1 m apart down to the bottom hole (57 m b.g.l.) for s1 borehole and 47 m b.g.l. for S2 borehole The horizontal spacing between the seismic source and the borehole is 3 m (S1) and 3.5 m (S2).

First-arrival times picked from recorded seismograms were drawn on a reduced time – depth panel, obtaining the layer velocities from the slopes of the time-depth curves by regression analysis.

Interval velocities were also calculated using different spacing (1m and 2m) and compared with the values obtained by time-depth as will be described in the following.

Borehole S1

P-wave

In Fig 5 we report the reduced time – depth curve for P-waves and borehole S1. Four different slopes were identified which are associated with different layer velocities (Table 1).

Layer	Depth (m)	VS (m/s)
1	0-6	800
2	6-34	1700
3	34-53	2000
4	54-57	2200

Table 1

S-wave

S wave velocities were obtained using the same processing described above.

The reduced time-depth curve is reported in fig. 6.a. Four layers can be identified: (Table 2)

Layer	Depth (m)	VS (m/s)
1	0-6	150
2	6-34	240
3	34-53	380
4	54-57	750

Table 2

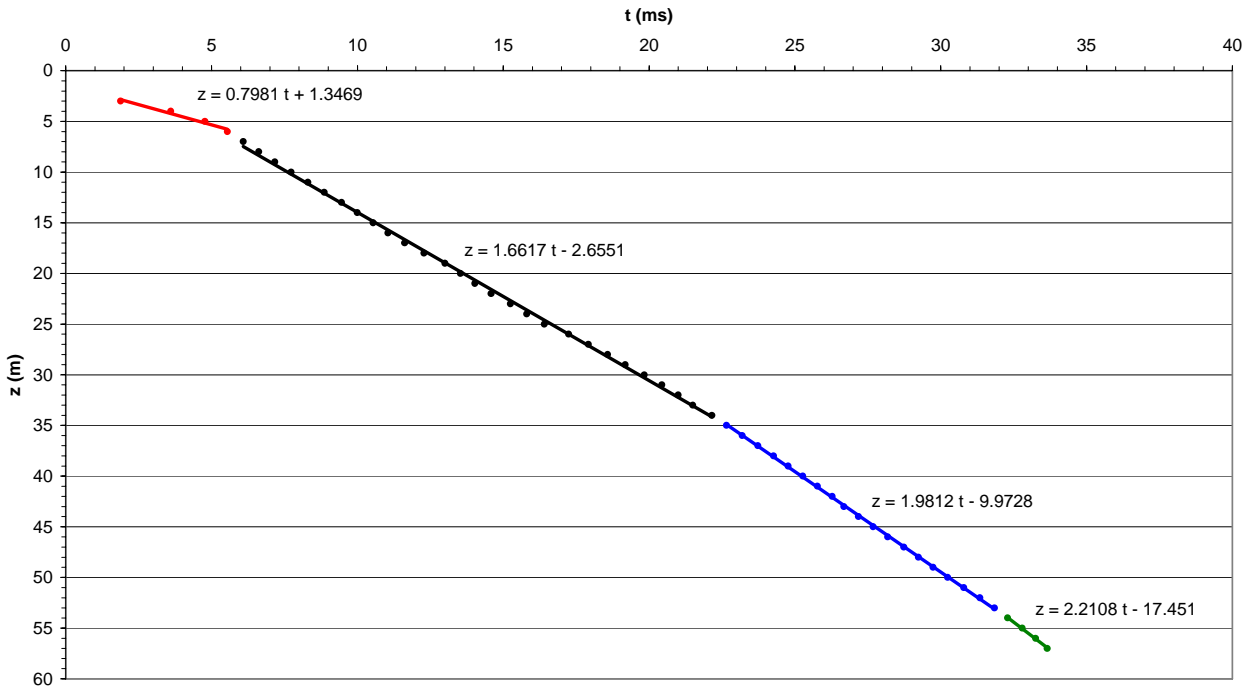


Fig. 5 Reduced time-depth curve for P-waves (Different colors are related to different velocity values).

The interval-velocity profiles are shown in Figure 6b together with the time-depth regression profile.

There is an excellent agreement between the different methods.

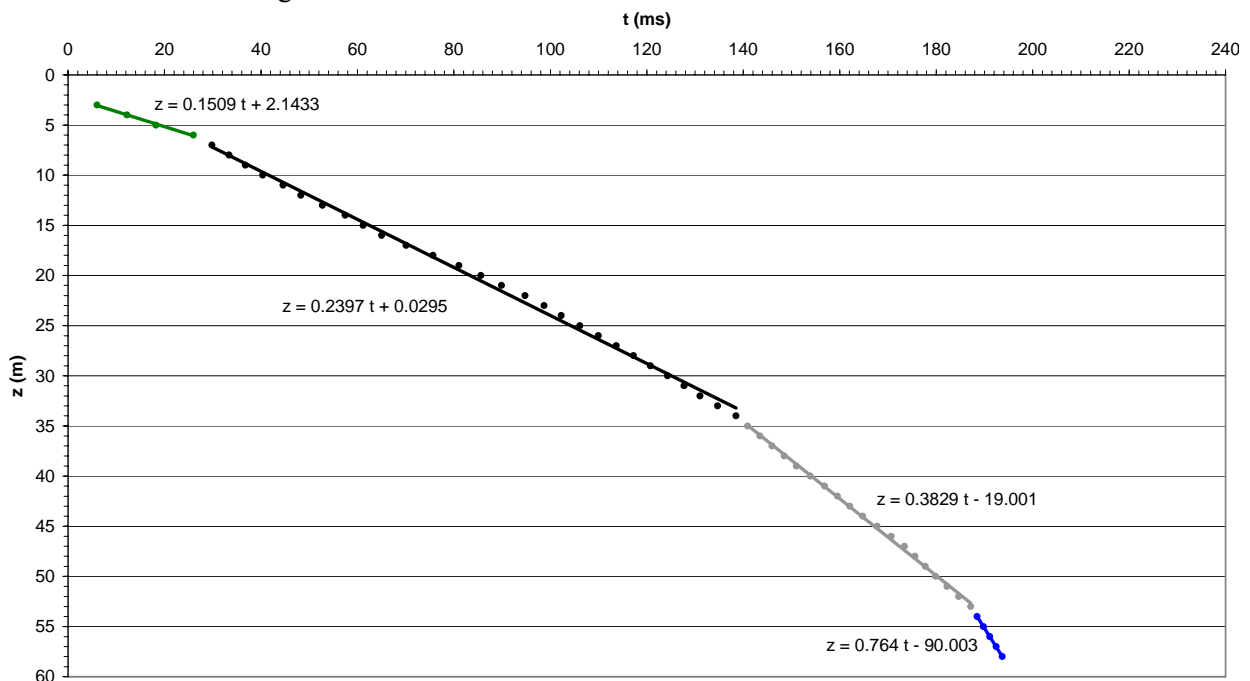


Fig. 6 a) Reduced time-depth curve for S-waves (Different colors are related to different velocity values).

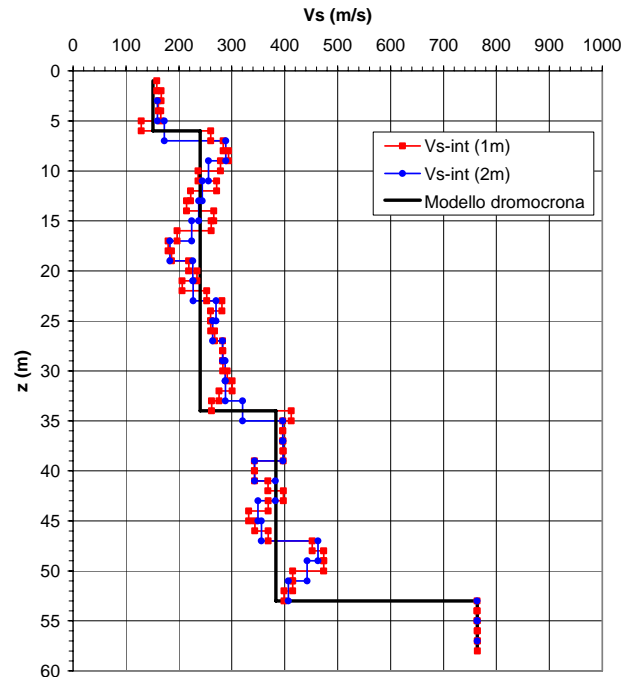


Fig. 6 b) S-wave Interval velocities (different colors are associated, respectively, to 1m or 2m spacing used for. The black solid line is the profile retrieved from analysis in the time-space domain).

Borehole S2

P-wave survey

In Fig. 7 it is displayed the reduced time-depth curve retrieved from P-wave first arrival picking (borehole S2). Differently from borehole S1, 3 main velocity layers are identified: a near surface layer of 5m thickness and 1250 m/s velocity, an intermediate layer from 5m to 44m depth marked by a velocity of 1600 m/s and a deeper layer reaching the bottom hole having a P-wave velocity of 2000 m/s.

S-wave survey

S-wave velocity were calculated using both the method of regression in the reduced-time depth domain and the technique of uinterval velocity. The reduced time –depth curve for S-wave (S2 borehole) is reported in figure 8a. One can clearly identify four velocity layers. Starting from the ground level, a shallower 11m-thick layer of 160 m/s S-wave velocity is found, then a layer marked by a 250 m/s velocity is identified between 11 and 36 m depth. Below this depth and down to 44 m depth the calculated velocity is 350 m/s. The deeper layer reaching the bottom hole is marked by a velocity of 600 m/s

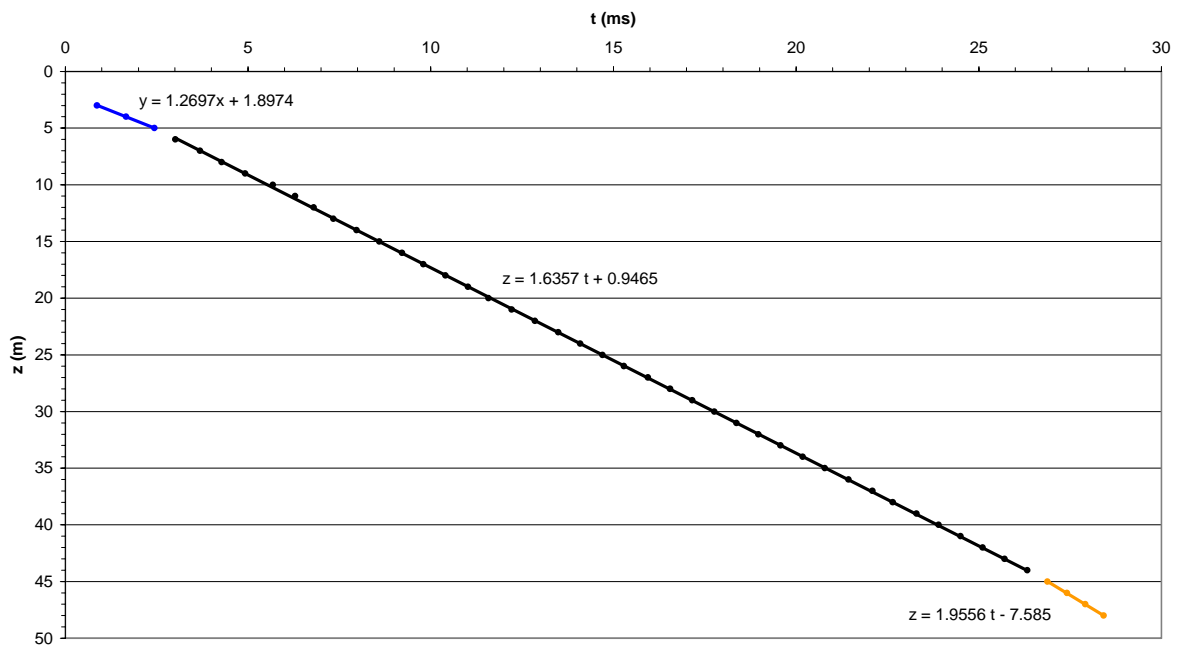


Fig. 7 Reduced time-depth curve for P-waves (Different colors are related to different velocity values).

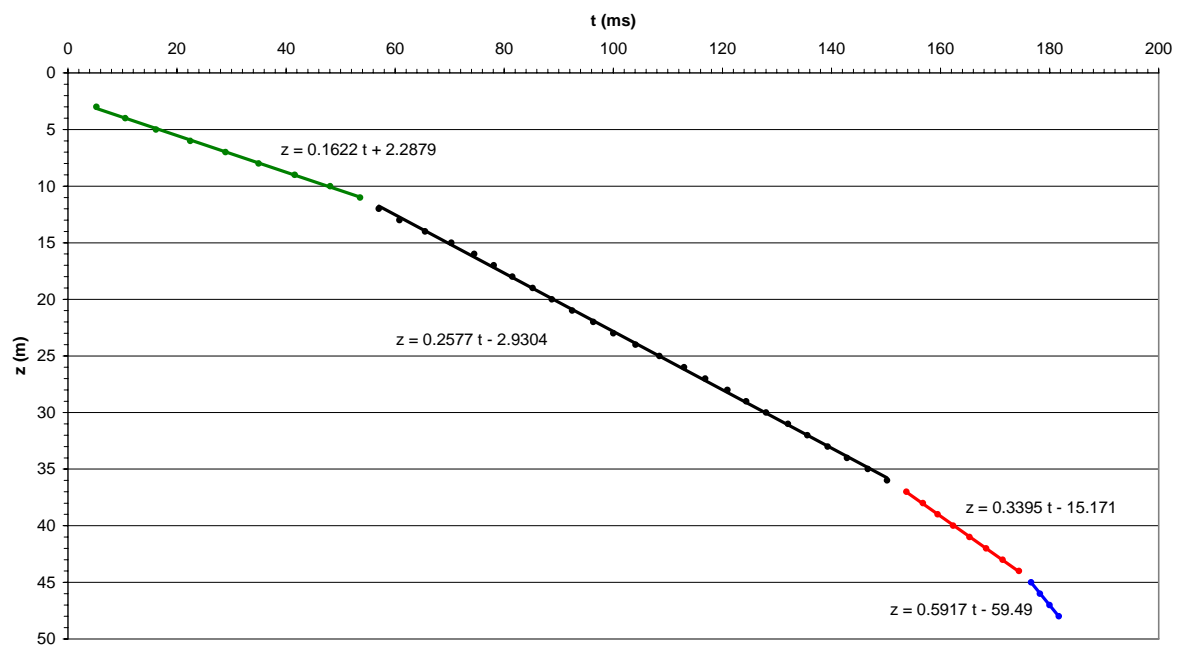


Fig. 8 a) Reduced time-depth curve for S-waves (Different colors are related to different velocity values).

In Figure 8b we display the interval velocities determined using depth interval of both 1m and 2m. The velocities retrieved from regression of the reduced time-depth curves show a very good agreement with the interval velocities.

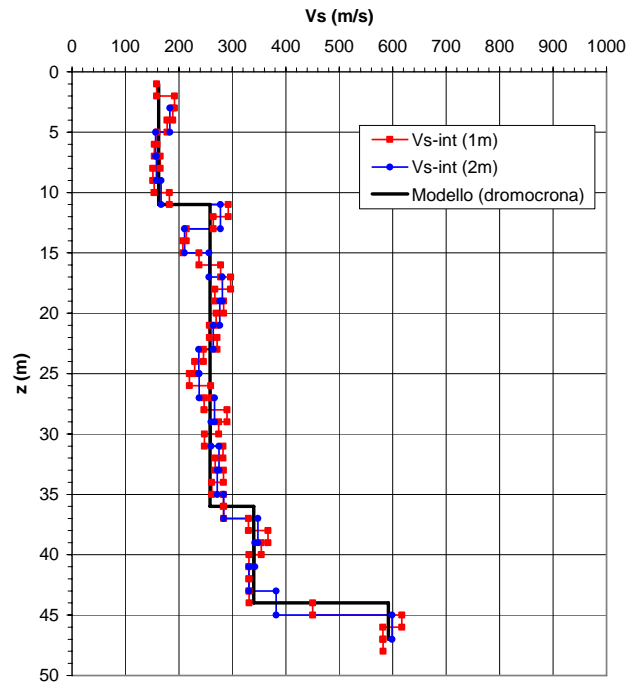


Fig. 8 b) S-wave Interval velocities (different colors are associated, respectively, to 1m or 2m spacing used for. The black solid line is the profile retrieved from analysis in the time-space domain.

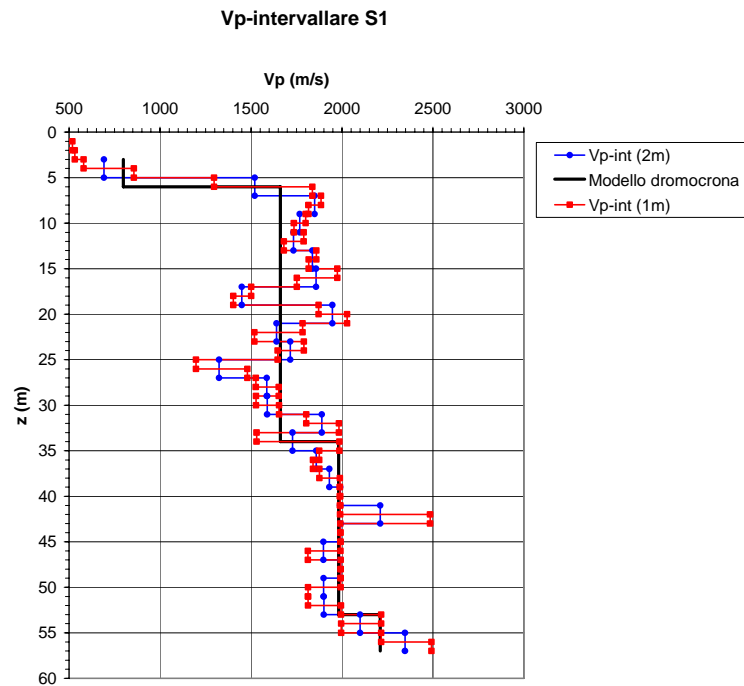


Fig.1A P-wave Interval velocities for borehole S1 (different colors are associated, respectively, to 1m or 2m spacing used for. The black solid line is the profile retrieved from analysis in the time-space domain.

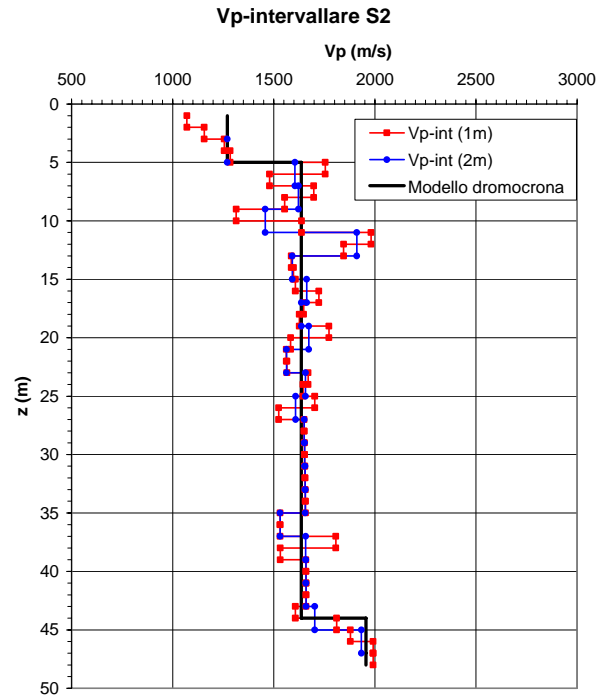


Fig. 2A P-wave Interval velocities for borehole S2 (different colors are associated, respectively, to 1m or 2m spacing used for. The black solid line is the profile retrieved from analysis in the time-space domain.

Site: Valle dell’Aterno

Crosshole seismics (for P- and S-wave velocity) aimed to low-strain (elastic) material characterization was performed in the Coppito municipality (AQ).

The geological formation under investigation is mainly calcareous gravel with sandy matrix, with the exception of sandy and silty deposits between 29m and 46m.

At 55 m depth the limestone bedrock was encountered.

Seismic P-wave transmission tomography was performed using 25 sensors (22 downhole geophones and 3 surface geophones) in borehole S1 and 26 shot locations in borehole 2. Horizontal spacing between boreholes is 7.5m. tomography inversion was performed using the ray-tracing technique to account for significant differences between layer velocities.

As displayed in fig. 9, after a surface weathered layer of several meters marked by a velocity of 500 m/s, P-wave velocity is progressively increasing with depth, up to values of 2000 – 2200 m/s with the exception in the depth range 28-32m where a moderate velocity inversion (1800 – 2000 m/s). this level is associated with silt and sand interbedded with thin level of gravel.

Below 45 m, P-wave velocities sharply increase to 4500 – 5000 m/s which can be associated to the limestone bedrock. In figure 9b the seismic raypath is displayed.

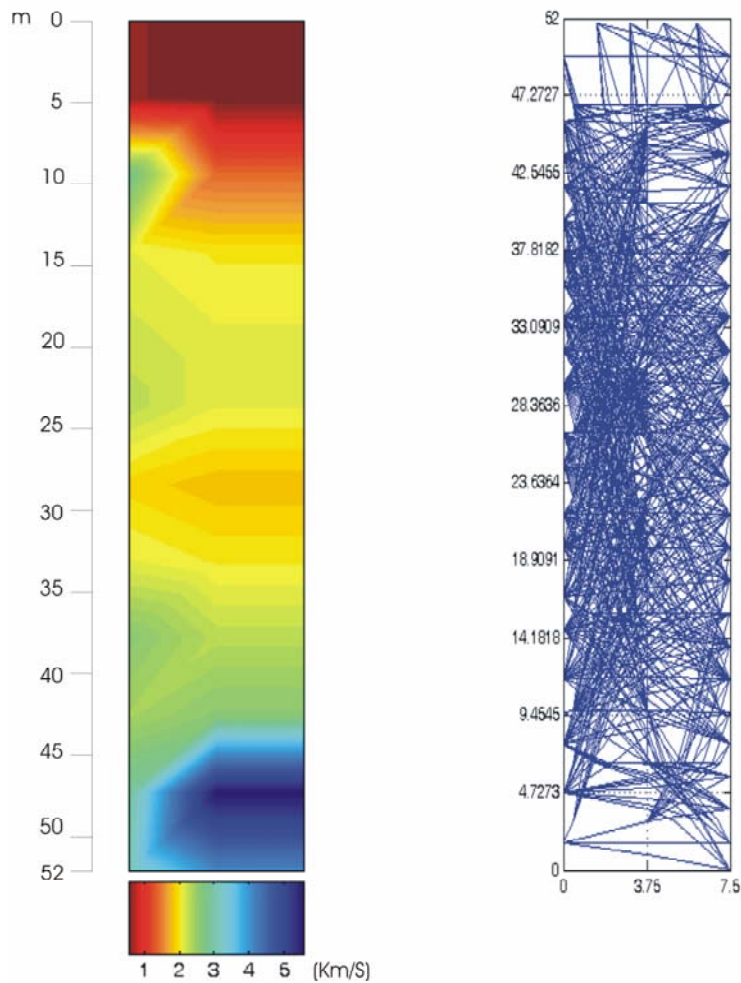


Fig. 9 P-wave velocity seismic tomography: a) P-wave velocity field, b) seismic raypath.

The S-wave profile (measured at 1m vertical spacing) shows (Figura10) a progressive increase in velocity down to 10 m. In the depth range between 10 m and 24 m the S-wave velocity is nearly constant at about 700 m/s. From 24m to 32 m a velocity inversion is clearly detected. Within this depth interval the s-wave velocity are confined to the 300-500 m/s range. Below 32m depth, the VS is higher, reaching its maximum value between 48-52 m depth where the measured values are about 1200 m/s.

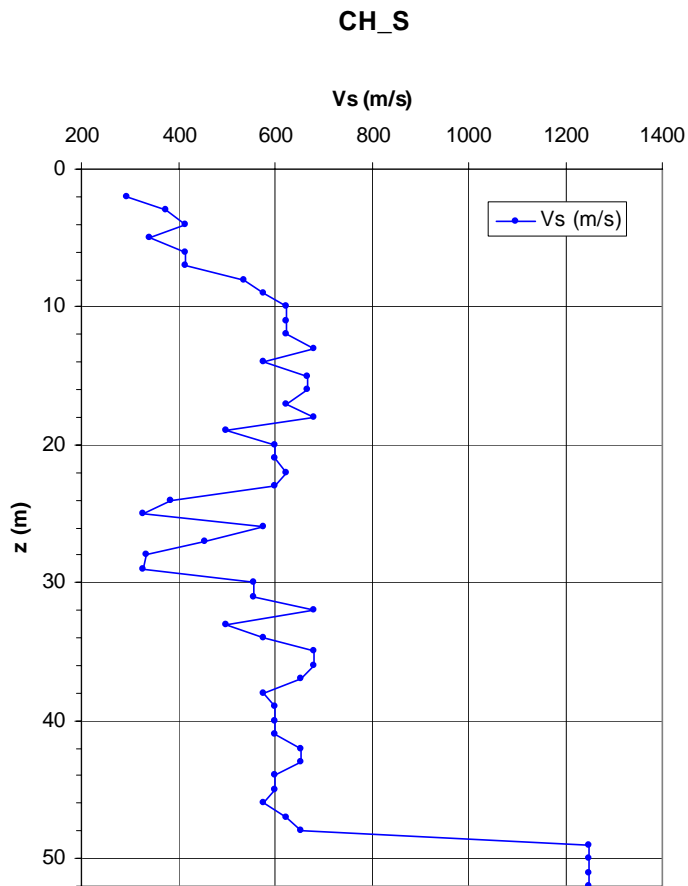


Fig.10 SH-wave profile

Site: Bevagna

During June and July 2007 cross-hole P-wave and S-wave surveys were performed in the municipality of Bevagna (PG). The P-wave tomography survey was performed setting 21 geophones downhole in borehole 1 and three on the ground level, using 25 shot locations. Spacing between boreholes is 6.6 m. A vertical spacing of 1 m is adopted for s-wave profiling.. Data are currently under processing.